

Finite Larmor radius contributions
to anomalous transport in plasmas
with stochastic magnetic fields

Inaugural-Dissertation

zur

Erlangung des Doktorgrades der
Mathematisch-Naturwissenschaftlichen Fakultät
der Heinrich-Heine-Universität Düsseldorf

vorgelegt von
Marcus Neuer
aus Düsseldorf

Dezember 2005

Aus dem Institut für Theoretische Physik
der Heinrich-Heine-Universität Düsseldorf

Gedruckt mit der Genehmigung der
Mathematisch-Naturwissenschaftlichen Fakultät der
Heinrich-Heine-Universität Düsseldorf

Referent: Prof. Dr. K.-H. Spatschek

Korreferent: Prof. Dr. D. Bruß

Tag der mündlichen Prüfung: 27.1.2006

Table of contents

1 Introduction	1
1.1 Physical motivation	1
1.2 Stochastic differential equations approach to anomalous transport	3
1.3 Mean squared displacement and the diffusion coefficient	5
1.4 Lagrangian and Eulerian correlations	5
1.5 Percolation structures of the flux function	7
1.6 Overview of this work	7
2 Velocity correlations based on the A-Langevin equation	9
2.1 The velocity of a particle in a stochastic magnetic field with collisions	9
2.1.1 General magnetic geometry and the description with the A-Langevin equation	9
2.1.2 The solution of the A-Langevin equation	11
2.2 Velocity products from the A-Langevin solution	15
2.2.1 The Green-Kubo formalism as link between correlation function and transport	15
2.2.2 Classical transport and the classical diffusion coefficients	15
2.2.3 Velocity correlation functions in the limit of strong guiding fields	16
3 Transport for small Kubo numbers	19
3.1 The Corrsin approximation for Lagrangian correlation functions	19
3.1.1 The Lagrangian coordinate system	19
3.1.2 Corrsin's independence hypothesis	19
3.1.3 Correlation function of the derivative of the perturbation field	21
3.2 Lagrangian velocity correlations	23
3.2.1 The guiding field term $\mathcal{L}^{(0)}$	23
3.2.2 The Larmor radius correction term $\mathcal{L}^{(1)}$	25
3.3 Diffusion regimes	27
3.3.1 The A-MSD-equation for the description of anomalous transport	27
3.3.2 The quasilinear limit	27
3.3.3 Occurance of a subdiffusive situation	30
3.3.4 The Rechester-Rosenbluth regime	31
3.3.5 The Kadomtsev-Pogutse -I regime	35
3.3.6 The Kadomtsev-Pogutse-II regime	36
3.4 Particles in vanishing mean fields	38
3.4.1 Velocity correlation function for vanishing mean fields	38
3.4.2 The relaxation function γ	38
3.4.3 The transport coefficients for vanishing mean field regimes	40

3.5 The Kubo number restriction of the Corrsin approximation	42
4 Transport in percolative magnetic environments	43
4.1 Percolative magnetic structures and the DCT	43
4.1.1 The flux function ϕ and the trapping effect in percolative structures	43
4.1.2 The stochastic properties of the flux function ϕ	46
4.2 The decorrelation trajectory approximation (DCT)	48
4.2.1 The subensemble decomposition of the Eulerian correlator	48
4.2.2 Averaged b -field in a subensemble	50
4.2.3 Conditional averages for perpendicular and parallel motion	52
4.2.4 The DCT approximation for $\mathcal{L}^{(0)}$ and the structure function $\mathcal{S}_0(t)$	57
4.2.5 The DCT approximation for $\mathcal{L}^{(1)}$	58
4.2.6 Properties of the $\mathcal{S}_i(t)$ structure functions in certain limits	63
4.3 Diffusion within the DCT approximation	64
5 Numerical simulations of the A-Langevin equation	69
5.1 Verification of the diffusion predictions for small Kubo numbers	69
5.1.1 Motivation for numerical analysis	69
5.1.2 Comparisons in the Rechester-Rosenbluth parameter regime	69
5.1.3 Verification of the regime with dominant stochastic fields	71
5.2 Numerical simulations in the percolation regime	73
5.2.1 Test of the predicted reduction of the diffusion rate for high Kubo numbers	73
5.2.2 Validation of the diffusion rates for high Kubo numbers and large Larmor radii	74
6 Conclusion	77
Appendix A	79
Appendix B	83
Appendix C	87
Appendix D	89
Bibliography	91

1 Introduction

1.1 Physical motivation

Transport phenomena are of major interest in several areas of modern physics and appear with great diversity in many applications of plasma physics. A very urgent topic is the heat and particle transport in magnetically confined plasmas used for thermonuclear fusion devices. These devices are intended to create an extremely hot and dense plasma which should be confined for sufficiently long times. Mainly two different concepts, the tokamak and the stellarator, are being proposed at the moment to reach this objective.

The necessary confinement of the plasma is achieved by magnetic fields that should keep the particles within a certain area of the machine [1]. From the beginning of the magnetic fusion research, the problem of particle transport is in the focus of theoretical and experimental investigations. In the basic concept of classical transport, a magnetic field preferentially binds the particles along the field line and reduces their ability to move in the perpendicular direction of the field. It is convenient to define transport quantities, namely the mean square displacement and the diffusion coefficient, and to distinguish the transport in perpendicular and parallel direction. Of course, in this classical picture large magnetic guiding fields reduce the perpendicular diffusion decisively. Collisions appear as an obstacle for the free motion along the field line and decrease the transport in parallel direction. Contrary they increase the ability of the particles to diffuse perpendicularly, because collisions transfer the particle to other field lines.

A reason for the extraordinary interest in the mechanisms of diffusion lies in the unexpected large losses caused by anomalous transport [2]. The term anomalous refers hereby to the strong deviation of the diffusion rate from the classical and neoclassical predictions [3], caused by fluctuations of the electric and magnetic field. To understand and control this type of transport is a major aim particularly with regard to the future designs of thermonuclear fusion reactors.

In the physics of fusion plasmas there is also an additional, very recent motivation for the investigation of particles in stochastic fields. Beneath the intrinsic perturbations of the magnetic field structure, which are more or less unavoidable because of errors in the coil arrangements of the devices, auxiliary coils are being added to existing configurations in several tokamaks [4]. These additional coils are an artificial source of stochasticity and generate magnetic fluctuations in order to control and observe the particle and heat loads on the wall. Examples can be found on the tokamaks Tore-Supra, DIII-D, and TEXTOR, and are being planned for JET.

The vast majority of works dedicated to anomalous transport starts with a Langevin type treatment, as can be found e.g. in [5], based solely on the guiding center assumption. In common fusion reactors the magnetic fields are sufficiently strong to assume infinitely small gyro-radii, at least for the electrons. The question remains in what way finite Larmor radii

influence the transport, especially in regions where the guiding center assumption fails. Indeed in tokamaks such areas can be found e.g. in the vicinity of hyperbolic points. Our central intention is the description of these finite Larmor radius effects by analytical and numerical means.

The knowledge of charged particle transport is also a long-standing problem in many astrophysical issues [6,7], such as low-energy cosmic ray penetration into the heliosphere, the transport of galactic cosmic rays in and out of the interstellar magnetic field, and the Fermi acceleration mechanism.

Galactic magnetic fields are parallel to the galactic disk and mostly aligned with the galactic spiral arms. The typical Larmor radius of a cosmic ray particle in this field is several orders smaller than the height of the galactic disk in which most of the solar systems are located. In astrophysical plasmas of this dimensions, collisions are neglected and from the classical theory cosmic ray particles may be expected to remain very effectively trapped within the disk. Observations do not agree with this picture. Cosmic rays are transported in perpendicular direction at several magnitudes higher than predicted.

Obviously a model based on entirely parallel magnetic fields is insufficient for a successful description of the cosmic rays. With a mean field in parallel direction, there have to be additional perpendicular components that enable the particles to leave the galactic plasma. These components are induced by nonlinearities of the galactic field and can be regarded as stochastic. It is also an intention of this work, to provide useful predictions of the diffusion that can be introduced into the models of cosmic rays. Magnetic fields occurring in the galaxy consist of very small guiding fields. Then it is required to include the complete gyration motion. One of the new important questions added from the astrophysical point of view is: What are the transport properties in stochastic magnetic fields when the mean field becomes small? The latter case is also realized in other astrophysical situations with random magnetic fields, e.g. the Earth magnetic field. In such plasmas with small guiding fields the Larmor radius effects become essential. Obviously in situations with mean fields smaller than the fluctuation amplitude, the stochastic component has to be regarded as the dominating one. For this case a completely new kind of approach is needed.

Despite the special interests in both, magnetic fusion plasmas and astrophysical plasmas, a general aspect of the transport in stochastic magnetic fields concerns the structure of the perturbation field. Due to the peculiar nature of the fluctuations, magnetic structures arise under certain circumstances and disrupt the displacement mechanisms of the particles. Fieldlines become trapped within areas of the magnetic flux, the so-called fluxtubes [6], and the transport is changed significantly.

1.2 Stochastic differential equations approach to anomalous transport

A common strategy to treat anomalous plasma transport is the use of kinetic theory, which primarily focusses on the analysis of the distribution function in phase space. The principle of this kind of description is to identify the state of the plasma, that is determined by a suitable number of macroscopical physical quantities, and to find the law of evolution, the kinetic equation of this state [5]. The advantage of the kinetic description is the possibility of a self-consistent model of the system, incorporating the alternating interactions between particles and fields. Typically the electromagnetic field is linked to the distribution function by applying the Maxwell equations. Within such an approach it is of course also possible to include the effects of magnetic fluctuations. Unfortunately, the distribution function may then contain a certain amount of stochasticity as it evolves now irregularly and randomly. Due to this extremely nonlinear character of the evolution equation, it is nearly impossible to use the kinetic approach for the transport quantities and one needs extensive numerical efforts for the treatment of fluctuating systems. Instead reduced and simpler models have become fashionable to describe such systems from a different point of view and on a substantially more practicable level of mathematical expense.

A more feasible way to find reliable predictions, especially for transport phenomena is based on the use of stochastic differential equations [8]. These are differential equations in which one or more terms are of stochastic nature. The solution of the equation is a stochastic value. This approach allows us to assume the magnetic field to be a random source. One has to abandon the self-consistent description here for the benefit of a more simple formulation. The loss of the complete interacting kinetic properties is expressed in the requirement to introduce a priori statistical information about the stochastic quantities in the differential equation. Despite this constraints, the approach with stochastic equations provides a highly efficient access to the analytical description of anomalous transport.

Modern fusion devices like tokamaks have a very special magnetic configuration containing toroidal and poloidal magnetic fields. The geometry of this fields is inhomogenous and curved, and a global analysis is very difficult to be incorporated. Fortunately the effect of the complex geometry often can be neglected for the involved model zones and the qualitative understanding of the underlying physical mechanisms of transport is studied in a standard slab configuration [9]: a guiding field in z -direction and fluctuations mainly in the perpendicular directions x and y .

Basically, three different stochastic quantities can be identified in our problem, the collisions, the magnetic fluctuations and, of course, the velocity of the particle. We use the stochastic differential equations approach based on the Accelerated-(A)-Langevin equation [5,10]. The name denotes that the origin of the equation is the Newton-Lorentz equation for the acceleration of a charged particle in a magnetic field $\mathbf{B} = B_0 (b_0 \mathbf{e}_z + \mathbf{b})$ with the stochastic component \mathbf{b} ,

$$\dot{\mathbf{u}} = \Omega \mathbf{u} \times (b_0 \mathbf{e}_z + \mathbf{b}) - \nu \mathbf{u} + \mathbf{a}. \quad (1.1)$$

Here $\Omega = ZeB_0/(mc)$ is the Larmor frequency, ν is the collision frequency and \mathbf{a} a white noise acceleration process. The latter is assumed as random acceleration with a δ -distributed correlation function. From this perspective a stochastic function like $\mathbf{a}(t)$ is not determined. It can only be described by its stochastic properties. A detailed introduction of (1.1) is presented in Sec. 2.

Another option to treat the topic theoretically starts from the Velocity-(V)-Langevin equations [11]. In strongly magnetized plasmas, charged particles move on gyration orbits around the field lines. Depending on the strength of the magnetic guiding as well as on the thermal velocities of the particles, the Larmor radius may be sufficiently small. Then it may be allowed to replace the exact position of a particle virtually by the position of the field line it gyrates along. In this approach one considers stochastic equations for guiding centers of test particles [9,10,11,12]. It approximates the A-Langevin equation for small gyro-radii. It can be derived from the A-Langevin equation by integration in time and application of the drift approximation, yielding

$$\begin{aligned}\frac{d\mathbf{r}_\perp}{dt} &= \mathbf{b} \eta_\parallel + \boldsymbol{\eta}_\perp, \\ \frac{dz}{dt} &= \eta_\parallel.\end{aligned}\tag{1.2}$$

These are the V-Langevin equations. Collisions are now introduced via the stochastic velocities $\boldsymbol{\eta}_\perp$ and η_\parallel . The V-Langevin equations are approximations and assume large (guiding) magnetic fields such that the guiding center picture becomes meaningful. Note that the stochastic component of the magnetic field is usually weak, i.e. the stochastic fields alone do not justify the drift approximation directly. Only if a strong confining magnetic field is additionally present, such as in tokamaks, the V-Langevin approach is justified. The same reason indicates that the V-Langevin equations are not suited for astrophysical applications.

In the present work, we concentrate on the solution of the A-Langevin equation. That invokes the stochastic equation of motion (1.1) for a single test particle. On the basis of the solution of the equation of motion one can calculate a velocity correlation function that leads to the diffusion tensor. Generally, the exact analytical solution of the problem is not. Nevertheless it is still possible to make some estimations in different limiting cases assuming that the perturbation of the magnetic field is weak.

The main assumptions of the present work are the following. First, we assume static magnetic disturbances and thereby neglect the electric force on the particles. This is justified as long as the propagation velocity of the magnetic fluctuations is small compared to the typical velocity of the particles. Furthermore we assume Gaussian Eulerian correlation functions (fulfilling the constraint $\text{div } \mathbf{B} = 0$).

1.3 Mean squared displacement and the diffusion coefficient

Transport can be systematically described in terms of two quantities: the diffusion coefficient and the mean square displacement (MSD), that is e.g. the quadratic perpendicular displacement, averaged over a given ensemble of realizations,

$$\langle \delta x^2(t) \rangle = \langle [x(t) - \langle x(t) \rangle]^2 \rangle = \langle x^2(t) \rangle - \langle x(t) \rangle^2. \quad (1.3)$$

With the MSD we divide transport roughly into three different regimes, distinguished by the dependence of the MSD on time,

$$\langle \delta x^2(t) \rangle \sim t^\alpha. \quad (1.4)$$

For $\alpha < 1$ the transport is subdiffusive. The MSD tends asymptotically to a constant value and transport in the corresponding direction breaks down. Diffusive behaviour is given for $\alpha = 1$. If this kind of transport prevails and the MSD is asymptotically proportional to time, a constant D may be introduced as

$$\langle \delta x^2(t) \rangle = 2Dt, \quad (1.5)$$

which we call the asymptotic diffusion coefficient. Similarly a quantity called running diffusion coefficient is defined as $D(t) = \frac{1}{2} \frac{d}{dt} \langle \delta x^2(t) \rangle$. In a subdiffusive situation $D(t)$ would vanish with increasing time t . At last, for $\alpha > 1$ the transport is called superdiffusive. A typical example of such a domain of diffusion is the ballistic motion of particles.

1.4 Lagrangian and Eulerian correlations

The dynamical law that governs the motion of the particles, in our case namely the A-Langevin equation (1.1) should lead to the MSD and the diffusion coefficient. The solution of the A-Langevin equation is the velocity of a particle. An ensemble averaged product of two particle velocities at two different points in space is called Eulerian velocity correlation function (we will also refer to correlation functions as correlations, correlators, or the Eulerian) and can be directly deduced from the solution of (1.1). Eulerian correlations are well established quantities [10,11]. They can often be calculated directly for a given problem and even their measurement is possible.

Another, much more complicated quantity is directly related to the transport properties we are interested in: the Lagrangian velocity correlation function [13,14]. Contrary to the Eulerian correlation, it is calculated as the averaged product of two velocities of the particle, that lie exactly on the trajectory at two times. The spatial dependence has been replaced by the trajectory and the correlation is only time-dependent. If the correlation function is known, the Green-Kubo formalism provides an elegant way to relate it with the MSD in form of an ordinary differential equation in time.

One of the major difficulties we are confronted with in this work is the derivation of the Lagrangian correlators. An exact calculation of this quantity would require the evaluation of the dynamical equation (1.1) for each realization of the stochastic terms, which is an impossible task. Estimates are needed to find a relation between Lagrangian and Eulerian correlations.

We will discuss two different approximations in order to find expressions for the Lagrangian velocity correlators. The first one, well-known throughout various areas of theoretical turbulence research, is the Corrsin approximation [13,15]. It provides a very intuitive and straightforward way to derive the Lagrangian correlator from the corresponding Eulerian. Unfortunately it is restricted to a specific domain of turbulence, defined in terms of the Kubo number [17,18], which is defined as the ratio of the distance which a particle travels during an autocorrelation time and the correlation distance. This is expressed in terms of the fluctuating velocity $V = \beta\lambda_{\parallel}/(b_0\tau_c)$, the decorrelation time τ_c and the perpendicular correlation length λ_{\perp} ,

$$\kappa = \frac{V\tau_c}{\lambda_{\perp}} = \frac{\beta\lambda_{\parallel}}{b_0\lambda_{\perp}}. \quad (1.6)$$

Here β is the fluctuation amplitude, b_0 the dimensionless strength parameter of the guiding field, λ_{\parallel} the parallel correlation length of the magnetic field and λ_{\perp} the perpendicular correlation length. The Kubo number is a dimensionless parameter, which we use frequently to specify the degree of magnetic turbulence. High Kubo numbers characterize systems with strong turbulence. With λ_{\parallel} and λ_{\perp} two different length scales are introduced that have decisive impact, not only on the transport itself, but also on the choice of the method required to find the Lagrangian correlator. The second way to find the Lagrangian correlation is called the decorrelation trajectory method (DCT) [18,19,20]. It is a rather new and more complex method than the Corrsin approximation, which includes effects of the magnetic structure into the correlator. The DCT has no restrictions for the values of the Kubo number.

1.5 Percolation structures of the flux function

A very recent topic discussed in the context of anomalous diffusion is the occurrence of certain magnetic flux structures [6] that can change the transport behaviour decisively [20,21,22]. The perturbations can be regarded to be generated from a stochastic flux function. In some cases that are related to Kubo numbers greater than one, the flux function gets percolative contours [23]. Additionally in such a case the field lines are forced to move around this contour lines [24]. This can lead to the very interesting fact, that a certain number of field lines are trapped within the percolative map of the flux function and can no longer contribute to transport. On the other hand, larger Larmor radii help the particles to detach from these field lines more efficiently. The method used in connection with this systems is the DCT mentioned in 1.4, developed by Vlad et al. in [20].

Since neither a complete review of the percolation regime on the basis of stochastic differential equations was not discussed in detail nor a consequent comparison between the Corrsin approximation and the DCT was not done so far, it is a central intention of our work to provide an analytical relation between the Corrsin correlation functions and the DCT correlation functions, as well as an in depth investigation of the combined effects of percolation structures and finite Larmor radii.

1.6 Overview of this work

The phenomenon of anomalous transport has been under investigation for a long time. Several previous works covered this topic by concentrating on guiding center motions alone. For any rigorous description and understanding of anomalous transport in plasmas, it is necessary to include the complete motion of the particles. A detailed analysis starting from the complete A-Langevin equation was not done so far, but appears unavoidable as we are primarily interested in the particle transport and not in the deviation of neighboring field lines. Furthermore, we want to identify especially the influence of the particle gyration around the field line, namely the Larmor radius effect.

Consequently a couple of important questions come into the focus of interest:

How do the fluctuations contribute to the diffusion of the particles?

What is the influence of the Larmor radius on the diffusion?

What happens with the transport if a mean guiding field is not present?

Is the diffusion affected by the percolative structure of the perturbation field?

Throughout the following investigations we will answer these questions and give analytical as well as numerical descriptions of the anomalous transport in stochastic plasmas.

This work is composed of 6 sections and is organized as follows:

In Sec. 2 we solve the A-Langevin equation with a sequence of transformations and derive an explicit expression for the velocity of a particle that experiences collisions and the effects of the perturbative magnetic field. From this expression we calculate unaveraged correlation functions, namely the products of velocities at two different times. The Green-Kubo formalism is presented and illustrated with the example of classical transport. With the assumption of strong guiding fields a series expansion of the correlation function is obtained, where the zeroth order represents the guiding center motion and the higher orders correspond to the Larmor radius effects.

Section 3 deals with the diffusion regimes for small Kubo numbers. The Corrsin approximation is explained and applied. It transfers the correlation function (derived in Sec. 2) to Lagrangian coordinates. Using the Green-Kubo formalism we discuss the diffusion regimes of anomalous transport analytically. First, the quasilinear limit is presented and the corresponding Larmor radius correction is determined. Here we show in detail how estimates for the diffusion can be derived. Another, somehow artificial regime, the subdiffusive situation is reviewed, which regards to a case where the diffusion coefficient has a zero asymptotic value and the transport stops. The well-known Rechester-Rosenbluth diffusion scaling follows from the present analysis. By numerical simulations of the Green-Kubo differential equation we integrate finite Larmor radius effects and discuss their impact on the diffusion. Two further regimes due to Kadomtsev and Pogutse are also shown to be reproduced by the A-Langevin approach. The last part of Sec. 3 is dedicated to the transport in dominant stochastic magnetic fields, where no mean field is present. A three-dimensional stochastic perturbation alone is considered in the A-Langevin equation. We give also analytical formulas for the diffusion coefficient and the MSD in such a scenario.

Section 4 extends our insights to high Kubo numbers. The latter correspond to certain magnetic structures that have great impact on the diffusion. We give a short introduction on the stochasticity of the flux function and on the percolative structures that are imposed for high Kubo numbers. The occurrence of flux tubes is demonstrated and their connection with the diffusion rate is explained. An involved method, the decorrelation trajectory approximation, is used to derive enhanced Lagrangian correlation functions that contain the effects of percolative flux structures. The explicit analytical relation between Corrsin correlators and DCT correlators is presented. Finite Larmor radius corrections are included into the analysis and the effects of the magnetic structure in combination with finite Larmor radii is investigated.

A numerical verification of the efforts of Secs. 3 and 4 is presented in Sec. 5. Using a Monte-Carlo simulation code of the A-Langevin equation we confirm our analytical predictions by the exact computer model.

The work is concluded in Sec. 6 by a summary of the efforts and results. We also give a short outlook for future activities on the topic of anomalous transport.

2 Velocity correlations based on the A-Langevin equation

2.1 The velocity of a particle in a stochastic magnetic field with collisions

2.1.1 General magnetic geometry and the description with the A-Langevin equation

In general, we consider a magnetic field of the form

$$\mathbf{B} \equiv B_0 (b_0 \mathbf{e}_z + b_x \mathbf{e}_x + b_y \mathbf{e}_y + b_z \mathbf{e}_z). \quad (2.1)$$

composed of a guiding field $B_0 b_0$ in z -direction and a perturbation field \mathbf{b} . Here the parameter b_0 and the vector \mathbf{b} are dimensionless. The factor B_0 takes care of the dimension of the magnetic field and will sometimes be referred to as magnetic field reference strength. We call the x - and y -components of $\mathbf{b} = (b_x, b_y, b_z)$ the perpendicular components.

Obviously we have to distinguish different realisations of the magnetic environment:

- The first case corresponds to a situation with a strong magnetic guiding field, $b_0 \gg b_z$. We can neglect the fluctuation in the z -direction and restrict to perpendicular fluctuations. For tokamak applications it will be appropriate to assume such a strong field. The B -Field is then proposed in the simpler form,

$$\mathbf{B} \equiv B_0 (b_0 \mathbf{e}_z + b_x \mathbf{e}_x + b_y \mathbf{e}_y). \quad (2.2)$$

In this case, it is expected that results derived from the A-Langevin equation will agree with those from the V-Langevin equation to the lowest order in the Larmor radius.

- The second situation is defined by a weak magnetic guiding field $b_0 \ll 1$. In that case we have only contributions of the stochastic field components and we will call it the vanishing guiding field regime. The B -Field is given as

$$\mathbf{B} \equiv B_0 (b_x \mathbf{e}_x + b_y \mathbf{e}_y + b_z \mathbf{e}_z). \quad (2.3)$$

Guiding center theories do not cover this situation [7].

We define a gyro-frequency unit $\Omega = \frac{Ze B_0}{m c}$. Here m is the test-particle (ion or electron) mass and Ze is the total charge. With this definition, the typical Larmor frequency is given, e.g. for the guiding field by $\Omega_L = \Omega b_0$. The Larmor radius is defined as $\rho_L = v_t / (\Omega b_0 + \Omega |\mathbf{b}|) \approx v_t / (\Omega b_0)$, introducing the thermal velocity v_t .

The A-Langevin equation (ALE) is the equation of motion for a single particle, which experiences the effects of the magnetic field and its stochastic contributions as well as random collisions $\mathbf{a}(t)$,

$$\dot{\mathbf{u}}(t) = \frac{Ze}{mc} \mathbf{u}(t) \times \{\mathbf{B}_0[b_0 \mathbf{e}_z + \mathbf{b}(t)]\} - \nu \mathbf{u}(t) + \mathbf{a}(t). \quad (2.4)$$

Similar to the theory of Brownian motion [8], a term characterized by the parameter ν mimicks the friction caused by the collisions. So far we will keep the most general form of the B -Field (2.1). The approach with stochastic equations requires additional postulates on the statistics of the random processes that are involved, so our mathematical description has to be completed by suitable assumptions on the averages and correlations of the initial velocities, the random collisions and the perturbation field.

Initial velocities in all direction obey a three dimensional Gaussian distribution,

$$P(\mathbf{u}_0) = \pi^{-3/2} v_t^{-3} \exp\left(-\frac{u_0^2}{v_t^2}\right),$$

so the average

$$\langle \mathbf{u}_0 \rangle_{u_0} \equiv \int \mathbf{u}_0 P(\mathbf{u}_0) d\mathbf{u}_0 = 0$$

vanishes and $\langle u_0^2 \rangle = v_t^2/2$. v_t is the thermal velocity of the particles. Here we also introduced a common bracket notation for the average. We denote the brackets with an index regarding to the stochastic variable which is averaged.

The white noise collisional events are modelled by a sharp δ -distributed correlation

$$\langle \mathbf{a}(t) \rangle = 0, \quad \langle \mathbf{a}(t_1) \mathbf{a}(t_2) \rangle = \mathbf{1} A \delta(t_1 - t_2), \quad (2.5)$$

introducing a free constant A . The assumption of the δ -correlation is a quite usual way to describe events with instantaneous correlation and which are uncorrelated everywhere else. We will use the free constant to ensure that the correlation function is a function of the time difference $\tau = t_1 - t_2$ and therefore stationary.

The stochastic properties of the magnetic field are defined by

$$\langle \mathbf{b}(t_1) \otimes \mathbf{b}(t_2) \rangle = \beta^2 \mathcal{L}_M(\tau), \quad \tau = t_1 - t_2, \quad (2.6)$$

where we introduced the Lagrangian correlation function of the magnetic field. That is the correlation of the stochastic field components determined at two different times t_1 and t_2 .

The matrix \mathcal{L}_M is principally unknown [11] and it is required that the magnetic field correlation is stated in the co-moving frame of reference, the Lagrangian coordinates. We dedicated Secs. 3 and 4 to find appropriate expressions for the Lagrangian correlation functions. The average of the magnetic field vanishes, $\langle \mathbf{b}(t) \rangle = 0$.

2.1.2 The solution of the A-Langevin equation

A couple of mathematical tools are helpful for the solution the ALE. Especially the rotational matrices $R_i(\alpha)$, a base of the $SO(3)$ group,

$$R_1 \equiv \begin{pmatrix} 1 & 0 & 0 \\ 0 & \cos \alpha & -\sin \alpha \\ 0 & \sin \alpha & \cos \alpha \end{pmatrix}, R_2 \equiv \begin{pmatrix} \cos \alpha & 0 & \sin \alpha \\ 0 & 1 & 0 \\ -\sin \alpha & 0 & \cos \alpha \end{pmatrix}, R_3 \equiv \begin{pmatrix} \cos \alpha & -\sin \alpha & 0 \\ \sin \alpha & \cos \alpha & 0 \\ 0 & 0 & 1 \end{pmatrix}, \quad (2.7)$$

and their infinitesimal generators

$$L_1 = \begin{pmatrix} 0 & 0 & 0 \\ 0 & 0 & -1 \\ 0 & 1 & 0 \end{pmatrix}, \quad L_2 = \begin{pmatrix} 0 & 0 & 1 \\ 0 & 0 & 0 \\ -1 & 0 & 0 \end{pmatrix}, \quad L_3 = \begin{pmatrix} 0 & -1 & 0 \\ 1 & 0 & 0 \\ 0 & 0 & 0 \end{pmatrix}, \quad \mathbf{L} \equiv \begin{pmatrix} L_1 \\ L_2 \\ L_3 \end{pmatrix}. \quad (2.8)$$

provide an elegant way to rewrite the vector-product in the ALE using the identity $\mathbf{a} \times \mathbf{b} = -(\mathbf{b} \mathbf{L}) \mathbf{a}$,

$$\dot{\mathbf{u}}(t) = -\Omega b_0 L_3 \mathbf{u} - \Omega \mathbf{b}(t) \mathbf{L} \mathbf{u}(t) - \nu \mathbf{u}(t) + \mathbf{a}(t).$$

Obviously the constant factors can be handled easily and by substituting,

$$\mathbf{u}(t) = e^{-\Omega_0 b_0 L_3 t - \nu t} \tilde{\mathbf{u}}(t) = R^- \tilde{\mathbf{u}}(t),$$

one obtains a simpler form of the ALE,

$$\dot{\tilde{\mathbf{u}}}(t) = -R^+ \Omega_0 \mathbf{b} \mathbf{L} R^- \tilde{\mathbf{u}} + R^+ \mathbf{a}(t).$$

The operator R^\pm makes use of the rotational matrices and is given by $R^\pm(t) \equiv R_3(\pm \Omega_0 b_0 t) e^{\pm \nu t}$. We introduce the operator V (see also App. A.1), defined by

$$V = -\Omega_0 R^+ (\mathbf{b} \mathbf{L}) R^-, \quad (2.9)$$

as well as $\tilde{\mathbf{a}} = R^+ e^{\nu t} \mathbf{a}(t)$ and recover the typical differential equation of the Brownian motion problem,

$$\dot{\tilde{\mathbf{u}}} = V \tilde{\mathbf{u}} + \tilde{\mathbf{a}},$$

yielding the solution

$$\tilde{\mathbf{u}}(t) = G(t) \mathbf{u}_0 + \int_0^t G(\tau, t) \tilde{\mathbf{a}}(\tau) d\tau. \quad (2.10)$$

The latter is given in terms of the Green's function $G(t_2, t_1)$, [25]

$$G(t_2, t_1) \equiv T \left[\exp \left\{ \int_{t_2}^{t_1} V(q) dq \right\} \right], \quad G(t_1) \equiv G(0, t_1), \quad (2.11)$$

where T is the time-ordering operator. All necessary details of the operator V are presented in Appendix A.1. In the original variables, one obtains

$$\mathbf{u}(t) = R^- G(t) \mathbf{u}_0 + R^- \int_0^t G(\tau, t) R^+ \mathbf{a}(\tau) d\tau. \quad (2.12)$$

Three fundamental influences dominate the motion of the particle: the gyration around the field lines, the random collisions and the fluctuating perturbation component of the magnetic field. A special solution exists when this last perturbation is not present $\mathbf{b} = 0$,

$$\boldsymbol{\eta}(t) \equiv \mathbf{u}(t) |_{\mathbf{b}=0} = R^- \mathbf{u}_0 + R^- \int_0^t R^+ \mathbf{a}(\tau) d\tau. \quad (2.13)$$

To mark the importance of this special solution for vanishing perturbation fields, we denote it with the letter $\boldsymbol{\eta}$, distinguishing again the two possible orientations $\boldsymbol{\eta}_\perp = (\eta_x, \eta_y)$ and η_z . The average of this stochastic quantity is zero, $\langle \langle \boldsymbol{\eta} \rangle_{\mathbf{u}_0} \rangle_{\mathbf{a}} = 0$. The velocities η_i are equivalent to the random collisional velocities that appear in the V-Langevin [10].

One further step is the calculation of the trajectory of a single particle, which requires an additional integration in time,

$$\mathbf{R}(t) = \mathbf{r}_0 + \int_0^t \mathbf{u}(t') dt'. \quad (2.14)$$

$\mathbf{R}(t)$ is the trajectory vector and should not be confused with the rotational matrices. For vanishing perturbations the condition

$$\lim_{\mathbf{b} \rightarrow 0} \mathbf{R}(t) = \mathbf{R}^{(0)}(t), \quad (2.15)$$

holds, where $\mathbf{R}^{(0)}$ is given by the classical damped helical particle motion,

$$\mathbf{R}^{(0)}(t) = \mathbf{r}_0 + \int_0^t \boldsymbol{\eta}(t') dt'. \quad (2.16)$$

Figure 2.1 shows the trajectory of a particle that experiences collisions and magnetic fluctuations. The gyro-motion is extremely disturbed by the stochastic perturbations. Collisions relocate the particle at once in form of an spontaneous random acceleration and the perpendicular fluctuations lead to additional deviations from the unperturbed orbit.

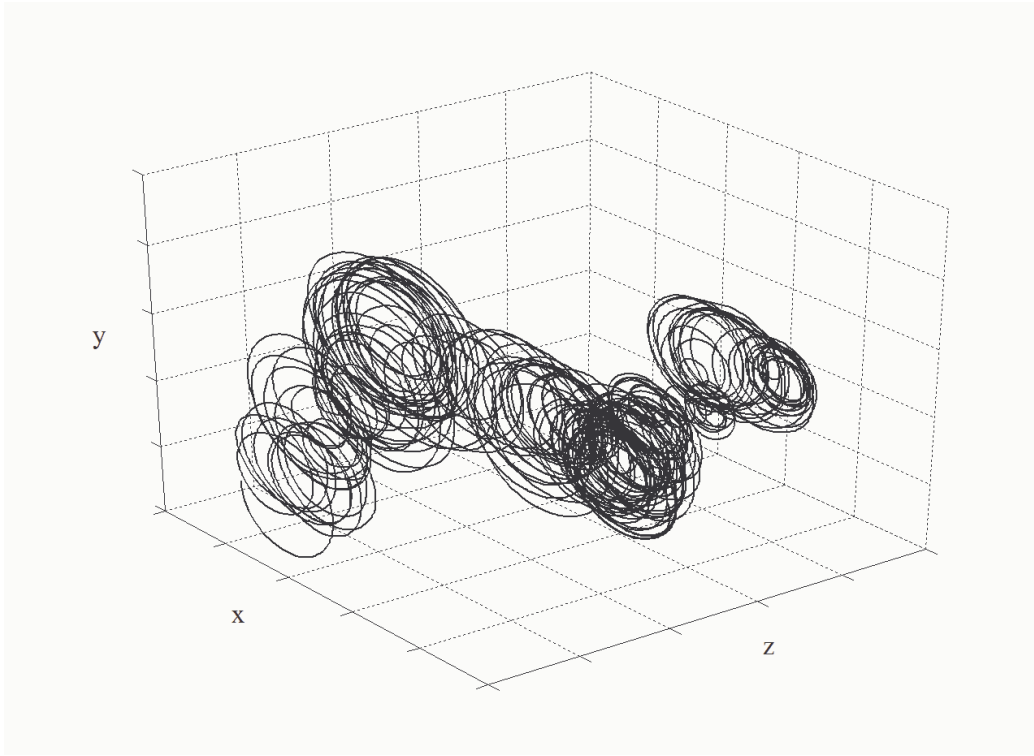


Figure 2.1: Sketch of a particle trajectory, undergoing collisions in the presence magnetic fluctuations.

We make now contact between the unperturbed and the perturbed solution of the ALE. Solving eqs. (2.12) and (2.13) for \mathbf{u}_0 , we can identify the influence of the perturbation field in form of an propagation equation,

$$\mathbf{u}(t) = R^- G(0, t) R^+ \boldsymbol{\eta} - R^- G(0, t) \int_0^t R^+ \mathbf{a}(\tau) d\tau + R^- \int_0^t G(\tau, t) R^+ \mathbf{a}(\tau) d\tau. \quad (2.17)$$

which essentially simplifies by the cancellation of the last two terms on the right hand side,

$$\mathbf{u}(t) = R^- G(0, t) R^+ \boldsymbol{\eta}(t). \quad (2.18)$$

The perturbation field \mathbf{b} acts as propagator on $\boldsymbol{\eta}$. All effects of \mathbf{b} are contained in G . For small values $\beta \ll b_0$, we can expand G in a power series

$$G(t_2, t_1) \approx 1 + \int_{t_2}^{t_1} V(q) dq, \quad \text{für } t_1 > t_2, \quad (2.19)$$

and use the properties of V from the previous Sec.,

$$\mathbf{u}(t) = \boldsymbol{\eta}(t) + \int_0^t V(\tau - t, t) \boldsymbol{\eta}(\tau) d\tau. \quad (2.20)$$

The latter formula is the starting point for our derivation of the velocity correlation functions. It is not applicable for vanishing guiding fields, because the condition $\beta \ll b_0$ is not valid any more. In this case we have to use the more general Eq. (2.18). The relation between the velocity $\mathbf{u}(t)$ of the A-Langevin equation and the collisional velocities $\boldsymbol{\eta}$ was not derived in any previous work.

2.2 Velocity products from the A-Langevin solution

2.2.1 The Green-Kubo formalism as link between correlation function and transport

We are interested in the macroscopic transport properties of ensembles with a large number of particles. The intention of our efforts is therefore to derive suitable descriptions of the mean square displacement $\langle \delta r_i^2(t) \rangle$ and the running diffusion coefficient $D(t)$, which are related by

$$\frac{1}{2} \frac{d}{dt} \langle \delta r_i^2(t) \rangle = D(t). \quad (2.21)$$

This relation can be deduced in the diffusive regimes from the VCF in Lagrangian coordinates. Once the Lagrangian correlation function (LCF) is known, the mean square displacement (MSD) and the running diffusion coefficient $D(t)$ are typically obtained from the Green-Kubo formula,

$$\frac{d^2}{dt^2} \langle \delta r_i^2(t) \rangle = 2 \frac{d}{dt} D(t) = \langle u_i(t_1) u_i(t_2) \rangle. \quad (2.22)$$

This equation should be solved with the initial conditions $D(0) = 0$ and $\langle \delta r_i(0) \rangle = 0$. In this formalism, the problem of the determination of transport properties has been reduced to the problem of finding the correct Lagrangian correlation function.

It should be noted, that the Green-Kubo formula is the one of the most essential equations for our analysis. Further details on the formalism can be found in [5].

2.2.2 Classical transport and the classical diffusion coefficients

We summarize the results from the Green-Kubo formalism for classical transport. The correlations of the velocity $\boldsymbol{\eta}$ with the stochastic properties of the collisions \boldsymbol{a} , are given by

$$\begin{aligned} \langle \boldsymbol{\eta}_\perp(t_1) \boldsymbol{\eta}_\perp(t_2) \rangle_\perp &= \frac{v_t^2}{2} e^{-\nu|t_1-t_2|} \cos(\Omega b_0 |t_1 - t_2|), \\ \langle \boldsymbol{\eta}_\parallel(t_1) \boldsymbol{\eta}_\parallel(t_2) \rangle_\parallel &= \frac{v_t^2}{2} e^{-\nu|t_1-t_2|}. \end{aligned} \quad (2.23)$$

Details on the calculation are given in App. A.2. The constant $A = \nu v_t^2$ is determined by the restriction, that the correlation function should only depend on the time difference $\tau = |t_1 - t_2|$. Otherwise an unphysical dependence on the absolute times t_1 or t_2 would occur. Finally the MSD and the diffusion coefficient are completely determined by the velocity correlation functions and derived by the Green-Kubo formula. The integration is straightforward and yields the following asymptotical results for classical transport,

$$\langle \delta x^2(t) \rangle = \frac{v_t^2}{v^2 + \Omega^2 b_0^2} vt = 2 \chi_{\perp} t, \quad \langle \delta z^2(t) \rangle = \frac{v_t^2}{v} t = 2 \chi_{\parallel} t. \quad (2.24)$$

Here the classical diffusion coefficients are defined as

$$\chi_{\perp} = \frac{v_t^2 v}{2(v^2 + \Omega^2 b_0^2)} \approx \frac{v_t^2 v}{2\Omega^2 b_0^2}, \quad \chi_{\parallel} = \frac{v_t^2}{2v}. \quad (2.25)$$

With the information about the classical transport data, Wang et al. suggested in [11] a suitable approximation of $\boldsymbol{\eta}_{\perp}$, to take care of the difficult oscillating terms induced by Ωb_0 ,

$$\langle \boldsymbol{\eta}_{\perp}(t_1) \boldsymbol{\eta}_{\perp}(t_2) \rangle_{\perp} = \chi_{\perp} v e^{-\nu|t_1-t_2|}, \quad \langle \eta_{\parallel}(t_1) \eta_{\parallel}(t_2) \rangle_{\parallel} = \chi_{\parallel} v e^{-\nu|t_1-t_2|}. \quad (2.26)$$

In further derivations it will be convenient to use these correlation functions. Of course correlations between different directions vanish, e.g. $\langle \eta_x(0) \eta_y(t) \rangle_{\perp} = 0$.

2.2.3 Velocity correlation functions in the limit of strong guiding fields

Our observations of disturbed orbits of the trajectories motivate the question, how magnetic fluctuations do contribute to the transport of the particles. So we extend the ideas of the previous section and include magnetic fluctuations. The velocity products for strong guiding fields are obtained from the solution (2.20),

$$\begin{aligned} \mathbf{u}(t_1) \otimes \mathbf{u}(t_2) &= \boldsymbol{\eta}(t_1) \otimes \boldsymbol{\eta}(t_2) \\ &+ \int_0^{t_1} V(\tau_1 - t_1, \tau_1) \boldsymbol{\eta}(\tau_1) d\tau_1 \otimes \int_0^{t_2} V(\tau_2 - t_2, \tau_2) \boldsymbol{\eta}(\tau_2) d\tau_2. \end{aligned} \quad (2.27)$$

They will also be referred to as correlation function (or to be more precisely, unaveraged correlation function). In Appendix A.1 we present the entries of the matrix V and some useful properties. Substituting the V_{ij} we immediately find the perpendicular correlation

$$\begin{aligned} u_x(t_1) u_x(t_2) &= \eta_x(t_1) \eta_x(t_2) \\ &+ \Omega^2 \eta_z(t_1) \eta_z(t_2) \int_0^{t_1} \{ \sin[\Omega b_0(\tau_1 - t_1)] b_x(\tau_1) + \cos[\Omega b_0(\tau_1 - t_1)] b_y(\tau_1) \} d\tau_1 \\ &\times \int_0^{t_2} \{ \sin[\Omega b_0(\tau_2 - t_2)] b_x(\tau_2) + \cos[\Omega b_0(\tau_2 - t_2)] b_y(\tau_2) \} d\tau_2 \\ &+ \Omega^2 \eta_z(t_1) \eta_z(t_2) \int_0^{t_1} \int_0^{t_2} b_z(\tau_1) b_z(\tau_2) d\tau_1 d\tau_2. \end{aligned} \quad (2.28)$$

and for the parallel component

$$\begin{aligned}
u_z(t_1) u_z(t_2) &= \eta_z(t_1) \eta_z(t_2) \\
&+ \Omega^2 \eta_x(t_1) \eta_x(t_2) \int_0^{t_1} \{-\sin[\Omega b_0(\tau_1 - t_1)] b_x(\tau_1) - \cos[\Omega b_0(\tau_1 - t_1)] b_y(\tau_1)\} d\tau_1 \\
&\quad \times \int_0^{t_2} \{-\sin[\Omega b_0(\tau_2 - t_2)] b_x(\tau_2) - \cos[\Omega b_0(\tau_2 - t_2)] b_y(\tau_2)\} d\tau_2 \\
&+ \Omega^2 \eta_y(t_1) \eta_y(t_2) \int_0^{t_1} \{\cos[\Omega b_0(\tau_1 - t_1)] b_y(\tau_1) - \sin[\Omega b_0(\tau_1 - t_1)] b_x(\tau_1)\} d\tau_1 \\
&\quad \times \int_0^{t_2} \{\cos[\Omega b_0(\tau_2 - t_2)] b_y(\tau_2) - \sin[\Omega b_0(\tau_2 - t_2)] b_x(\tau_2)\} d\tau_2.
\end{aligned} \tag{2.29}$$

Note the important fact that the two expressions (2.28) and (2.29) coincide for $b_0 \rightarrow 0$. Without the guiding field, there is no preferred direction, and the transport coefficients for parallel and perpendicular transport are evidently equal. In [7] this tendency was observed numerically. It is an essential advantage of the A-Langevin approach to include this limiting case consistently. Any method based on the guiding center assumption fails to describe this transition.

Using the approximation method for large b_0 sketched in Appendix A.3, we find the functions

$$\begin{aligned}
u_x(t_1) u_x(t_2) &= \eta_x(t_1) \eta_x(t_2) \\
&+ \frac{1}{b_0^2} \eta_z(t_1) \eta_z(t_2) b_y(t_1) b_y(t_2) + \frac{1}{\Omega^2 b_0^4} b_x'(t_1) b_x'(t_2) + \mathcal{O}(\Omega^{-4} b_0^{-6}),
\end{aligned} \tag{2.30}$$

and

$$\begin{aligned}
u_z(t_1) u_z(t_2) &= \eta_z(t_1) \eta_z(t_2) + [\eta_x(t_1) \eta_x(t_2) + \eta_y(t_1) \eta_y(t_2)] \\
&\times \left\{ \frac{1}{b_0^2} b_y(t_1) b_y(t_2) + \frac{1}{\Omega^2 b_0^4} b_x'(t_1) b_x'(t_2) \right\} + \mathcal{O}(\Omega^{-4} b_0^{-6}).
\end{aligned} \tag{2.31}$$

This case corresponds to the situation $b_{x,y} \gg b_z$, so the influence of the z -components of the perturbation field can be neglected. The velocity correlation functions still require averaging with respect to the stochastic variables,

$$\begin{aligned}
& \langle \langle \langle u_x(t_1) u_x(t_2) \rangle_{\mathbf{b}} \rangle_{\perp} \rangle_{\parallel} = \langle \eta_x(t_1) \eta_x(t_2) \rangle_{\perp} \\
& + \frac{1}{b_0^2} \langle \eta_z(t_1) \eta_z(t_2) \langle \langle b_y(t_1) b_y(t_2) \rangle_{\mathbf{b}} \rangle_{\perp} \rangle_{\parallel} \\
& + \frac{1}{\Omega^2 b_0^4} \langle \eta_z(t_1) \eta_z(t_2) \langle \langle b_x'(t_1) b_x'(t_2) \rangle_{\mathbf{b}} \rangle_{\perp} \rangle_{\parallel} + \mathcal{O}(\Omega^{-4} b_0^{-6}).
\end{aligned} \tag{2.32}$$

The influences of the magnetic perturbations appear explicitly. We shall call the contributions of the perturbations the anomalous contribution, thereby distinguishing between the classical transport already discussed in the previous section and the anomalous transport due to the magnetic fluctuations. The fluctuations are stochastically determined by the products $\langle b_i(t_1) b_j(t_2) \rangle$ and $\langle b_i'(t_1) b_j'(t_2) \rangle$. We identify the anomalous parts (denoted with the symbol \mathcal{L} for Lagrangian),

$$\langle \langle \langle u_x(t_1) u_x(t_2) \rangle_{\mathbf{b}} \rangle_{\perp} \rangle_{\parallel}^{\text{AN}} \equiv \mathcal{L}^{(0)} + \mathcal{L}^{(1)}. \tag{2.33}$$

designating the functions $\mathcal{L}^{(0)}$ and $\mathcal{L}^{(1)}$,

$$\mathcal{L}^{(0)}[\langle \delta r_i^2(t) \rangle, \psi_{\parallel}, \varphi_{\parallel}, t] = \frac{1}{b_0^2} \langle \eta_z(t_1) \eta_z(t_2) \langle \langle b_y(t_1) b_y(t_2) \rangle_{\mathbf{b}} \rangle_{\perp} \rangle_{\parallel}, \tag{2.34}$$

$$\mathcal{L}^{(1)}[\psi_{\parallel}, \varphi_{\parallel}, \psi_{\perp}, \varphi_{\perp}, t] = \frac{\rho_L^2}{v_i^2 b_0^2} \langle \eta_z(t_1) \eta_z(t_2) \langle \langle b_x'(t_1) b_x'(t_2) \rangle_{\mathbf{b}} \rangle_{\perp} \rangle_{\parallel}. \tag{2.35}$$

A specific order of averages occurs. The average of the parallel collisional velocities, covered by η_z , is especially involved since we must also include all dependencies on η_z remaining in the perturbation fields \mathbf{b} . The first term on the right hand side of (2.33), $\mathcal{L}^{(0)}$, does not include any effects of the finite Larmor radii. Correlation functions similar to $\mathcal{L}^{(0)}$ were derived in [12] and in [17,18,19] with the V-Langevin framework based on a pure guiding center perspective.

First order Larmor radius effects are included in the second term $\mathcal{L}^{(1)}$ (all higher order corrections can also be found by the method sketched in Appendix A.3). At this stage we are left with the problem to insert appropriate expressions for the Lagrangian b -field correlations, respectively the correlations for the derivations of the b -fields.

Lagrangian correlation functions appear as the the central ingredient for the description of anomalous transport. These are correlations of the velocities evaluated at two points along the trajectory. An exact calculation is impossible, because it would be necessary to solve the dynamical equation (2.4) for all realizations of the stochastic quantities.

Estimates are required to find a relation [16] between the Lagrangian and the Eulerian correlations. We will therefore proceed with an intuitive method that helps us to approximate the Lagrangian correlations.

3 Transport for small Kubo numbers

3.1 The Corrsin approximation for Lagrangian correlation functions

3.1.1 The Lagrangian coordinate system

In the Eulerian frame of reference a certain physical value of a particle, let it be $\alpha(\mathbf{r}, t)$, is given as function of its position and the time. Such coordinates have a fixed origin, for example realized in the laboratory system. Lagrangian coordinates are given within the co-moving frame of reference. The particles center is the origin of the coordinates. Obviously both systems are connected with each other by the trajectory of the particle, which means the value α in the Eulerian domain leads to the value $\lambda(t) = \alpha(\mathbf{R}(t), t)$ in the Lagrangian domain. The transformation is in principle,

$$\lambda(t) = \alpha[\mathbf{R}(t), t] = \int_{-\infty}^{\infty} d\mathbf{r} \delta(\mathbf{r} - \mathbf{R}(t)) \alpha(\mathbf{r}, t), \quad (3.1)$$

as long as the complete trajectory $\mathbf{R}(t)$ is known. This imposes the following problem: the integration of the Green-Kubo formula becomes implicit.

3.1.2 Corrsin's independence hypothesis

The situation becomes notably more complicated whenever the involved variables are stochastic. Averaging methods have to be applied similar to the ones presented in the introductory section. Of course, the trajectory becomes stochastic as well and the transformation (3.1) has to be evaluated in a different way. Especially the average over the fluctuating magnetic field requires an advanced approach. A widely adopted approximation due to Corrsin [13] assumes that the correlation function and the trajectory can be averaged independently. Details of this procedure can also be found in [15]. The approximation was confirmed and applied in many works of Balescu et al. [10,11]. Saffman et al. [17] performed tests of the Corrsin approximation for various cases.

Appropriate estimates for the Lagrangian correlation function have been intensively discussed in literature. Common approaches start with the Eulerian correlation function (ECF) of the magnetic field,

$$\langle \mathbf{b}_{\perp}(\mathbf{r}) \mathbf{b}_{\perp}(0) \rangle = \mathcal{E}[\mathbf{r}(t)] = \beta^2 \begin{pmatrix} 1 - \frac{y^2}{\lambda_{\perp}^2} & 0 \\ 0 & 1 - \frac{x^2}{\lambda_{\perp}^2} \end{pmatrix} \exp\left(-\frac{x^2 + y^2}{2\lambda_{\perp}} - \frac{z^2}{2\lambda_{\parallel}^2}\right), \quad (3.2)$$

which describes the correlation within the laboratory frame. Here we explicitly assume the Eulerian correlator to have a Gaussian form. Two important length scales define the

stochastic magnetic field, the correlation lengths λ_{\parallel} and λ_{\perp} . Several authors covered the topic of relating Eulerian and Lagrangian functions, e.g. [18]. The Eulerian correlator fulfills the condition for the complete magnetic field: $\text{div } \mathbf{B} = 0$.

It is convenient to introduce also the Fourier transform of $\mathbf{b}(\mathbf{r})$,

$$\mathbf{b}(\mathbf{r}) = \int \mathbf{b}(\mathbf{k}) \exp(-i\mathbf{k}\mathbf{r}(t)) d\mathbf{k}. \quad (3.3)$$

Now the complete dependence on the trajectory $\mathbf{r}(t)$ is capsuled in the exponential term and further collisional averages can be applied more easily using the cumulant expansion. The integration vector is $\mathbf{k} = (k_x, k_y, k_z)$. The correlation spectrum of the ECF is given by

$$\langle \mathbf{b}(\mathbf{k}_1) \mathbf{b}(\mathbf{k}_2) \rangle = \tilde{\mathcal{E}}(\mathbf{k}) \delta(\mathbf{k}_1 + \mathbf{k}_2), \quad (3.4)$$

defining the Eulerian correlation function in k -space,

$$\tilde{\mathcal{E}}(\mathbf{k}) = (\mathbf{k}_{\perp}^2 \delta_{ij} - k_i k_j) A(\mathbf{k}) \stackrel{e.g.}{\Leftrightarrow} \tilde{\mathcal{E}}_{yy}(\mathbf{k}) = k^2 A(\mathbf{k}), \quad (3.5)$$

and the correlation function of the vector potential in k -space,

$$A(\mathbf{k}) = (2\pi)^{-3/2} \lambda_{\perp}^4 \lambda_{\parallel} \beta^2 \exp\left(-\frac{1}{2} \mathbf{k}_{\perp}^2 \lambda_{\perp}^2 - \frac{1}{2} k_z \lambda_{\parallel}^2\right). \quad (3.6)$$

Our rigorous analysis of the procedure follows [14]. Using the formula (3.1), we transform from Eulerian to Lagrangian space

$$\mathbf{b}(t) = \int d\mathbf{r} \mathbf{b}(\mathbf{r}) \delta(\mathbf{r} - \mathbf{R}(t)). \quad (3.7)$$

The representation of the δ -function in k -space allows us to write the latter as

$$\mathbf{b}(t) = \frac{1}{(2\pi)^{3/2}} \int d\mathbf{k}_1 \int d\mathbf{r} \mathbf{b}(\mathbf{r}) e^{i\mathbf{k}_1 \mathbf{r} - i\mathbf{k}_1 \mathbf{R}(t)}. \quad (3.8)$$

Let $\mathbf{b}(\mathbf{k}_1)$ be the Fourier transform of $\mathbf{b}(t_1)$, then the backtransformation yields

$$\mathbf{b}(t) = \int d\mathbf{k}_1 \mathbf{b}(\mathbf{k}_1) e^{-i\mathbf{k}_1 \mathbf{R}(t)}. \quad (3.9)$$

So far we simply succeeded in rewriting $\mathbf{b}(t)$ in a distinct form. Next we concentrate on the unaveraged correlation,

$$\mathbf{b}(t_1) \mathbf{b}(t_2) = \int \int d\mathbf{k}_1 d\mathbf{k}_2 \mathbf{b}(\mathbf{k}_1) \mathbf{b}(\mathbf{k}_2) e^{-i\mathbf{k}_1 \mathbf{R}(t_1) - i\mathbf{k}_2 \mathbf{R}(t_2)}. \quad (3.10)$$

The average over the fluctuation field \mathbf{b} leads to

$$\langle \mathbf{b}(t_1) \mathbf{b}(t_2) \rangle_{\mathbf{b}} = \int \int d\mathbf{k}_1 d\mathbf{k}_2 \langle \mathbf{b}(\mathbf{k}_1) \mathbf{b}(\mathbf{k}_2) e^{-i\mathbf{k}_1 \mathbf{R}(t_1) - i\mathbf{k}_2 \mathbf{R}(t_2)} \rangle_{\mathbf{b}}, \quad (3.11)$$

and causes a severe problem in the integrand. The implicit dependencies of $\mathbf{R}(t)$ and \mathbf{b} rule out any possibility to average the last terms. It is exactly the next step, which is called Corrsin approximation or sometimes independence hypothesis to overcome this problem. By assumption we demand the stochastic independence of the product $\mathbf{b}(\mathbf{k}_1) \mathbf{b}(\mathbf{k}_2)$ and the exponential function in the last term. Averaging both terms separately, the situation is simplified to

$$\langle \mathbf{b}(\mathbf{k}_1) \mathbf{b}(\mathbf{k}_2) e^{-i\mathbf{k}_1 \mathbf{R}(t_1) - i\mathbf{k}_2 \mathbf{R}(t_2)} \rangle_{\mathbf{b}} \stackrel{\text{Corrsin}}{\approx} \langle \mathbf{b}(\mathbf{k}_1) \mathbf{b}(\mathbf{k}_2) \rangle_{\mathbf{b}} \langle e^{-i\mathbf{k} \mathbf{R}(t_1) - i\mathbf{k} \mathbf{R}(t_2)} \rangle_{\mathbf{b}}. \quad (3.12)$$

Please note that the independence assumption only refers to the average over magnetic fluctuations. The correlation of the fluctuating magnetic field is given in the Corrsin approximation by

$$\langle \mathbf{b}(t_1) \mathbf{b}(t_2) \rangle_{\mathbf{b}} = \int d\mathbf{k} \tilde{\mathcal{E}}(\mathbf{k}) \langle e^{-i\mathbf{k} \mathbf{R}(t_1) + i\mathbf{k} \mathbf{R}(t_2)} \rangle_{\mathbf{b}}. \quad (3.13)$$

Since the trajectory depends on $\boldsymbol{\eta}$, it has to be included in further averaging procedures regarding parallel and perpendicular motion. Perpendicular collisions can hereby be included easily using the cumulant expansion,

$$\langle \langle e^{-i\mathbf{k} \mathbf{R}(t_1) - i\mathbf{k} \mathbf{R}(t_2)} \rangle_{\mathbf{b}} \rangle_{\perp} = e^{-ik_z(z_0(t_1) - z_0(t_2))} e^{-\frac{1}{2} k_x^2 \langle \delta x^2(\tau) \rangle_{\perp} - \frac{1}{2} k_y^2 \langle \delta y^2(\tau) \rangle_{\perp}}. \quad (3.14)$$

3.1.3 Correlation function of the derivative of the perturbation field

We know that the VCF presented in 2.2.3 also contains the correlation function of the magnetic field derivatives. We differentiate Eq. (3.3),

$$\mathbf{b}'(t) = -i \int d\mathbf{k}_1 \mathbf{b}(\mathbf{k}_1) (\mathbf{k}_1 \cdot \mathbf{R}'(t)) e^{-i\mathbf{k}_1 \mathbf{R}(t)}. \quad (3.15)$$

and use the Corrsin method again to find

$$\begin{aligned} \langle \mathbf{b}'(t_1) \mathbf{b}'(t_2) \rangle_{\mathbf{b}} &= (-1) \int d\mathbf{k} \tilde{\mathcal{E}}(\mathbf{k}) \\ &\times (k_x^2 \eta_x(t_1) \eta_x(t_2) + k_y^2 \eta_y(t_1) \eta_y(t_2) + k_z^2 \eta_z(t_1) \eta_z(t_2)) e^{-ik_z \int_{t_2}^{t_1} \eta_z(t') dt'} \\ &\times e^{-ik_x \int_{t_2}^{t_1} \eta_x(t') dt' - ik_y \int_{t_2}^{t_1} \eta_y(t') dt'}. \end{aligned} \quad (3.16)$$

This expression is far more complicated than Eq. (3.13). Averages over η_i cannot be applied directly, because products of the exponential function and the η_i appear. We will proceed with this averages, after we substituted Eq. (3.16) into the correlation function.

3.2 Lagrangian velocity correlations

3.2.1 The guiding field term $\mathcal{L}^{(0)}$

At the end of Sec. 2 we derived the anomalous parts,

$$\langle\langle u_x(t_1) u_x(t_2) \rangle_b \rangle_{\perp}^{\text{AN}} \equiv \mathcal{L}^{(0)} + \mathcal{L}^{(1)} + \mathcal{O}(\rho_L^4). \quad (3.17)$$

which are caused by the magnetic fluctuations. We identify a term $\mathcal{L}^{(0)}$ in the zeroth order of the Larmor radius, connected to the guiding center limit,

$$\mathcal{L}^{(0)}[\langle \delta r_i^2(t) \rangle, \psi_{\parallel}, \varphi_{\parallel}, t] = \frac{1}{b_0^2} \langle \eta_z(t_1) \eta_z(t_2) \langle \langle b_y(t_1) b_y(t_2) \rangle_b \rangle_{\perp} \rangle_{\parallel}, \quad (3.18)$$

and an additional perturbation term $\mathcal{L}^{(1)}$

$$\mathcal{L}^{(1)}[\psi_{\parallel}, \varphi_{\parallel}, \psi_{\perp}, \varphi_{\perp}, t] = \frac{\rho_L^2}{v_t^2 b_0^2} \langle \eta_z(t_1) \eta_z(t_2) \langle \langle b_x'(t_1) b_x'(t_2) \rangle_b \rangle_{\perp} \rangle_{\parallel}, \quad (3.19)$$

which shows quadratic scaling with the Larmor radius. We will now calculate $\mathcal{L}^{(0)}$ and apply the Corrsin approximation for the magnetic field,

$$\langle \langle b_y(t_1) b_y(t_2) \rangle_b \rangle_{\perp} = \int d\mathbf{k} \tilde{\mathcal{E}}(\mathbf{k}) e^{-i k_z \int_{t_2}^{t_1} \eta_z(t') dt'} e^{-\frac{1}{2} k_x^2 \langle \delta x^2(\tau) \rangle_{\perp} - \frac{1}{2} k_y^2 \langle \delta y^2(\tau) \rangle_{\perp}}. \quad (3.20)$$

This transforms the correlation function into the Lagrangian frame of reference,

$$\mathcal{L}^{(0)} = \int d\mathbf{k} \tilde{\mathcal{E}}(\mathbf{k}) \left\langle \eta_z(t_1) \eta_z(t_2) e^{-i k_z \int_{t_2}^{t_1} \eta_z(t') dt'} \right\rangle_{\parallel} e^{-\frac{1}{2} k_x^2 \langle \delta x^2(\tau) \rangle_{\perp} - \frac{1}{2} k_y^2 \langle \delta y^2(\tau) \rangle_{\perp}}. \quad (3.21)$$

We will now introduce two functions which are closely related with the $\boldsymbol{\eta}$ motion. Both are supplementary stochastic functions helping to generalize the concept of the MSD and the running diffusion coefficient. In general, one defines

$$\begin{aligned} \varphi_a &= \int_{t_2}^{t_1} \langle a(t_1) a(\theta) \rangle d\theta = \int_{t_2}^{t_1} \langle a(\theta) a(t_2) \rangle d\theta, \\ \psi_a &= \int_{t_2}^{t_1} \int_{t_2}^{t_1} \langle a(\theta_1) a(\theta_2) \rangle d\theta_2 d\theta_1. \end{aligned} \quad (3.22)$$

For the classical transport these functions are given by

$$\varphi_{\parallel}(t) \equiv \int_{t_2}^{t_1} \langle \eta_z(t_1) \eta_z(\theta_2) \rangle d\theta_2 = \chi_{\parallel} (1 - e^{-\nu\tau}), \quad (3.23)$$

$$\varphi_{\perp}(t) \equiv \int_{t_2}^{t_1} \langle \eta_x(t_1) \eta_x(\theta_2) \rangle d\theta_2 = \chi_{\perp} (1 - e^{-\nu\tau}),$$

$$\psi_{\parallel}(t) \equiv \int_{t_2}^{t_1} \int_{t_2}^{t_1} \langle \eta_z(\theta_1) \eta_z(\theta_2) \rangle d\theta_1 d\theta_2 = \frac{2\chi_{\parallel}}{\nu} (\nu\tau - 1 + e^{-\nu\tau}), \quad (3.24)$$

$$\psi_{\perp}(t) \equiv \int_{t_2}^{t_1} \int_{t_2}^{t_1} \langle \eta_x(\theta_1) \eta_x(\theta_2) \rangle d\theta_1 d\theta_2 = \frac{2\chi_{\perp}}{\nu} (\nu\tau - 1 + e^{-\nu\tau}).$$

The variable $\varphi_{\parallel,\perp}$ represents the running diffusion coefficient and $\psi_{\parallel,\perp}$ equals the MSD. We use this kind of notation to be consistent with the majority of contributions in the literature, see e.g. [11,12,18,19,20].

Note, that the $\langle \delta x^2 \rangle$ and $\langle \delta y^2 \rangle$ terms in (3.20) and (3.21) still contain the influences respectively anomalous transport and should not be confused with the classical $\psi_{\parallel,\perp}$ terms. The combined average of the parallel motion is performed using the prescription shown in Appendix B.1,

$$\mathcal{L}^{(0)} = \int d\mathbf{k} \tilde{\mathcal{E}}(\mathbf{k}) \left\{ \frac{v_t^2}{2} e^{-\nu t} - m^2 \varphi_{\parallel}^2 \right\} e^{-\frac{1}{2} k_z^2 \psi_{\parallel}} e^{-\frac{1}{2} k_x^2 \langle \delta x^2(\tau) \rangle - \frac{1}{2} k_y^2 \langle \delta y^2(\tau) \rangle} \quad (3.25)$$

Performing the k -integration we finally find the Lagrangian correlation function of the guiding center motion,

$$\mathcal{L}^{(0)} = \frac{\beta^2}{b_0^2} \mathcal{M} \left\{ \chi_{\parallel} \nu e^{-\nu t} - \frac{\varphi_{\parallel}^2}{\lambda_{\parallel}^2} \mathcal{M}^2 \right\} \mathcal{N}. \quad (3.26)$$

In the last step we used the symmetry of the system, $\langle \delta x^2 \rangle = \langle \delta y^2 \rangle$. Hereby the functions \mathcal{M} and \mathcal{N} are defined by

$$\mathcal{M} = \frac{1}{\left(1 + \frac{\psi_{\parallel}(\nu t)}{\lambda_{\parallel}^2}\right)^{1/2}}, \quad \mathcal{N} = \frac{1}{\left(1 + \frac{\langle \delta x^2(t) \rangle}{\lambda_{\perp}^2}\right)^2}. \quad (3.27)$$

Equation (3.26) can now be introduced into the Green-Kubo formalism (2.22), to obtain a differential equation for the transport data. The terms in (3.26) have the following interesting properties: Infinite limits of the correlation lengths reduce the terms to unity as

$$\mathcal{M}_{\lambda_{\parallel} \rightarrow \infty} = 1, \quad \mathcal{N}_{\lambda_{\perp} \rightarrow \infty} = 1. \quad (3.28)$$

3.2.2 The Larmor radius correction term $\mathcal{L}^{(1)}$

In the case of strong guiding fields, the main advantage of the A-Langevin approach is the capability to calculate finite Larmor radius corrections. As long as the guiding center approximation can be applied, the system is determined by $\mathcal{L}^{(0)}$. For smaller guiding fields, the gyration around the field lines contributes to the transport, and finite values of the Larmor radius must be taken into account. Depending on the ratio β/b_0 of fluctuations and the guiding field, the finite Larmor radius effects become important. For $b_0 \gg \beta$, the Larmor radius is identified by $\rho_L = v_t/(\Omega b_0)$. Finite Larmor radii change the transport behavior and appear in (3.17) via the additional (first order) perturbation term $\mathcal{L}^{(1)}$. We will still assume that the guiding field is predominantly stronger than the fluctuations and that higher order corrections may still be neglected. We can use our Corrsin approximated results of the derivative of the correlation function. Applying the average over perpendicular and parallel collisions leads to the rather complicated formula

$$\begin{aligned}
\mathcal{L}^{(1)} = & \langle \eta_z(t_1) \eta_z(t_2) \langle \langle \mathbf{b}'(t_1) \mathbf{b}'(t_2) \rangle_b \rangle_{\perp} \rangle_{\parallel} = (-1) \int \left\{ \tilde{\mathcal{E}}(\mathbf{k}) \right. \\
& \times \left. \left((k_x^2 \eta_x(t_1) \eta_x(t_2) + k_y^2 \eta_y(t_1) \eta_y(t_2)) e^{-i k_x \int_{t_2}^{t_1} \eta_x(t') dt' - i k_y \int_{t_2}^{t_1} \eta_y(t') dt'} \right) \right\}_{\perp} \\
& \times \left. \left(\eta_z(t_1) \eta_z(t_2) e^{-i k_z \int_{t_2}^{t_1} \eta_z(t') dt'} \right) \right\}_{\parallel} \tag{3.29} \\
& + k_z^2 \left(\eta_z(t_1) \eta_z(t_2) \eta_z(t_1) \eta_z(t_2) e^{-i k_z \int_{t_2}^{t_1} \eta_z(t') dt'} \right) \Big|_{\parallel} \\
& \times e^{-\frac{1}{2} k_x^2 \langle \delta x^2(\tau) \rangle - \frac{1}{2} k_y^2 \langle \delta y^2(\tau) \rangle} \Big\} d\mathbf{k}.
\end{aligned}$$

The major difficulty in the derivation of the term $\mathcal{L}^{(0)}$ was the complicated combined average of the product of η_z and the exponential function. This kind of averages appear here in three different forms. Although the calculation of this terms is not trivial it just requires the prescription from Appendix B.1 to solve the averages $\mathcal{L}^{(1)}$ step by step,

$$\begin{aligned}
\mathcal{L}^{(1)} \approx & -(2\pi)^{-3/2} \int \left(\frac{v_t^2}{2} e^{-\nu t} - k_z^2 \varphi_{\parallel}^2 \right) e^{-\frac{1}{2} k_z^2 (\psi_{\parallel} + \lambda_{\parallel}^2)} dk_z \\
& \times \left\{ \int k_x^2 [k_x^2 \chi_{\perp} \nu e^{-\nu t} - k_x^4 \varphi_{\perp}^2] e^{-\frac{1}{2} k_x^2 (\psi_{\perp} + \lambda_{\perp}^2)} e^{-\frac{1}{2} k_y^2 (\psi_{\perp} + \lambda_{\perp}^2)} dk_x dk_y \right. \\
& + \left. \int k_y^2 [k_y^2 \chi_{\perp} \nu e^{-\nu t} - k_y^4 \varphi_{\perp}^2] e^{-\frac{1}{2} k_x^2 (\psi_{\perp} + \lambda_{\perp}^2)} e^{-\frac{1}{2} k_y^2 (\psi_{\perp} + \lambda_{\perp}^2)} \right\} dk_x dk_y \\
& - (2\pi)^{-3/2} \int m^2 \frac{v_t^4}{4} e^{-\frac{1}{2} m^2 (\psi_{\parallel} + \lambda_{\parallel}^2)} dk_z \\
& \times \int k_x^2 e^{-\frac{1}{2} k_x^2 (\psi_{\perp} + \lambda_{\perp}^2)} e^{-\frac{1}{2} k_y^2 (\psi_{\perp} + \lambda_{\perp}^2)} dk_x dk_y.
\end{aligned} \tag{3.30}$$

The last term on the right-hand side of Eq. (3.29) was estimated by

$$k_z^2 \left\langle \eta_z^2(t_1) \eta_z^2(t_2) e^{-i k_z \int_{t_2}^{t_1} \eta_z(t') dt'} \right\rangle \approx v_t^4 k_z^2 \exp\left(-\frac{1}{2} k_z^2 \psi_{\parallel}\right).$$

This approximation has been verified a posteriori. Evaluating the integrals leads to the correction terms for the correlator,

$$\begin{aligned}
\mathcal{L}^{(1)} = & -\frac{\rho_L^2}{v_t^2 b_0^2} \mathcal{L}^{(0)}_{\lambda_{\perp} \rightarrow \infty} \left[\chi_{\perp} \nu e^{-\nu t} \frac{4}{\left(1 + \frac{\psi_{\perp}}{\lambda_{\perp}^2}\right)^3 \lambda_{\perp}^2} - \frac{\varphi_{\perp}^2}{\lambda_{\perp}^4} \frac{18}{\left(1 + \frac{\psi_{\perp}}{\lambda_{\perp}^2}\right)^4} \right] \\
& - \frac{\rho_L^2 \beta^2}{b_0^2} \frac{v_t^2}{4 \lambda_{\parallel}^2 \left(1 + \frac{\psi_{\parallel}}{\lambda_{\parallel}^2}\right)^{3/2} \left(1 + \frac{\psi_{\perp}}{\lambda_{\perp}^2}\right)^2}.
\end{aligned} \tag{3.31}$$

Here, $\mathcal{L}^{(0)}_{\lambda_{\perp} \rightarrow \infty}$ means the result for the zeroth order, in the limit $\lambda_{\perp} \rightarrow \infty$, which corresponds to the correlation function that describes the quasilinear limit in combination with collisions. $\mathcal{L}^{(1)}$ is a correction term, affecting each regime predicted by $\mathcal{L}^{(0)}$. For small Larmor radii this correction vanishes.

Only a few diffusion regimes allow the analytical evaluation of this correction formula. Principally it describes a reduction of the diffusion. For $\lambda_{\perp} \gg \lambda_{\parallel}$ it will be always negative. Small values of λ_{\perp} lead to states where the correction formula may be positive and amplifies the diffusion. Such states are ruled out by the condition that the Kubo number has to be small.

3.3 Diffusion regimes

3.3.1 The A-MSD-equation for the description of anomalous transport

The Green-Kubo formalism (2.22) allows us to find the MSD and the running diffusion coefficient of anomalous transport by the solution of an ordinary differential equation,

$$\frac{d^2}{dt^2} \langle \delta x^2(t) \rangle = 2 \frac{d}{dt} D(t) = \mathcal{L}^{(0)} + \mathcal{L}^{(1)}. \quad (3.32)$$

In the following we will sometimes refer to this equation as A-MSD equation to denote that it originates from the A-Langevin equation. The complete diffusion coefficient consists of both, the classical diffusion rate and the diffusion rate of the anomalous transport. Equation (3.32) refers to anomalous transport only. Substituting our expressions for $\mathcal{L}^{(0)}$ and $\mathcal{L}^{(1)}$, we find the explicit form

$$\begin{aligned} \frac{d^2}{dt^2} \langle \delta x^2(t) \rangle = \\ 2 \frac{d}{dt} D(t) = \frac{\beta^2}{b_0^2} \left[\frac{\chi_{\parallel} \nu e^{-\nu t}}{\left(1 + \frac{\psi_{\parallel}(\nu t)}{\lambda_{\parallel}^2}\right)^{1/2}} - \frac{\varphi_{\parallel}^2}{\lambda_{\parallel}^2} \frac{1}{\left(1 + \frac{\psi_{\parallel}(\nu t)}{\lambda_{\parallel}^2}\right)^{3/2}} \right] \frac{1}{\left(1 + \frac{\langle \delta x^2(t) \rangle}{\lambda_{\perp}^2}\right)^2} \\ - \frac{\rho_L^2}{v_t^2 b_0^2} \mathcal{L}^{(0)}_{\lambda_{\perp} \rightarrow \infty} \left[\frac{4 \chi_{\perp} \nu e^{-\nu t}}{\left(1 + \frac{\psi_{\perp}}{\lambda_{\perp}^2}\right)^3 \lambda_{\perp}^2} - \frac{\varphi_{\perp}^2}{\lambda_{\perp}^4} \frac{18}{\left(1 + \frac{\psi_{\perp}}{\lambda_{\perp}^2}\right)^4} \right] \\ - \frac{\rho_L^2 \beta^2}{b_0^2} \frac{v_t^2}{4 \lambda_{\parallel}^2 \left(1 + \frac{\psi_{\parallel}}{\lambda_{\parallel}^2}\right)^{3/2} \left(1 + \frac{\psi_{\perp}}{\lambda_{\perp}^2}\right)^2}. \end{aligned} \quad (3.33)$$

Without constraints, the A-MSD equation cannot be solved analytically and has to be evaluated by numerical methods. Note that (3.33) represents the most general form of the equation, of course containing all of the different diffusion regimes.

Fortunately, it is possible to find analytical results within certain limits and under special assumptions, which simplify the A-MSD equation. The most important and famous anomalous transport regimes (for small Kubo numbers) are presented in the upcoming sections.

3.3.2 The quasilinear limit

The quasilinear regime [11] refers to a domain in which the perpendicular correlation length tends to infinity, $\lambda_{\perp} \rightarrow \infty$ and collisions are absent, $\nu = 0$. It is the manifested test regime for any theory describing anomalous transport. The functions φ_{\parallel} and ψ_{\parallel} can be expanded in power series at $\nu = 0$, yielding

$$\varphi_{\parallel} = \frac{v_t^2}{2} t, \quad \psi_{\parallel} = \frac{v_t^2}{2} t^2. \quad (3.34)$$

Obviously, only a ballistic motion along the field lines prevails, because the z-motion is not disrupted by collisions. No implicit dependence on the perpendicular MSD remains within the Green-Kubo formula,

$$\frac{d^2}{dt^2} \langle \delta x^2(t) \rangle^{(0)} = 2 \frac{d}{dt} D_{\text{ql}}^{(0)}(t) = \frac{v_t^2 \beta^2}{b_0^2} \frac{1}{\left(1 + \frac{v_t^2 t^2}{2\lambda_{\parallel}^2}\right)^{3/2}}. \quad (3.35)$$

Additionally the condition $\kappa \ll 1$ always holds for $\lambda_{\perp} \rightarrow \infty$ and the results of Corrsin approximation are valid. The latter equation can be directly integrated,

$$D_{\text{ql}}^{(0)} = \frac{v_t^2 \beta^2}{\sqrt{2} b_0^2} \int_0^{\infty} \frac{1}{\left(1 + \frac{v_t^2 t^2}{2\lambda_{\parallel}^2}\right)^{3/2}} dt, \quad (3.36)$$

to find the asymptotic diffusion coefficient for particles in the quasilinear limit,

$$D_{\text{ql}}^{(0)} = \frac{v_t}{\sqrt{2}} \frac{\beta^2}{b_0^2} \lambda_{\parallel}. \quad (3.37)$$

So far, we retrieved the famous quasilinear scaling from our $\mathcal{L}^{(0)}$ correlation function. But the assumptions for this regime simplify also the correction terms. For the first order correction, we substitute $\mathcal{L}^{(1)}_{\lambda_{\perp} \rightarrow \infty}$ into the Green-Kubo equation,

$$D_{\text{ql}}^{(1)} = -\frac{\rho_L^2 \beta^2}{4\lambda_{\parallel}^2 b_0^2} \int_0^{\infty} \frac{1}{\left(1 + \frac{v_t^2 t^2}{2\lambda_{\parallel}^2}\right)^{3/2}} dt, \quad (3.38)$$

applying the same integral as above, and obtain the correction

$$D_{\text{ql}}^{(1)} = -\frac{v_t \rho_L^2 \beta^2}{4\sqrt{2} b_0^2 \lambda_{\parallel}}. \quad (3.39)$$

Introducing dimensionless quantities, by substituting

$$\tau = \Omega b_0 t, \quad \bar{D}_{\text{ql}} = \frac{D_{\text{ql}}}{v_t \rho_L} \quad \text{and} \quad \bar{\lambda}_{\parallel} = \frac{\lambda_{\parallel}}{\rho_L} \quad (3.40)$$

and using the ratio $\varepsilon = \beta/b_0$, Eq. (3.33) for the anomalous parts in the quasilinear limit becomes,

$$2 \frac{d}{d\tau} \bar{D}_{\text{ql}}^{(0+1)}(\tau) = \frac{\varepsilon^2}{\left(1 + \frac{\tau^2}{2\bar{\lambda}_{\parallel}^2}\right)^{3/2}} - \frac{\varepsilon^2}{4\bar{\lambda}_{\parallel}^2 \left(1 + \frac{\tau^2}{2\bar{\lambda}_{\parallel}^2}\right)^{3/2}} \quad (3.41)$$

yielding the results

$$\bar{D}_{\text{ql}}^{(0)} = \frac{1}{\sqrt{2}} \varepsilon^2 \bar{\lambda}_{\parallel} \quad \text{and} \quad \bar{D}_{\text{ql}}^{(1)} = -\frac{\varepsilon^2}{4\sqrt{2}\bar{\lambda}_{\parallel}}. \quad (3.42)$$

The analytical predictions and the dimensionless running diffusion coefficient $\bar{D}_{\text{ql}}(t)$ as a function of time are shown in Fig. 3.1. For $\bar{\lambda}_{\parallel} \rightarrow \infty$ both curves coincide. An obvious reduction of the diffusion can be observed, when comparing the guiding center result and the Larmor corrections. Equations (3.42) is also a good analytical estimate for other regimes, as it shows that the effect of the gyro-radii vanishes for large λ_{\parallel} .

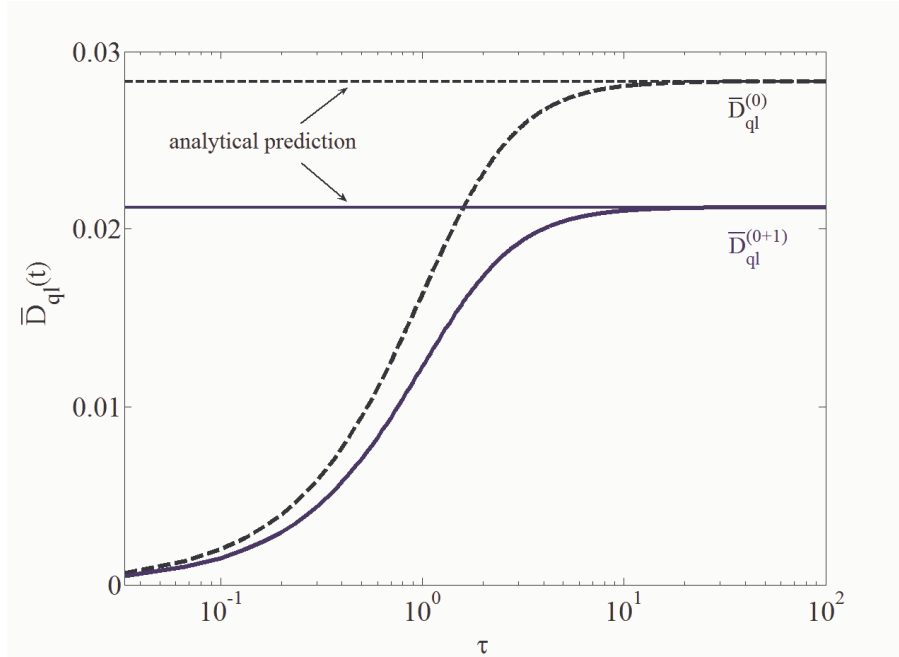


Figure 3.1: Solution of Eq. (3.41) (blue) for $\bar{\lambda}_{\parallel} = 1$ and $\varepsilon = 0.2$. The dashed line describes the corresponding quasilinear result without finite Larmor corrections. The constant lines are the analytical predictions (3.42).

3.3.3 Occurance of a subdiffusive situation

Contrary to the quasilinear regime, we now include collisions along the the field lines. This assumption is somehow artificial as we still keep the condition $\lambda_{\perp} \rightarrow \infty$, i.e. no decorrelation in the perpendicular dimension. As a matter of fact, this case is also not affected by any insufficiency of the Corrsin approximation. The parallel collisions induce a diffusive transport in the z -direction. Using $\psi_{\parallel} = \frac{2\chi_{\parallel}}{\nu} (\nu t - 1 + e^{-\nu t}) \approx 2\chi_{\parallel} t$, we have to solve the equation

$$\frac{d^2}{dt^2} \langle \delta x^2(t) \rangle^{(0)} = 2 \frac{d}{dt} D_{\text{sub}}^{(0)}(t) = \frac{\beta^2}{b_0^2} \left\{ \frac{v_t^2 e^{-\nu t}}{2 \left(1 + \frac{\psi_{\parallel}(t)}{\lambda_{\parallel}^2}\right)^{1/2}} - \frac{\varphi_{\parallel}^2}{\lambda_{\parallel}^2} \frac{1}{\left(1 + \frac{\psi_{\parallel}(t)}{\lambda_{\parallel}^2}\right)^{3/2}} \right\}. \quad (3.43)$$

This differential equation yields subdiffusive behavior for the perpendicular transport. Introducing the dimensionless quantities

$$\tau = \nu t, \quad \bar{\chi}_{\parallel,\pm} = \frac{2 \chi_{\parallel,\pm}}{\lambda_{\parallel,\pm}^2 \nu} \quad \text{and} \quad \bar{D}_{\text{sub}} = \frac{D_{\text{sub}}}{\lambda_{\parallel}^2 \nu}, \quad (3.44)$$

the Eq. (3.43) leads to

$$\frac{d^2}{d\tau^2} \sigma^{(0)} = 2 \frac{d}{d\tau} \bar{D}_{\text{sub}}^{(0)}(\theta) = \frac{\varepsilon^2 e^{-\tau}}{(1 + \bar{\chi}_{\parallel} \tau)^{1/2}} - \frac{\varepsilon^2 \bar{\chi}_{\parallel}^2 (1 - e^{-\tau})^2}{4(1 + \bar{\chi}_{\parallel} \tau)^{3/2}}. \quad (3.45)$$

Note that we use different ways to introduce dimensionless quantities. Especially our definition of \bar{D} differs in each regime and is therefore denoted with an index, referring to the specified regime.

Figure 3.2 shows subdiffusive decays of the running diffusion coefficient for different values of the characteristic parameter $\bar{\chi}_{\parallel}$.

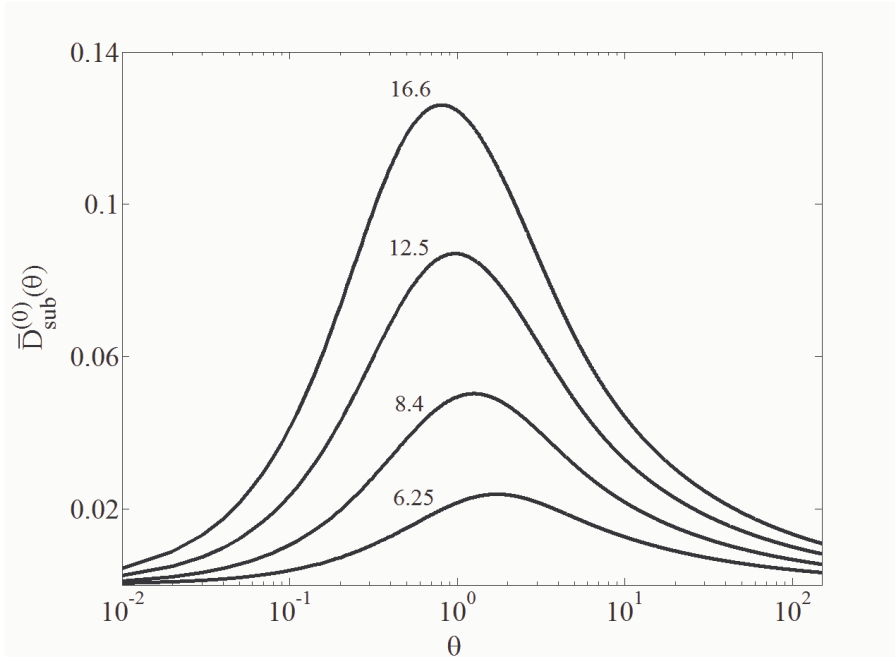


Figure 3.2: Solution in the subdiffusive regime ($\lambda_{\perp} \rightarrow \infty$, $\nu > 0$). Diffusion coefficient $\bar{D}^{(0)}$ as function of the reduced time for different values of $\bar{\chi}_{\parallel}$.

The long time asymptotics for $\tau \gg 1$ of the running diffusion coefficient $D(\theta)$ is determined by the integral

$$\bar{D}_{\text{sub}}^{(0)}(\theta) = -\frac{\varepsilon^2 \bar{\chi}_{\parallel}^2}{8} \int \frac{1}{(\bar{\chi}_{\parallel} \theta)^{3/2}} d\theta = \frac{1}{4} \varepsilon^2 \bar{\chi}_{\parallel}^{1/2} \theta^{-1/2} \quad (3.46)$$

verifying the dependency $D(\theta) \sim \sqrt{\theta^{-1}}$. This regime is also discussed in the literature [10] using different approaches and its results are well established. Finite Larmor radius corrections do not lead to a change of the subdiffusive nature.

3.3.4 The Rechester-Rosenbluth regime

A very important and often stated diffusion scaling was found by Rechester and Rosenbluth [26]. It is a paradigm for anomalous transport and can be derived from the A-MSD equation analytically. Contrary to the limiting cases presented above, we now assume finite correlation length. The differential equation for the MSD is given by

$$\frac{d^2}{dt^2} \langle \delta x^2(t) \rangle^{(0)} = \frac{\beta^2}{b_0^2} \frac{1}{\left(1 + \frac{\psi_{\perp} + \langle \delta x^2(t) \rangle^{(0)}}{\lambda_{\perp}^2}\right)^2} \left\{ \frac{v_{\perp}^2 e^{-\nu t}}{2 \left(1 + \frac{\psi_{\parallel}(t)}{\lambda_{\parallel}^2}\right)^{1/2}} - \frac{\varphi_{\parallel}^2}{\lambda_{\parallel}^2} \frac{1}{\left(1 + \frac{\psi_{\parallel}(t)}{\lambda_{\parallel}^2}\right)^{3/2}} \right\}. \quad (3.47)$$

Introducing the quantities,

$$\begin{aligned} \xi &= \frac{2 \langle \delta x^2(t) \rangle}{\lambda_{\perp}^2}, \quad \tau = \nu t, \quad \bar{\chi}_{\parallel, \pm} = \frac{2 \chi_{\parallel, \pm}}{\lambda_{\parallel, \pm}^2 \nu}, \\ \bar{\psi}_{\parallel, \pm} &= \frac{\psi_{\parallel, \pm}}{\lambda_{\parallel, \pm}^2}, \quad \bar{\varphi}_{\parallel, \pm} = \frac{\varphi_{\parallel, \pm}}{\lambda_{\parallel, \pm}^2} \quad \text{and} \quad \bar{D}_{\text{RR}} = \frac{D_{\text{RR}}}{\lambda_{\parallel}^2 \nu} \end{aligned} \quad (3.48)$$

and using the Kubo number $\kappa = \beta \lambda_{\parallel} / b_0 \lambda_{\perp}$ we obtain the dimensionless form of Eq. (3.47),

$$\begin{aligned} \frac{d^2}{d\tau^2} \xi^{(0)}(\tau) &= \left(\kappa^2 \bar{\chi}_{\parallel} e^{-\tau} (1 + \bar{\psi}_{\parallel})^{-\frac{1}{2}} - \right. \\ &\left. \kappa^2 \bar{\chi}_{\parallel}^2 (1 - e^{-\tau}) (1 + \bar{\psi}_{\parallel})^{-\frac{3}{2}} \right) \left(1 + \bar{\psi}_{\perp} + \frac{1}{2} \xi(t) \right)^{-2}. \end{aligned} \quad (3.49)$$

In the limit $\tau \gg 1$ the equation becomes

$$\frac{d^2}{d\tau^2} \xi^{(0)}(\tau) = -\kappa^2 \bar{\chi}_{\parallel}^2 (1 + \bar{\psi}_{\parallel})^{-\frac{3}{2}} \left(1 + \bar{\psi}_{\perp} + \frac{1}{2} \xi(t) \right)^{-2}. \quad (3.50)$$

For estimates of the diffusion in this regime, we use a separation method presented in [12] based on the following argument: The motion can be divided into two anomalous contributions,

- a displacement $\sigma^{(0)}(t)$ caused by the motion of the particle with the field line alone. This situation corresponds to the subdiffusive case and was already discussed in the previous section.

- a decorrelation $\mu^{(0)}(t)$ from the field lines mainly caused by collisions, which is called the Rechester-Rosenbluth diffusion.

The MSD which can be retrieved by (3.47) or (3.50) is a superposition of this two contributions,

$$\xi^{(0)}(t) = \sigma^{(0)}(t) + \mu^{(0)}(t).$$

To single out the asymptotic diffusion due to the magnetic nonlinearity, we have to find a solution for $\mu(t)$ and introduce,

$$d^2 \sigma / dt^2 = -\kappa^2 \bar{\chi}_{\parallel}^2 (1 + \bar{\psi}_{\parallel})^{-\frac{3}{2}}, \quad (3.51)$$

leading to

$$\frac{d^2}{d\tau^2} \mu^{(0)}(\tau) = \kappa^2 \bar{\chi}_{\parallel}^2 (1 + \bar{\psi}_{\parallel})^{-\frac{3}{2}} (1 - (1 + \bar{\psi}_{\perp} + \xi(t))^{-2}). \quad (3.52)$$

In appendix B.2 we split this equation into two time domains and present a fitting method to find a solution $\mu^{(0)}(t)$ and the corresponding diffusion coefficient \bar{D}_{RR} . The result scales like the famous Rechester-Rosenbluth diffusion coefficient and is given by,

$$\bar{D}_{\text{RR}}^{(0)}(t) = \frac{16 \kappa^4 \bar{\chi}_{\parallel}}{\log^2(16 \sqrt{2\pi} \kappa^4 \bar{\chi}_{\parallel} \bar{\chi}_{\perp}^{-1})}. \quad (3.53)$$

Introducing a reduced dimensionless Larmor radius and friction

$$\bar{\rho}_L = \frac{\rho_L}{\lambda_{\parallel}}, \quad \bar{\nu} = \frac{\nu}{\Omega b_0} \quad (3.54)$$

the dimensionless form of the correction formula,

$$\begin{aligned} \frac{d^2}{dt^2} \langle \delta x^2(t) \rangle^{(1)} = & -\frac{\rho_L^2}{v_t^2 b_0^2} \mathcal{L}^{(0)}_{\lambda_{\perp} \rightarrow \infty} \left[\chi_{\perp} \nu e^{-\nu t} \frac{4}{\left(1 + \frac{\psi_{\perp}}{\lambda_{\perp}^2}\right)^3 \lambda_{\perp}^2} - \frac{\varphi_{\perp}^2}{\lambda_{\perp}^4} \frac{18}{\left(1 + \frac{\psi_{\perp}}{\lambda_{\perp}^2}\right)^4} \right] \\ & - \frac{\rho_L^2 \beta^2}{b_0^2} \frac{v_t^2}{4 \lambda_{\parallel}^2 \left(1 + \frac{\psi_{\parallel}}{\lambda_{\parallel}^2}\right)^{3/2} \left(1 + \frac{\psi_{\perp}}{\lambda_{\perp}^2}\right)^2}, \end{aligned} \quad (3.55)$$

reads

$$\begin{aligned} \frac{d^2}{d\tau^2} \xi^{(1)} = & -\frac{1}{2} \bar{\rho}_L^2 \bar{\nu}^2 \kappa^2 \mathcal{L}^{(0)}_{\lambda_{\perp} \rightarrow \infty} [4 e^{-\tau} (1 + \bar{\chi}_{\perp} \tau)^{-3} - 18 \bar{\chi}_{\perp} (1 - e^{-\tau})^2 (1 + \bar{\chi}_{\perp} \tau)^{-4}] \\ & - \frac{1}{2} \bar{\rho}_L^2 \kappa^2 \bar{\chi}_{\parallel} (1 + \bar{\chi}_{\parallel} \tau)^{-3/2} (1 + \bar{\chi}_{\perp} \tau)^{-2}. \end{aligned} \quad (3.56)$$

In Fig. 3.3 the diffusion coefficient is shown as a function of κ . We used values for κ that are within the valid range of the Corrsin approximation. It shows the typical quadratic scaling (3.53) for the Rechester-Rosenbluth regime in the guiding center limit. For increasing Larmor radii the transport is (again) reduced severely.

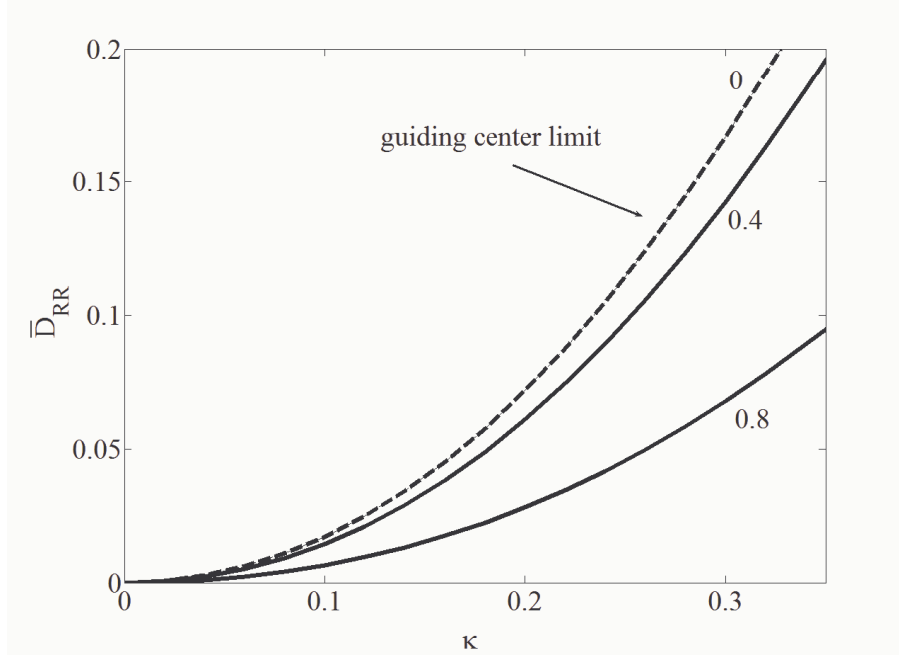


Figure 3.3: Influence of the Larmor radii on the diffusion in the Rechester-Rosenbluth regime. Total diffusion coefficient $\bar{D}_{\text{RR}} = \bar{D}_{\text{RR}}^{(0)} + \bar{D}_{\text{RR}}^{(1)}$ from the solution of the dimensionless Eqs. (3.42) and (3.48) for different values of $\bar{\rho}_L$. The classical diffusion rates were chosen in the typical Rechester-Rosenbluth range to be $\bar{\chi}_\perp = 0.4$ and $\bar{\chi}_\parallel = 20$.

Figure 3.4 shows the asymptotic dimensionless diffusion coefficient \bar{D}_{RR} as a function of the dimensionless Larmor radius $\bar{\rho}_L$. The reduction caused by (3.56) is compared with the guiding center result (3.50) (which is a constant in $\bar{\rho}_L$) and the parabolic deviation from the predicted value in the zeroth order can be seen.

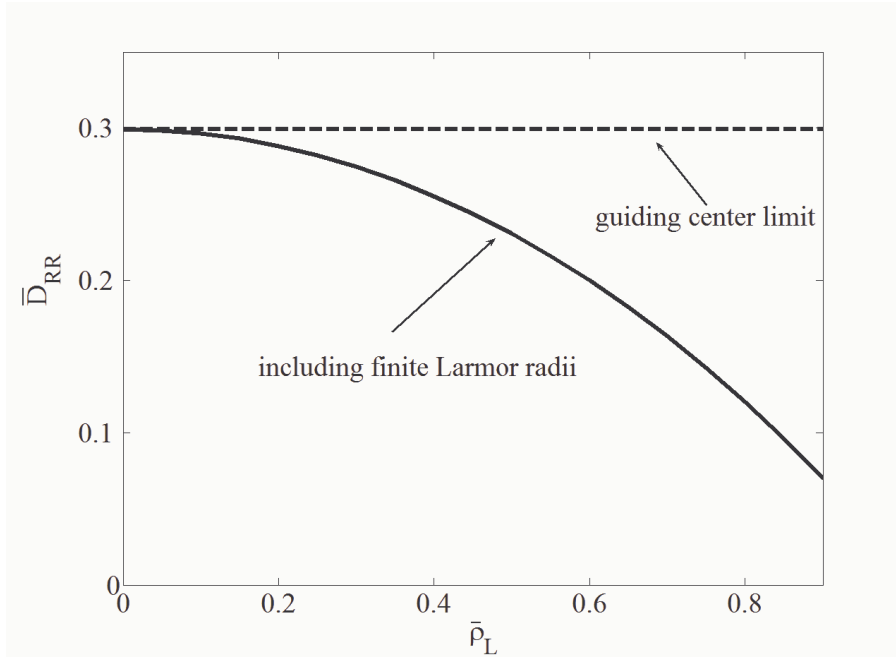


Figure 3.4: Diffusion coefficient as a function of the Larmor radius. Solution of the dimensionless Eqs. (3.42) and (3.48) for $\kappa = 0.4$, $\bar{\chi}_\perp = 0.2$ and $\bar{\chi}_\parallel = 20$.

3.3.5 The Kadomtsev-Pogutse -I regime

Basically, two diffusion scalings are referred to as Kadomtsev-Pogutse limit. The first one (Kadomtsev-Pogutse-I), which we will refer to as percolation limit is characterized by an infinite parallel correlation length $\lambda_\parallel \rightarrow \infty$, [24]. The second one (Kadomtsev-Pogutse-II) describes collisional transport within weak stochastic fields and is discussed in detail in the next section. Evidently the first case violates the validity condition of the Corrsin approximation and is assumed to give wrong predictions for the transport properties. Nevertheless it is very elucidating to discuss this regime first under presumably wrong assumptions. Kadomtsev and Pogutse proposed that in this case the asymptotic diffusion coefficient scales like

$$D \sim v_t \frac{\beta}{b_0} \lambda_\perp. \quad (3.57)$$

Indeed such a scaling is observed analytically, if we use the correlation functions derived with the independence hypothesis,

$$D_{\text{KP}}^{(0)} = \frac{v_t^2 \beta^2}{2 b_0^2} \int_0^\infty \frac{1}{\left(1 + \frac{D_{\text{KP}} \tau}{\lambda_\perp^2}\right)^2} d\tau = \frac{v_t^2 \beta^2 \lambda_\perp^2}{2 b_0^2 D_{\text{KP}}^{(0)}} \quad (3.58)$$

leading to the asymptotic (positiv) solution for $D_{\text{KP}}^{(0)}$,

$$D_{\text{KP}}^{(0)} = \frac{1}{\sqrt{2}} v_t \frac{\beta}{b_0} \lambda_{\perp}. \quad (3.59)$$

Unfortunately, this scaling is wrong [18]. For $\lambda_{\parallel} \rightarrow \infty$, the turbulence may be regarded as frozen. The trajectories of the particles will then be trapped within the closed contour lines of the stream function ϕ and the diffusion vanishes because a linear grow of the MSD is no longer possible. Obviously this behaviour is not reflected in (5.10). As $D \sim \kappa^0$ which is a Bohm-like scaling, D will be constant for $\kappa \rightarrow \infty$. Many works pointed out this failure of the Corrsin method [18,19] for strong magnetic turbulence.

Isichenko et al. applied in [22] methods of the percolation theory and predicted that the diffusion coefficient depends crucially on the fractal dimension ν of the contours of ϕ ,

$$D^{(0)} = \beta \lambda_{\perp} \kappa^{-1/\nu+2}. \quad (3.60)$$

Numerical simulations, as shown e.g. in [27], lead to the well-established result for large Kubo numbers,

$$D^{(0)} \sim \kappa^{-0.3}. \quad (3.61)$$

We shall come back to this point in Sec. 4. A detailed review of the percolation theory approach to transport in random media can e.g. be found in [23].

3.3.6 The Kadomtsev-Pogutse-II regime

The Kadomtsev-Pogutse-II regime is a situation where the collisional effects are more important than the magnetic perturbation field. It is often referred to as weakly anomalous regime. It is characterized by the conditions $\bar{\chi}_{\perp} \gg \bar{D}_{\text{KP2}}$ and $\bar{\chi}_{\perp} \ll \bar{\chi}_{\parallel}$. Obviously the classical diffusion coefficient may not become zero in this regime. Using the dimensionless A-MSD equation from the last section. in its asymptotic limit $\tau \rightarrow \infty$, we have

$$2 \frac{d}{d\tau} \bar{D}_{\text{KP2}}^{(0)}(\tau) = -\kappa^2 \bar{\chi}_{\parallel}^2 (1 + \bar{\chi}_{\parallel} \tau)^{-\frac{3}{2}} (1 + \bar{\chi}_{\perp} \tau)^{-2}, \quad (3.62)$$

which can be integrated explicitly to find the asymptotic diffusion coefficient in form of an expansion in $\bar{\chi}_{\perp}^{1/2}$,

$$\begin{aligned} \bar{D}_{\text{KP2}}^{(0)} &= -\frac{\kappa^2 \bar{\chi}_{\parallel}^2}{2} \int_0^{\infty} (1 + \bar{\chi}_{\parallel} \tau)^{-\frac{3}{2}} (1 + \bar{\chi}_{\perp} \tau)^{-2} d\tau \\ &= \frac{3\pi}{2} \kappa^2 \sqrt{\bar{\chi}_{\parallel} \bar{\chi}_{\perp}} + \mathcal{O}(\chi_{\perp}). \end{aligned} \quad (3.63)$$

This is the well-known Kadomtsev-Pogutse-(II)-regime for weakly anomalous influences. It shows the characteristic $\bar{D}_{\text{KP2}} \sim \sqrt{\bar{\chi}_{\parallel} \bar{\chi}_{\perp}}$ scaling of the diffusion constant and may be

regarded as a boundary situation for the more general Rechester-Rosenbluth regime.

We can now quantify the condition $D_{\text{KP2}} \ll \bar{\chi}_\perp \ll \bar{\chi}_\parallel$, which only holds as long as $\kappa^2 \bar{\chi}_\parallel \ll \bar{\chi}_\parallel$.

For the higher order correction $D^{(1)}$ a similar equation is found and we have again one of the rare cases in which the first order term $\mathcal{L}^{(1)}$ can be evaluated analytically,

$$\begin{aligned} \bar{D}_{\text{KP2}}^{(1)} &= -\frac{1}{4} \bar{\rho}_L^2 \kappa^2 \bar{\chi}_\parallel \int_0^\infty (1 + \bar{\chi}_\parallel \tau)^{-3/2} (1 + \bar{\chi}_\perp \tau)^{-2} \\ &= -\frac{3\pi}{2} \bar{\rho}_L^2 \kappa^2 \sqrt{\frac{\bar{\chi}_\perp}{\bar{\chi}_\parallel}}, \end{aligned} \quad (3.64)$$

revealing the influences of the Larmor radius. In dimensional form, the diffusion coefficients are given by

$$D_{\text{KP2}}^{(0)} = 3\pi \kappa^2 \frac{\lambda_\perp}{\lambda_\parallel} \sqrt{\chi_\parallel \chi_\perp}, \quad D_{\text{KP2}}^{(1)} = -\frac{3\pi}{2} \rho_L^2 \kappa^2 \frac{\lambda_\perp}{\lambda_\parallel} \sqrt{\frac{\chi_\perp}{\chi_\parallel}} v.$$

We show the influence of the finite Larmor radii in Fig. 3.5. The anomalous diffusion rate is magnitudes smaller than the classical diffusion coefficient. Still an effect of the correction term can be observed, that shows a quadratic reduction of \bar{D}_{KP2} with $\bar{\rho}_L$.

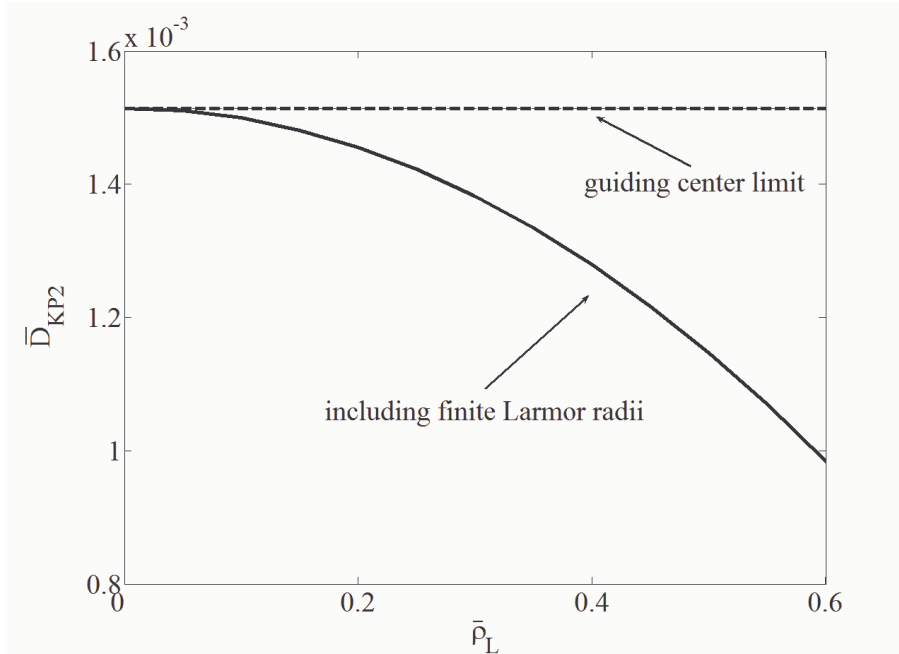


Figure 3.5: Influence of the Larmor radii on the Kadomtsev-Pogutse-II regime. We used here the values that lie within the conditions of this regime of $\kappa = 0.03$, $\bar{\chi}_\parallel = 10$ and $\bar{\chi}_\perp = 0.2$.

Though the classical transport coefficients in Fig. 3.5 have similar values as in the Rechester-Rosenbluth case, κ is small enough to satisfy the conditions for the Kadomtsev-Pogutse-II regime. Again, the reduction is antiproportional to λ_{\parallel} .

3.4 Particles in vanishing mean fields

3.4.1 Velocity correlation function for vanishing mean fields

So far we described the transport of particles in the presence of strong guiding fields and additional stochastic perturbations. The situation changes considerably when the mean (guiding) field is no longer present. The total B-field is then given by (2.3), and the particle transport takes place in a purely stochastic environment. Of course, the Larmor radius still exists and is now given by $\rho_L = v_t / (\Omega\beta)$. Some remarks on this case were already proposed in the appendix of [7]. We now present predictions for the collisional case.

The assumption of weak guiding fields simplifies the solution of the ALE. The rotational matrices are replaced by unity matrices and the operator V gets a simpler shape. Within this assumption the solution of the ALE reads,

$$\mathbf{u}(t) = G(0, t) \boldsymbol{\eta}(t). \quad (3.65)$$

It is not surprising that we have only one relevant component, as G is significantly reduced,

$$G(0, t) = T \left[\exp \left(\int_0^t V dt \right) \right], \quad V = -\Omega \begin{pmatrix} 0 & -b_z & b_y \\ b_z & 0 & -b_x \\ -b_y & b_x & 0 \end{pmatrix}. \quad (3.66)$$

The velocity correlator is given by the product $\mathbf{u}(t) \mathbf{u}(0)$ and has to be averaged over all stochastic variables,

$$\langle \mathbf{u}(t) \mathbf{u}(0) \rangle = \langle \langle \langle G(0, t) \boldsymbol{\eta}(t) \boldsymbol{\eta}(0) \rangle_b \rangle_{\parallel} \rangle_{\perp}. \quad (3.67)$$

We assume that the averages over the collisions $\boldsymbol{\eta}$ (we can no longer distinguish any directions) and the b -field in G can now be applied independently, yielding

$$\langle \mathbf{u}(t) \mathbf{u}(0) \rangle_{b \perp \parallel} = \langle G(0, t) \rangle_{b \perp \parallel} \langle \langle \boldsymbol{\eta}(t) \boldsymbol{\eta}(0) \rangle_{\parallel} \rangle_{\perp}. \quad (3.68)$$

3.4.2 The relaxation function γ

The average of the propagator is obtained by a cumulant expansion in the exponential. Using

$$\langle V(\tau') V(\tau'') \rangle_b = \Omega^2 \begin{pmatrix} -\langle b_y(\tau') b_y(\tau'') \rangle_b & 0 & 0 \\ -\langle b_z(\tau') b_z(\tau'') \rangle_b & -\langle b_z(\tau') b_z(\tau'') \rangle_b & 0 \\ 0 & -\langle b_x(\tau') b_x(\tau'') \rangle_b & -\langle b_x(\tau') b_x(\tau'') \rangle_b \\ 0 & 0 & -\langle b_y(\tau') b_y(\tau'') \rangle_b \end{pmatrix} \quad (3.69)$$

and $\langle b_x(\tau') b_x(\tau'') \rangle_b = \langle b_y(\tau') b_y(\tau'') \rangle_b = \langle b_z(\tau') b_z(\tau'') \rangle_b$ we finally get

$$\langle G(0, t) \rangle_{b_{\perp \parallel}} = \exp \left\{ -2 \Omega^2 \int_0^t \int_0^t \langle \langle b(\tau') b(\tau'') \rangle_b \rangle_{\perp \parallel} d\tau' d\tau'' \right\} \mathbf{1}. \quad (3.70)$$

The integration is not performed directly. We first assume that the magnetic fluctuations converge into a linear and diffusive state,

$$\langle G(0, t) \rangle_{b_{\perp \parallel}} = \exp(-2 \Omega^2 \gamma t). \quad (3.71)$$

defining the function $\gamma(t)$ as

$$\gamma(t) = \int_0^\infty \langle \langle b(\tau) b(0) \rangle_b \rangle_{\perp \parallel} d\tau. \quad (3.72)$$

We call $\gamma(t)$ the relaxation function. A similar definition can be found in the works of Kubo [20]. With the Corrsin approximation we can find estimates for this function, as the Kubo number is now equal to β/b_0 . Because there is no predominating direction in the weak field case and all directions can be treated on equal basis, the one-dimensional analysis is sufficient. The collisional diffusion coefficient for each direction is given by $\chi = \frac{v_e^2}{2\nu}$. With the cumulant expansion and the assumption of collisional diffusivity, $\langle \delta x^2 \rangle = 2 \chi t$,

$$\gamma = \int_0^\infty \int_{k \rho_L > 2\pi} \tilde{\mathcal{E}}(k) \exp\left[-\frac{1}{2} k^2 \chi \tau\right] dk d\tau. \quad (3.73)$$

Essential for the calculation is a heuristic estimate of the effective integration region, namely that the Larmor radius of the particles has to be larger than the wavelength of the modes in (3.65). Because the particles follow the field lines when their Larmor radius is smaller than the wavelength of the modes, we consider only the modes with $k > 2\pi/\rho_L$. This argument was successfully applied by Casse et al. in [7] in a comparable situation.

The integral over k should be evaluated as follows. Split the integration into two parts and neglect the interval $]-2\pi/\rho_L, 2\pi/\rho_L[$,

$$\begin{aligned} \gamma &= \int_0^\infty \left\{ \int_{2\pi/\rho_L}^\infty \tilde{\mathcal{E}}(k) \exp\left[-\frac{1}{2} k^2 \chi \tau\right] dk \right. \\ &\quad \left. - \int_{-2\pi/\rho_L}^{-\infty} \tilde{\mathcal{E}}(k) \exp\left[-\frac{1}{2} k^2 \chi \tau\right] dk \right\} d\tau. \end{aligned} \quad (3.74)$$

This leads to,

$$\gamma = \beta^2 \int_0^{\infty} \frac{\operatorname{erfc}\left[\frac{\sqrt{2} \pi \lambda \sqrt{1 + \frac{\chi \tau}{\lambda^2}}}{\rho_L}\right]}{\sqrt{1 + \frac{\chi \tau}{\lambda^2}}} d\tau. \quad (3.75)$$

This can be written as

$$\gamma = \frac{\sqrt{2} \pi \beta^2 \lambda}{\rho_L} \int_0^{\infty} \frac{\rho_L \operatorname{erfc}\left[\frac{\sqrt{2} \pi \lambda \sqrt{1 + \frac{\chi \tau}{\lambda^2}}}{\rho_L}\right]}{\sqrt{2} \pi \lambda \sqrt{1 + \frac{\chi \tau}{\lambda^2}}} d\tau. \quad (3.76)$$

The integrand can be approximated for real arguments and with $x \neq 0$ by $\operatorname{erfc}(x)/x \approx e^{-x^2}/x$ and becomes integrable,

$$\gamma = \frac{\sqrt{2} \pi \lambda}{\rho_L} \int_0^{\infty} \frac{\rho_L \exp\left[-\left(\frac{\sqrt{2} \pi \lambda \sqrt{1 + \frac{\chi \tau}{\lambda^2}}}{\rho_L}\right)^2\right]}{\sqrt{2} \pi \lambda \sqrt{1 + \frac{\chi \tau}{\lambda^2}}} d\tau, \quad (3.77)$$

and yields,

$$\gamma = \frac{\beta^2 \lambda \rho_L \operatorname{erfc}\left[\frac{\sqrt{2} \pi \lambda}{\rho_L}\right]}{\sqrt{2 \pi} \chi} = \frac{2 \beta^2 \lambda \nu}{\sqrt{2 \pi} \rho_L \Omega^2} \operatorname{erfc}\left[\frac{\sqrt{2} \pi \lambda}{\rho_L}\right]. \quad (3.78)$$

3.4.3 The transport coefficients for vanishing mean field regimes

Together with the definition of the propagator, we get the final MSD equation. Introducing Eq. (3.78) with (3.71) and (3.68) into the Green-Kubo formula, we immediately find asymptotic results for the MSD, as γ appears as a correction to the friction ν ,

$$\frac{d^2 \langle \delta x^2 \rangle}{dt^2} = \langle u(t) u(0) \rangle_{b \perp \parallel} = \frac{\nu_t^2}{2} e^{-\nu t - 2 \Omega^2 \gamma t}. \quad (3.79)$$

The solution of this differential equation is equal to the integration for classical transport and leads to

$$\langle \delta x^2 \rangle = \frac{\nu_t^2}{(\nu + 2 \Omega^2 \gamma)} t. \quad (3.80)$$

Small stochastic perturbation fields act like a collisions. They introduce friction-like deviations between particle and field and reduce the diffusion in the same way as the collisional frequency ν . The asymptotic diffusion coefficient can be deduced from (3.80),

$$D = \frac{v_t^2}{2(\nu + 2\Omega^2 \gamma)}. \quad (3.81)$$

We introduce dimensionless quantities, by dividing the classical diffusion coefficient χ and substituting expression (3.78),

$$\frac{D}{\chi} = \frac{1}{\left(1 + \frac{4\lambda}{\sqrt{2\pi} \rho_L} \operatorname{erfc}\left(\frac{\sqrt{2}\pi\lambda}{\rho_L}\right)\right)}. \quad (3.82)$$

The effect of the stochastic magnetic field is shown in Fig. 3.6, where the diffusion coefficient is given as a function of the dimensionless correlation length λ/ρ_L . Diffusion is reduced, compared to the classical rate, for a certain values of λ/ρ_L . This can be understood mainly as an effect of the correlation length: for large correlation lengths the magnetic field will not change and the particles are not affected by the field. A maximum of the magnetic influences is found for $\lambda/\rho_L \approx 0.1$. The spatial random variation of the magnetic field can be responsible for the random interactions between particle and field. They induce forces that are comparable to collisions that are described by the additional virtual friction term in the diffusion coefficient.

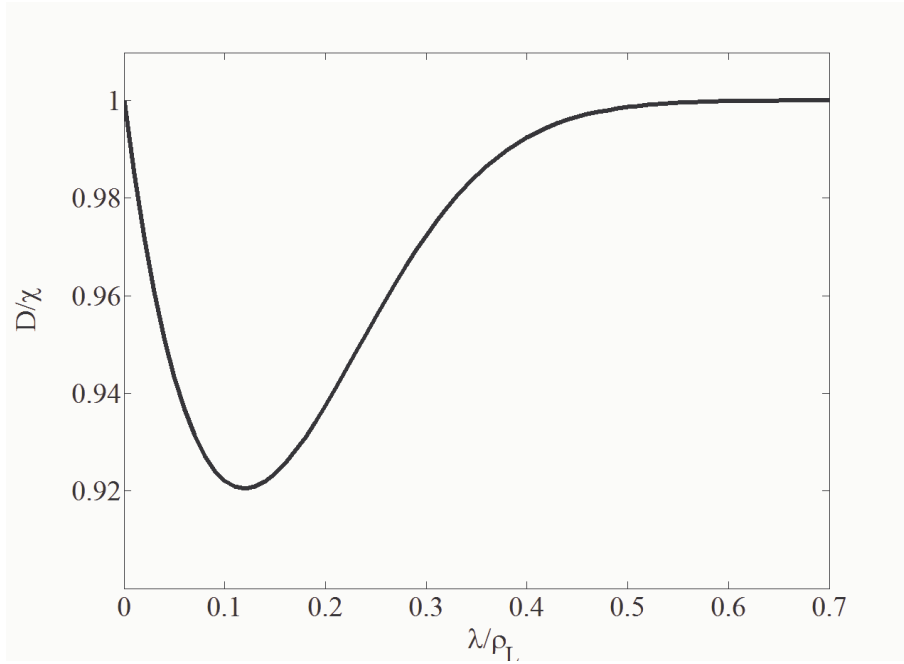


Figure 3.6: Ratio of the diffusion coefficient defined in (3.80) as a function of the reduced correlation length λ/ρ_L .

3.5 The Kubo number restriction of the Corrsin approximation

The Corrsin approximation is restricted to a certain domain of validity, defined in terms of the Kubo number (1.6). The Kubo number is generally defined as the ratio of the distance a particle travels during an autocorrelation time and the correlation distance. Large Kubo numbers $\kappa > 1$ lead to a failure of the independence hypothesis, and in this case Corrsin estimates give the wrong correlation behavior. Some recent works of Vlad et.al. [17,18,19,21] presented suitable replacements for the Corrsin approximation which are also valid for larger Kubo numbers. As a matter of fact, the decorrelation trajectory method (DCT) is more involved and its application within the A-Langevin framework will be presented in Sec. 4. Then our framework is extended to the percolative regimes.

For all results obtained within the Corrsin conjecture we are restricted to $\kappa \ll 1$.

A further, completely equivalent method is the MDIA, the modified interaction approximation discussed by Vanden-Eijnden et al. in [12]. It also uses the independence hypothesis and is restricted to the same ranges of turbulence as the Corrsin approximation.

4 Transport in percolative magnetic environments

4.1 Percolative magnetic structures and the DCT

4.1.1 The flux function ϕ and the trapping effect in percolative structures

We start our description of the stochastic properties of the magnetic field \mathbf{b} from a slightly different point of view. The perturbation field \mathbf{b} is now assumed to have only a two-dimensional structure. For sufficiently strong guiding fields, this condition is always fulfilled. Such a stochastic field \mathbf{b} is generated by the scalar magnetic potential $\phi(\mathbf{x}, z)$,

$$\mathbf{b}(\mathbf{x}, z) = \nabla\phi(\mathbf{x}, z) \times \mathbf{e}_z; \quad (4.1)$$

ϕ will be called flux function [18]. The vector $\mathbf{x} = (x, y)$ refers to the perpendicular coordinates, whereas z can be regarded as the parallel component. Magnetic field lines are determined by the flux function using the relation $d\mathbf{x}/dz = \mathbf{b}$. It yields two Hamiltonian-type equations for the field line motion

$$\frac{dx}{dz} = \frac{\partial\phi}{\partial y}, \quad \frac{dy}{dz} = -\frac{\partial\phi}{\partial x}. \quad (4.2)$$

For large Kubo numbers $\kappa = \beta\lambda_{\parallel}/(b_0\lambda_{\perp})$ we may assume that ϕ depends on z very slowly, so the partial derivative with z is zero, $\partial\phi/\partial z = 0$. From this condition and Eq. (4.2) it follows that the field lines have to remain on the equipotential lines of ϕ . We have for a field line trajectory

$$\frac{d\phi}{dz} \approx \frac{\partial\phi}{\partial x} \frac{dx}{dz} + \frac{\partial\phi}{\partial y} \frac{dy}{dz} = -\frac{dy}{dz} \frac{dx}{dz} + \frac{dx}{dz} \frac{dy}{dz} = 0. \quad (4.3)$$

In Fig. 4.1 we show a typical contour plot of ϕ as a function of the coordinates x and y , as two contour lines associated with the constant levels of ϕ . The initial value of ϕ will be called ϕ^0 . Depending on this level, the above condition implies that a fictive particle may be free to cross the topographical map (a), or may be trapped for certain ϕ^0 -values, which is shown in Fig. 4.1 as the line (b). For $\kappa \rightarrow \infty$, trapped field lines remain trapped. Smaller κ , for finite λ_{\parallel} , may lead to a detrapping with increasing z . When most lines are de-trapped after a correlation time, we are in the non-percolative limit.

Typically this situation is illustrated by the following analogy, [22,24]: ϕ is considered to be a landscape composed of hills and wells, which is filled with water to the level of ϕ^0 . If we start in the maximum of ϕ , where the landscape is completely flooded and decrease the waterlevel ϕ^0 , the number of hills increases as well as their dimensions.

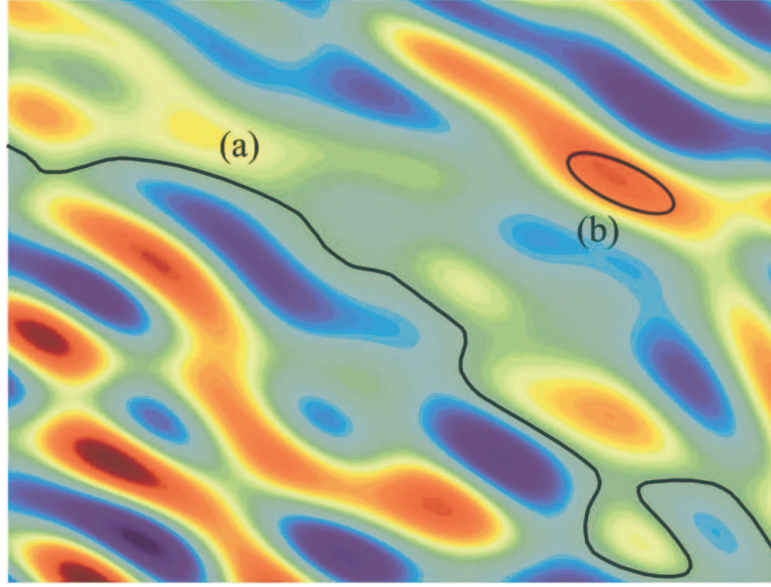


Figure 4.1: Contourplot of $\phi(x)$ plotted in an x - y -diagram for two realisations of field line motion, (a) a value of ϕ^0 near the threshold, where the field line can pass the complete topographical map and (b) the walk of a trapped field line near a potential extremum.

At certain levels the coalescence of different hills is observed, because ϕ^0 passes the hyperbolic points of the percolation map. Whenever such a coalescence takes place, the area and the contourline of the hill suddenly increase and with it the area along which a field line is allowed to travel. High Kubo numbers represent ϕ -regimes with distinct extremas, hence many hills. The particle diffusion is reduced essentially, because a certain number of particles remain in trapped states with their field lines. Such a particle contributes to the diffusion process again, if it is dislocated to a lower ϕ^0 value by a collision. Higher collisionality therefore reduces the trapping effect.

Contrary a situation with less hills or many united hills, a "smooth" landscape, is realized for small Kubo numbers. In such regimes trapping does not play an important role and is neglected. Our results from Sec. 3 belong to such a realisation.

If a potential is constant in t , or $z(t)$ respectively, it is called "frozen". Nearly all particles are then trapped around the hills and wells. Subdiffusive behaviour with $D \rightarrow 0$ emerges. The structure will change as the particle moves along the trajectory. The characteristic length of this process is the parallel correlation length λ_{\parallel} . For distances with $z \ll \lambda_{\parallel}$ the potential will not change at all. Figure 4.2 shows a three dimensional evolution of the x - y -contours of ϕ with z for $\lambda_{\parallel} > L$, where L is the maximal length in z . A notable alteration of the potential will happen on length scales predominantly longer than λ_{\parallel} . Here a nearly infinite parallel correlation length ensures the stability of the percolation structure along z . The lines of constant ϕ^0 do not change and form so called flux tubes [6]. Field lines stay on the equipotential lines and are forced to remain on the surfaces of the flux tubes.

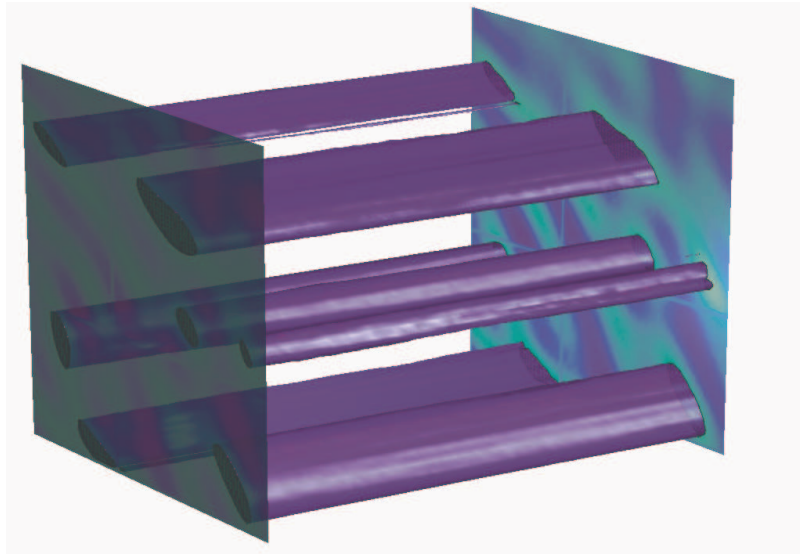


Figure 4.2: Flux structure illustration of the function ϕ in a regime with infinite high Kubo numbers, $\lambda_{\parallel} \rightarrow \infty$, $\beta = 0.2$ and $\lambda_{\perp} \ll 1$. Here the box length in x , y and z is $L = 1$.

In Fig. 4.3 we show the deformation of the flux tubes due to the variation of ϕ with z . In such a case the condition $\frac{\partial \phi}{\partial z} \approx 0$ is no longer valid, and field lines are no longer strictly bound to the lines of constant ϕ .

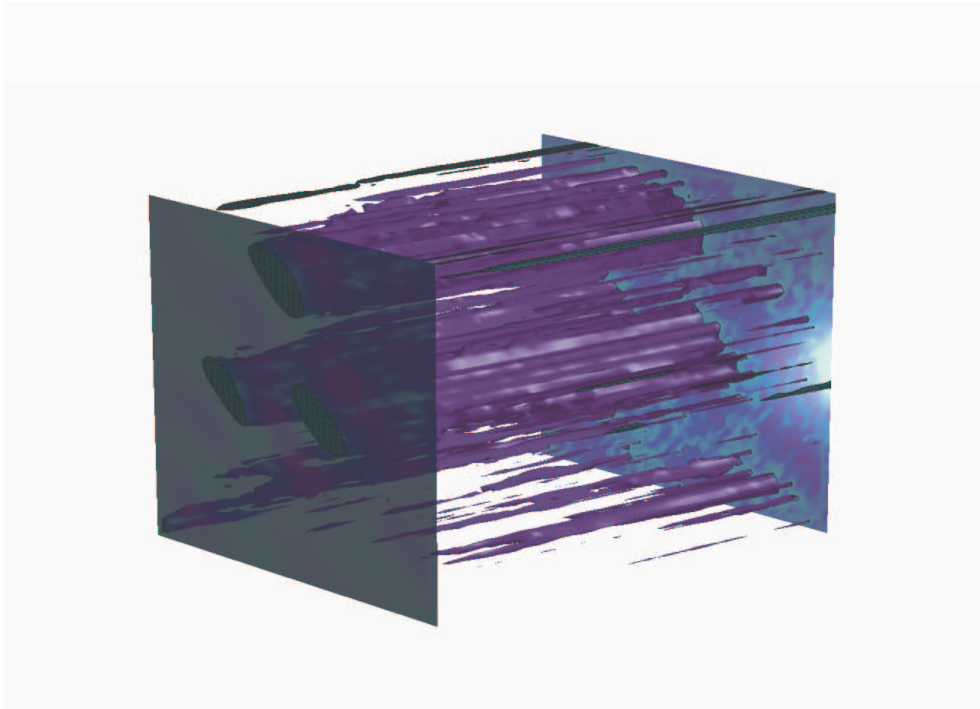


Figure 4.3: Flux decorrelation for small parallel correlation lengths, $\lambda_{\parallel} \approx \lambda_{\perp} < 1$ and $\beta = 0.2$. Flux tubes start to merge and new tubes emerge. The length of the box is $L = 1$.

Additionally, we now observe the case $L > \lambda_{\parallel}$. The tubes and with them their contourlines start to merge, so the field lines are allowed to explore larger areas of the ϕ map. Even new flux tubes emerge that join the other ones after certain distances z . The value of λ_{\parallel} belongs to situation with $\kappa \lesssim 1$. Field lines can nearly pass freely along the whole area and this state can be described with the Corrsin method.

Though the figures provide a good intuitive approach to understand the difficulties of the percolation regime, a detailed theory for this situation is needed. Effects of the percolation structure have to be included on the level of the flux function ϕ and so we proceed with the stochastic properties of this function.

4.1.2 The stochastic properties of the flux function ϕ

Of course, the flux-function itself is a stochastic object, too. Its correlation function is defined as,

$$A(\mathbf{x}, z) = \langle \phi(\mathbf{0}, 0) \phi(\mathbf{x}, z) \rangle = \beta^2 \lambda_{\perp}^2 \exp[-\Theta(\mathbf{x}, z)], \quad (4.4)$$

with the phase Θ

$$\Theta(\mathbf{x}, z) \equiv \frac{x^2 + y^2}{2\lambda_{\perp}^2} + \frac{z^2}{2\lambda_{\parallel}^2}. \quad (4.5)$$

In the previous section, we derived the LCF from the Eulerian correlator of the \mathbf{b} -field. The Eulerian correlation of the perturbation field \mathbf{b} is defined by

$$\mathcal{E} \equiv \langle \mathbf{b}(0) \otimes \mathbf{b}(x) \rangle = \langle (\nabla \times \phi \mathbf{e}_z) \otimes (\nabla \times \phi \mathbf{e}_z) \rangle = \begin{pmatrix} -\partial_{yy} A & \partial_{yx} A \\ \partial_{xy} A & -\partial_{xx} A \end{pmatrix} \equiv \begin{pmatrix} \mathcal{E}_{xx} & \mathcal{E}_{xy} \\ \mathcal{E}_{yx} & \mathcal{E}_{yy} \end{pmatrix}. \quad (4.6)$$

Additional cross-correlations [20] between the \mathbf{b} -field and the flux function ϕ are given by

$$\mathcal{E}_{\phi x} \equiv \langle \phi(0) b_x(\mathbf{x}, t) \rangle = -\partial_y A = -\mathcal{E}_{x\phi}, \quad \mathcal{E}_{y\phi} = -\mathcal{E}_{\phi x} = -\partial_x A. \quad (4.7)$$

Correlations of the derivatives with respect to the time t are denoted by a bar and are given by

$$\bar{\mathcal{E}}_{ii} \equiv \langle b_i'(t_1) b_i'(t_2) \rangle = \frac{d^2}{dt_1 dt_2} \langle b_i(t_1) b_i(t_2) \rangle. \quad (4.8)$$

We have

$$\begin{aligned}
\bar{A} &= \left(\frac{d^2}{dt_1 dt_2} A(x(t_1) - x(t_2), z(t_1) - z(t_2)) \right)_{\substack{t_1=t \\ t_2=0}} \\
&= \left\{ \left(\beta^2 - \frac{x^2 \beta^2}{\lambda^2} \right) \eta_x^0 \eta_x(t) + \left(\beta^2 - \frac{y^2 \beta^2}{\lambda^2} \right) \eta_y^0 \eta_y(t) + \left(\frac{\beta^2 \lambda^2}{l^2} - \frac{z^2 \beta^2 \lambda^2}{l^4} \right) \eta_z^0 \eta_z(t) \right\} \\
&\quad \times \exp[-\Theta(\mathbf{x}, z)],
\end{aligned} \tag{4.9}$$

yielding the correlation matrix

$$\bar{\mathcal{E}} = \begin{pmatrix} -\partial_{yy} \bar{A} & \partial_{yx} \bar{A} \\ \partial_{xy} \bar{A} & -\partial_{xx} \bar{A} \end{pmatrix} \tag{4.10}$$

by applying (4.8). We also used the property of the $\boldsymbol{\eta}$ -velocities that cross-correlations of the velocities, $\langle \eta_x(0) \eta_y(t) \rangle_{\perp} = 0$, vanish. The same reason causes $\mathcal{E}_{\phi b'} = \langle \phi(0) b_x'(t) \rangle = 0$, because only single η_i -elements appear.

4.2 The decorrelation trajectory approximation (DCT)

4.2.1 The subensemble decomposition of the Eulerian correlator

We have seen in Sec. 4.1 that the ϕ structure influences the transport decisively. The Corrsin approximation lacks the ability to include this influence. The position in the ϕ -map, characterized by ϕ^0 , b_x^0 and b_y^0 determines whether the field line can pass through large areas or is trapped. Now we collect a set of trajectories with the same distinct potential level ϕ^0 and b -field \mathbf{b}^0 at the position $\mathbf{x} = 0$. This set will be referred to as a subensemble $S(\phi^0, \mathbf{b}^0)$ [18,19,20]. An infinite number of these subensembles exists to include any possible magnetic field configuration. Indeed there will be ensembles with certain values of the magnetic parameters that allow trapping.

The ECF is now separated into contributions from each of these subensembles $S(\phi^0, \mathbf{b}^0)$ with the initial conditions $\phi^0 = \phi(0)$ and $\mathbf{b}^0 = \mathbf{b}(0)$. The complete ECF has then to be the superposition of all possible subensembles, expressed in terms of the integral

$$\mathcal{E}(\mathbf{x}) = \int_{-\infty}^{\infty} \int_{-\infty}^{\infty} d\phi^0 d\mathbf{b}^0 P(\mathbf{b}^0, \phi^0) \langle \mathbf{b}(\mathbf{0}) \otimes \mathbf{b}(\mathbf{x}, z) \rangle_S. \quad (4.11)$$

The probability $P(\mathbf{b}^0, \phi^0)$ is given in terms of standard Gaussian distributions and describes the probability to find the parameters ϕ^0 and \mathbf{b}^0 as well as it measures the contribution of the subensemble to the integral. All possible configurations in ϕ^0 and \mathbf{b}^0 are covered by the integration. So far we have only the subensemble description of the magnetic field alone, a pure magnetic field correlation function. We recall the velocity correlation found for strong guiding fields,

$$\langle \langle u_x(t_1) u_x(t_2) \rangle_{\mathbf{b}} \rangle_{\perp} \equiv \langle \eta_x(t_1) \eta_x(t_2) \rangle_{\perp} + \mathcal{L}^{(0)}[\mathbf{x}, z, t] + \mathcal{L}^{(1)}[\mathbf{x}, z, t], \quad (4.12)$$

with

$$\begin{aligned} \mathcal{L}^{(0)} &= \frac{1}{b_0^2} \langle \eta_z(t_1) \eta_z(t_2) \langle \langle b_y[\mathbf{x}(t_1)] b_y[\mathbf{x}(t_2)] \rangle_{\mathbf{b}} \rangle_{\perp} \rangle_{\parallel}, \\ \mathcal{L}^{(1)} &= \frac{\rho L^2}{v_i^2 b_0^2} \langle \eta_z(t_1) \eta_z(t_2) \langle \langle b_y'[\mathbf{x}(t_1)] b_y'[\mathbf{x}(t_2)] \rangle_{\mathbf{b}} \rangle_{\perp} \rangle_{\parallel}. \end{aligned} \quad (4.13)$$

It is evident, that the parallel collisional velocity modelled by η_z have also to be taken into account. The subensemble representations of the contributions from anomalous transport in the Eulerian correlator should read

$$\begin{aligned} \mathcal{L}_{\text{DCT}}^{(0)} &= \frac{1}{b_0^2} \int_{-\infty}^{\infty} \int_{-\infty}^{\infty} \int_{-\infty}^{\infty} P(\eta^0) P(\mathbf{b}^0) P(\phi^0) \eta^0 b_y^0 \\ &\times \langle \langle \eta_{\parallel}(t) b_y [\mathbf{x}(t), z(t), t] \rangle_S \rangle_{\perp} d\eta_z^0 d\mathbf{b}^0 d\phi^0, \end{aligned} \quad (4.14)$$

and

$$\begin{aligned} \mathcal{L}_{\text{DCT}}^{(1)} &= \left\langle \frac{\rho L^2}{v_t^2 b_0^2} \int_{-\infty}^{\infty} \int_{-\infty}^{\infty} \int_{-\infty}^{\infty} \int_{-\infty}^{\infty} \int_{-\infty}^{\infty} P(\eta_x^0) P(\eta_y^0) P(\eta_z^0) P(\mathbf{b}^0) P(\phi^0) \times \right. \\ &\left. \times \eta^0 b_y^0 \langle \eta_{\parallel}(t) b_y [\mathbf{x}(t), z(t), t] \rangle_S d\eta_x^0 d\eta_y^0 d\eta_z^0 d\mathbf{b}^0 d\phi^0 \right\rangle_{\perp}. \end{aligned} \quad (4.15)$$

We added the index DCT to denote the origin of the approximation technique and to distinguish the new correlation functions from the ones derived in Sec. 3.

Until this point Eqs. (4.15) and (4.16) remain exact and no approximation has been applied. Unfortunately, the same problem occurs that we encountered in the Corrsin approximation: We do not know the exact trajectory $\mathbf{r} = (\mathbf{x}, z)$. But the decomposition leads to a slightly different view. In each subensemble, the values of ϕ^0 , η^0 and \mathbf{b}^0 are fixed. Within a subensemble we can determine each trajectory for a mean field $\langle \mathbf{b}(\mathbf{x}, z) \rangle_S$ by solving the A-Langevin equation. The crucial simplification of this technique is that all contributions from the magnetic field are non-stochastic values.

The major approximation of the DCT [18] and therefore the transition from the Eulerian to the Lagrangian perspective, is to evaluate the formulas (4.15) or (4.16) by estimating the unknown trajectory $\mathbf{x}(t)$ with the decorrelation trajectory,

$$\mathbf{x}(t) \approx \mathbf{X}(t). \quad (4.16)$$

$\mathbf{X}(t)$ is the fictitious trajectory, along which a particle would travel if it is introduced into the subensemble magnetic mean field, is called the decorrelation trajectory. It is then substituted into the expression for the averaged field $\langle \mathbf{b}(\mathbf{x} = \mathbf{X}, z) \rangle_S$ and with the trajectory $\mathbf{X}(t)$ given by the A-Langevin equation, Eqs. (4.15) and (4.16) determine the Lagrangian velocity correlator. Our first task is now to find the average $\langle \mathbf{b}(\mathbf{x}, z) \rangle_S$ in each subensemble defined by \mathbf{b}^0 and ϕ^0 . Additionally we need expressions for the averages occurring in the DCT equations.

The DCT itself is given by the A-Langevin equation

$$\ddot{\mathbf{X}}(t) = \dot{\mathbf{U}}(t) = \frac{Ze}{mc} \mathbf{U}(t) \times \{B_0 [b_0 \mathbf{e}_z + \langle \mathbf{b}(\mathbf{x}, z) \rangle_S]\} - \nu \mathbf{U}(t) + \mathbf{a}(t), \quad (4.17)$$

containing the non-stochastic subensemble average $\langle \mathbf{b}(\mathbf{x}, z) \rangle_S$. Of course the collisions \mathbf{a} are still a stochastic quantity. In Fig. 4.4 we illustrated two solutions of this equation for a fixed

value of $\langle \mathbf{b}(\mathbf{x}, z) \rangle_S$. Two cases are shown, (a) without collisions and (b) with collisions. Beneath the typical Larmor orbit ρ_L , we observe in both cases an additional cyclic (in x and y directions) motion due to the averaged perturbation field. Of course, decorrelation trajectories from the V-Langevin equations do not contain the gyro-motion and are given by the motion of the trapped field line alone.

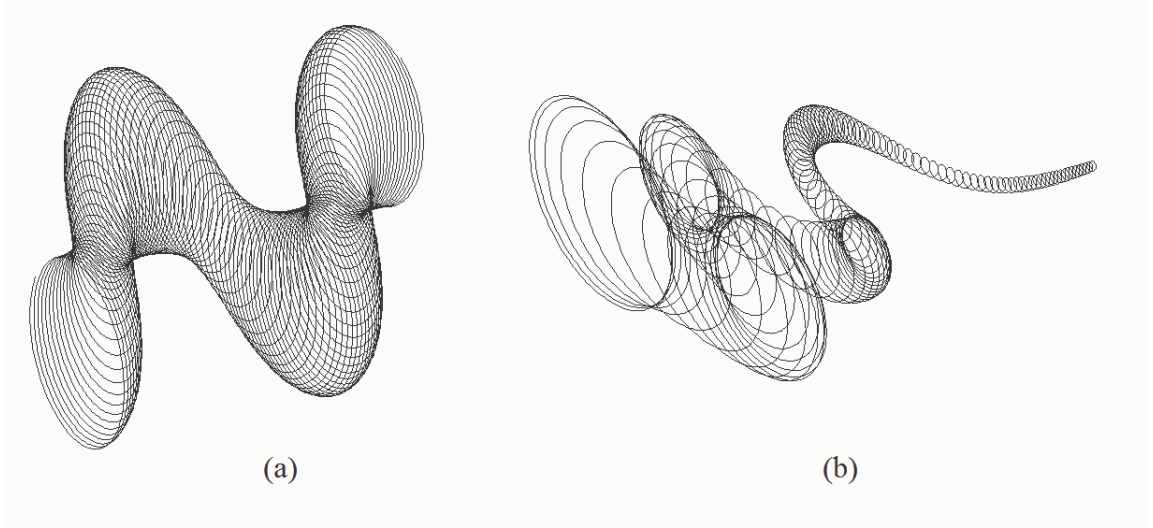


Figure 4.4: Two examples of decorrelation trajectories derived by a numerical solution of (4.18). The vector $\mathbf{R}(t)$ is plotted for (a) no collisions $\nu = 0$ and (b) with collisions $\nu = 0.02$. We used an area of a random magnetic potential in which already trapping is observed. The smaller cyclic motion represents the Larmor orbit of the particle.

We already connected the winding of the field lines around the ϕ -maximums to a trapping effect. Case (b) confirms our heuristic argument that the collisions will reduce the trapping because the winding goes not on forever. It is stopped by the frictional term in (4.18).

4.2.2 Averaged b -field in a subensemble

Each subensemble has an averaged b -field. We can calculate this average by using the conditional probability to be within the subensemble defined by ϕ^0 and \mathbf{b}^0 and having a b -field \mathbf{b} at the position \mathbf{x} ,

$$\langle \mathbf{b}(\mathbf{x}, z) \rangle_S = \int_{-\infty}^{\infty} d\mathbf{b} \mathbf{b} P(\mathbf{b}, \mathbf{x} | \phi^0 \mathbf{b}^0), \quad (4.18)$$

introducing,

$$P(\mathbf{b}, \mathbf{x} | \phi^0 \mathbf{b}^0) = \frac{\langle \delta(\mathbf{b} - \mathbf{b}(\mathbf{x}, z, t)) \delta(\phi^0 - \phi(\mathbf{0})) \delta(\mathbf{b}^0 - \mathbf{b}(\mathbf{0})) \rangle_S}{\langle \delta(\phi^0 - \phi(\mathbf{0})) \delta(\mathbf{b}^0 - \mathbf{b}(\mathbf{0})) \rangle_S}. \quad (4.19)$$

We want to simplify this expression further and evaluate the terms with the Fourier transformation of the δ -function,

$$\begin{aligned} \langle \delta(\mathbf{b} - \mathbf{b}(\mathbf{x}, t)) \delta(\phi^0 - \phi(\mathbf{0})) \delta(\mathbf{b}^0 - \mathbf{b}(\mathbf{0})) \rangle = \\ \int_{-\infty}^{\infty} \int_{-\infty}^{\infty} \int_{-\infty}^{\infty} \exp(i\mathbf{a}_1 \mathbf{b} + i\mathbf{a}_2 \mathbf{b}^0 + i\mathbf{a}_3 \phi^0) \\ \times \langle \exp(-i\mathbf{a}_1 \mathbf{b}(\mathbf{x}) - i\mathbf{a}_2 \mathbf{b}(\mathbf{0}) - i\mathbf{a}_3 \phi(\mathbf{0})) \rangle d\mathbf{a}_1 d\mathbf{a}_2 d\mathbf{a}_3. \end{aligned} \quad (4.20)$$

The exponential function from the Fourier representation helps us, similar as in Sec. 3, to apply the cumulant expansion,

$$\begin{aligned} \langle \exp(-i\mathbf{a}_1 \mathbf{b}(\mathbf{x}) - i\mathbf{a}_2 \mathbf{b}(\mathbf{0}) - i\mathbf{a}_3 \phi(\mathbf{0})) \rangle = \\ = \exp\left\{-\frac{1}{2} \langle (\mathbf{a}_1 \mathbf{b}(\mathbf{x}) + \mathbf{a}_2 \mathbf{b}(\mathbf{0}) + \mathbf{a}_3 \phi(\mathbf{0}))^2 \rangle\right\} \\ = \exp\left\{-\frac{1}{2} [a_{1,i}^2 \langle b_i b_i \rangle + a_{2,i}^2 \langle b_i b_i \rangle + \right. \\ \left. + a_3^2 \langle \phi \phi \rangle + 2 a_3 a_{1,i} \langle \phi b_i \rangle + 2 a_3 a_{2,i} \langle \phi, b_i \rangle + 2 a_{1,i} a_{2,j} \langle b_i b_j \rangle]\right\}. \end{aligned} \quad (4.21)$$

We can substitute this result into the integration (4.21), which yields similar as in appendix C.1 a mean perturbation field,

$$\langle \mathbf{b}(x, y) \rangle_S = \begin{pmatrix} b_x^0 \mathcal{E}_{xx} + b_y^0 \mathcal{E}_{xy} + \phi^0 \mathcal{E}_{\phi x} \\ b_x^0 \mathcal{E}_{yx} + b_y^0 \mathcal{E}_{yy} + \phi^0 \mathcal{E}_{\phi y} \end{pmatrix}. \quad (4.22)$$

Introducing the expressions for the \mathcal{E}_{ij} and separating the parallel dependencies in the averaged \mathbf{b} -field, using

$$\langle \mathbf{b}(x, y) \rangle_S = \mathbf{F}(\mathbf{x}) e^{-\Theta(0,z)} \quad (4.23)$$

the components of \mathbf{F} are given by

$$\begin{aligned} F_x(\mathbf{x}, \lambda_{\perp}) &= -\frac{\beta^2}{\lambda^2} \{y \lambda_{\perp}^2 \phi^0 + (y^2 - \lambda_{\perp}^2) b_x^0 - x y b_y^0\} e^{-\Theta(x,0)}, \\ F_y(\mathbf{x}, \lambda_{\perp}) &= \frac{\beta^2}{\lambda^2} \{x \lambda_{\perp}^2 \phi^0 + x y b_x^0 + (\lambda_{\perp}^2 - x^2) b_y^0\} e^{-\Theta(x,0)}. \end{aligned} \quad (4.24)$$

In our analysis of the DCT terms, we need only the y -component of \mathbf{F} . In summary:

- We derived a subensemble decomposition of the Eulerian correlation function for the magnetic field and for the velocity of a particle.
- Both decompositions depend on the averaged \mathbf{b} -field in each subensemble.
- This average, \mathbf{F} , is given as a function of \mathbf{x} and z .

A very similar result is obtained for the averaged derivative in the subensemble,

$$\langle \mathbf{b}'(x, y) \rangle_S = \begin{pmatrix} b_x^{i0} \mathcal{E}_{x'x'} + b_y^{i0} \mathcal{E}_{x'y'} \\ b_x^{i0} \mathcal{E}_{y'x'} + b_y^{i0} \mathcal{E}_{y'y'} \end{pmatrix}. \quad (4.25)$$

Note that the ϕ^0 -part vanishes. Using the definitions of the derivative correlations we immediately find for the x -component

$$\langle b_x'(x, y) \rangle_S = \{T_1(\mathbf{x}) \eta_x^0 \eta_x(t) + T_2(\mathbf{x}) \eta_y^0 \eta_y(t) + T_3(\mathbf{x}) \eta_z^0 \eta_z(t)\} e^{-\frac{z^2}{2\lambda_{\parallel}^2}}, \quad (4.26)$$

with the definition

$$T_1(\mathbf{x}, \lambda_{\perp}) = \left(\frac{x^2 y^2 \beta^2 b_x^{i0}}{\lambda_{\perp}^6} - \frac{x^2 \beta^2 b_x^{i0}}{\lambda_{\perp}^4} - \frac{y^2 \beta^2 b_x^{i0}}{\lambda_{\perp}^4} + \frac{\beta^2 b_x^{i0}}{\lambda_{\perp}^2} - \frac{x^3 y \beta^2 b_y^{i0}}{\lambda_{\perp}^6} + \frac{3xy \beta^2 b_y^{i0}}{\lambda_{\perp}^4} \right) \times e^{-\frac{x^2}{2\lambda_{\perp}^2} - \frac{y^2}{2\lambda_{\perp}^2}}, \quad (4.27)$$

$$T_2(\mathbf{x}, \lambda_{\perp}) = \left(\frac{y^4 \beta^2 b_x^{i0}}{\lambda_{\perp}^6} - \frac{6y^2 \beta^2 b_x^{i0}}{\lambda_{\perp}^4} + \frac{3\beta^2 b_x^{i0}}{\lambda_{\perp}^2} - \frac{xy^3 \beta^2 b_y^{i0}}{\lambda_{\perp}^6} + \frac{3xy \beta^2 b_y^{i0}}{\lambda_{\perp}^4} \right) \times e^{-\frac{x^2}{2\lambda_{\perp}^2} - \frac{y^2}{2\lambda_{\perp}^2}}, \quad (4.28)$$

$$T_3(\mathbf{x}, \lambda_{\perp}) = \left(\frac{\beta^2 b_x^{i0}}{\lambda_{\parallel}^2} - \frac{z^2 \beta^2 b_x^{i0}}{\lambda_{\parallel}^4} - \frac{y^2 \beta^2 b_x^{i0}}{\lambda_{\parallel}^2 \lambda_{\perp}^2} + \frac{y^2 z^2 \beta^2 b_x^{i0}}{\lambda_{\parallel}^4 \lambda_{\perp}^2} + \frac{xy \beta^2 b_y^{i0}}{\lambda_{\parallel}^2 \lambda_{\perp}^2} - \frac{xyz^2 \beta^2 b_y^{i0}}{\lambda_{\parallel}^4 \lambda_{\perp}^2} \right) \times e^{-\frac{x^2}{2\lambda_{\perp}^2} - \frac{y^2}{2\lambda_{\perp}^2}}. \quad (4.29)$$

4.2.3 Conditional averages for perpendicular and parallel motion

The perpendicular average

We will explain the averaging procedures by beginning with a simple example for a one dimensional case. The average of perpendicular collisions is incorporated in the following way: We use the coordinate transformation, see e.g. [20], $\tilde{x}(t) = x(t) + \xi_x(t)$ and define ξ_x to be responsible for all perpendicular deviations from the trajectory. With this definition an arbitrary Eulerian correlation function \mathcal{E} has to be calculated by

$$\langle \mathcal{E}(x, z) \rangle_{\perp} = \int_{-\infty}^{\infty} \mathcal{E}(x + \xi_x) \langle \delta(\xi_x - \xi_x(t)) \rangle_{\perp} d\xi_x. \quad (4.30)$$

This formulation is identical to the relation derived within the Corrsin approximation. Indeed we apply an independence assumption here for the perpendicular part of the motion. Using the Fourier representation of the δ function we can easily find

$$\langle \delta(\xi_x - \xi_x(t)) \rangle_{\perp} = \frac{1}{\sqrt{2\pi \langle \xi^2(t) \rangle}} \exp\left(-\frac{\xi_x^2}{2 \langle \xi^2(t) \rangle_{\perp}}\right) \equiv P_{\perp}(\xi_x), \quad (4.31)$$

i.e. Gaussian distribution in ξ_x denoted by the symbol $P_{\perp}(\xi_x)$. Because of symmetry reasons we have $\langle \xi_x^2 \rangle = \langle \xi_y^2 \rangle \equiv \langle \xi^2(t) \rangle$. For the zeroth order we can apply the average at the very beginning of the calculation, namely on the Eulerian correlator,

$$\begin{aligned} \langle A(\mathbf{x}, z; \lambda_{\perp}) \rangle_{\perp} = \\ \int_{-\infty}^{\infty} \int_{-\infty}^{\infty} \beta^2 \lambda_{\perp}^2 \exp\left[-\frac{(x + \xi_x)^2 + (y + \xi_y)^2}{2\lambda_{\perp}^2} - \frac{z^2}{2\lambda_{\parallel}^2}\right] P(\xi_x) P(\xi_y) d\xi_x d\xi_y, \end{aligned} \quad (4.32)$$

This gives the averaged Eulerian correlation in the form,

$$\langle A(\mathbf{x}, z; \lambda_{\perp}) \rangle_{\perp} = \mathcal{N}_{\text{DCT}} A(\mathbf{x}, z; \lambda_{\perp} + \langle \xi^2(t) \rangle), \quad (4.33)$$

with

$$\mathcal{N}_{\text{DCT}} = \left(1 + \frac{\langle \xi^2(t) \rangle}{\lambda_{\perp}^2}\right)^{-1}, \quad (4.34)$$

which was already encountered in Sec. 3 in a similar form with the Corrsin method. Here the exponent of \mathcal{N}_{DCT} differs from the term found with the Corrsin approximation. This scaling does not change the scalings derived with \mathcal{N} -term.

Subensemble conditional averages

Now we focus on the combined averages needed in the DCT equations. The subensemble averages are obtained by accounting for the conditional averages in the following way:

$$\begin{aligned} \langle \langle \eta_{\parallel}(t) \mathbf{b}[\mathbf{x}(t), z(t), t] \rangle_S \rangle_{\perp} = & \int_{-\infty}^{\infty} \int_{-\infty}^{\infty} \int_{-\infty}^{\infty} \frac{\langle \eta_z(t) \delta(z - z(t)) \delta(\eta_z^0 - \eta_z(0)) \rangle_{\parallel}}{P(\eta_0)} \\ & \times \frac{\langle \langle \delta(b - b(\mathbf{x} + \boldsymbol{\xi}, z, t)) \delta(\phi^0 - \phi(\mathbf{0})) \delta(\mathbf{b}^0 - \mathbf{b}(\mathbf{0})) \rangle_S \delta(\xi_x - \xi_x(t)) \delta(\xi_y - \xi_y(t)) \rangle_{\perp}}{\langle \delta(\phi^0 - \phi(\mathbf{0})) \delta(\mathbf{b}^0 - \mathbf{b}(\mathbf{0})) \rangle_S} \\ & \times d\xi_x d\xi_y dz, \end{aligned} \quad (4.35)$$

as well as

$$\begin{aligned}
\langle \langle \eta_{\parallel}(t) \mathbf{b}'[\mathbf{x}(t), z(t), t] \rangle_S \rangle_{\perp} &= \int_{-\infty}^{\infty} \int_{-\infty}^{\infty} \int_{-\infty}^{\infty} \frac{\langle \eta_z(t) \delta(z - z(t)) \delta(\eta_z^0 - \eta_z(0)) \rangle_{\parallel}}{P(\eta_0)} \\
&\times \frac{\langle \langle \delta(\mathbf{b}' - \mathbf{b}'(\mathbf{x} + \boldsymbol{\xi}, z, t)) \delta(\mathbf{b}^0 - \mathbf{b}(\mathbf{0})) \rangle_S \delta(\xi_x - \xi_x(t)) \delta(\xi_y - \xi_y(t)) \rangle_{\perp}}{\langle \delta(\mathbf{b}^0 - \mathbf{b}(\mathbf{0})) \rangle_S} d\xi_x d\xi_y dz.
\end{aligned} \tag{4.36}$$

The procedure of averaging will be performed as follows: The first conditional average term in both expressions depends on η_z and takes the parallel motion into account that appears within the \mathbf{b} -field as well as in the velocity correlator itself. Similar to the treatment of the Corrsin approximation we are not allowed to make a stochastic independence assumption for these terms. Perpendicular averaging is performed by applying two δ functions for ξ_x and ξ_y and finally using the method presented above. Unfortunately this method becomes more elaborate for the derivative average. Because of the η_x and η_y product terms in (4.27) we need the same procedure as for the parallel motion. The subensemble averages of the \mathbf{b} field and its derivation were already calculated in the previous section.

Combined average for parallel motion

Next, we determine the conditional average for the parallel motion. Starting with the leading term in the integrals (4.35) and (4.36),

$$M_{\parallel}(z) \equiv \frac{\langle \eta_z(t) \delta(z - z(t)) \delta(\eta_z^0 - \eta_z(0)) \rangle_{\parallel}}{\langle \delta(\eta_z^0 - \eta_z(0)) \rangle_{\parallel}}, \tag{4.37}$$

we basically have to find a generalization to the method found in appendix B.2. The Fourier representation of the δ functions helps us to rewrite the stochastic data in form of exponential functions and yields the following integrations,

$$M_{\parallel}(z) = \frac{1}{2\pi P(\eta^0)} \int \int \exp[-ikz - iq\eta_z^0] \langle \eta_z(t) \exp[ikz(t) + iq\eta_z(0)] \rangle_{\parallel} dk dq. \tag{4.38}$$

To simplify the last expression, we define the function

$$\langle H_{\parallel} \rangle_{\parallel} \equiv \langle \exp[a\eta_z(t) + ikz(t) + iq\eta_z(0)] \rangle_{\parallel}. \tag{4.39}$$

It is related to the unknown average by

$$\langle \eta_z(t) \exp[ikz(t) + iq\eta_z(0)] \rangle_{\parallel} = \left[\left\langle \frac{\partial}{\partial a} H_{\parallel} \right\rangle_{\parallel} \right]_{a=0}. \tag{4.40}$$

In this form the parallel average is applied to H by the standard cumulant expansion,

$$\begin{aligned} \langle H_{\parallel} \rangle_{\parallel} = \exp \left(-\frac{a^2}{2} \langle \eta_z(t) \eta_z(t) \rangle_{\parallel} - \frac{k^2}{2} \langle z^2(t) \rangle_{\parallel} - \frac{q^2}{2} \langle \eta_z(0) \eta_z(0) \rangle_{\parallel} \right. \\ \left. + iaq \langle \eta_z(0) \eta_z(t) \rangle_{\parallel} - kq \langle z(t) \eta_z(0) \rangle_{\parallel} + iak \langle z(t) \eta_z(t) \rangle_{\parallel} \right) \end{aligned} \quad (4.41)$$

in which the well-known stochastic properties of η_z can be identified,

$$\begin{aligned} \langle \eta_z(t) \eta_z(t) \rangle_{\parallel} &= \langle \eta_z(0) \eta_z(0) \rangle_{\parallel} = 1, \\ \langle \eta_z(t_1) \eta_z(t_2) \rangle_{\parallel} &= \chi_{\parallel} \nu e^{-\nu |t_1 - t_2|} \equiv C_{\parallel}(t), \\ \langle z(t) \eta_z(t) \rangle_{\parallel} &= \langle z(t) \eta_z(0) \rangle_{\parallel} = \varphi_{\parallel}(t), \\ \langle z^2(t) \rangle_{\parallel} &= \psi_{\parallel}(t). \end{aligned} \quad (4.42)$$

The average H_{\parallel} simplifies to

$$\langle H_{\parallel} \rangle_{\parallel} = \exp \left(-\frac{a^2}{2} - \frac{k^2}{2} \psi_{\parallel}(t) - \frac{q^2}{2} + iaq C_{\parallel}(t) - kq \varphi_{\parallel}(t) + iak \varphi_{\parallel}(t) \right), \quad (4.43)$$

and the derivative at $a = 0$ is then

$$\left. \frac{\partial}{\partial a} \langle H_{\parallel} \rangle_{\parallel} \right|_{a=0} = [iq C_{\parallel}(t) + ik \varphi_{\parallel}(t)] \exp \left(-\frac{q^2}{2} - \frac{k^2}{2} \psi_{\parallel}(t) - kq \varphi_{\parallel}(t) \right). \quad (4.44)$$

Returning to the original problem to find M_{\parallel} . We use the definition of H_{\parallel} in the expression for M_{\parallel}

$$\begin{aligned} M_{\parallel}(z) &= \frac{1}{2\pi P(\eta^0)} \int \int [iq C_{\parallel}(t) + ik \varphi_{\parallel}(t)] \exp[-ikz - iq \eta_z^0] \\ &\quad \times \exp \left(-\frac{q^2}{2} - \frac{k^2}{2} \psi_{\parallel}(t) - kq \varphi_{\parallel}(t) \right) dk dq. \end{aligned} \quad (4.45)$$

Performing the integration over q leads to

$$\begin{aligned} M_{\parallel}(z) &= \frac{1}{\sqrt{2\pi} P(\eta_z^0)} \int [\eta_z^0 C_{\parallel}(t) - ik(R-1) \varphi_{\parallel}(t)] \\ &\quad \times \exp \left(-\frac{1}{2} (\eta_z^0 - ik \varphi_{\parallel}(t))^2 - ikz - \frac{k^2}{2} \psi_{\parallel}(t) \right) dk. \end{aligned} \quad (4.46)$$

Finally the integration over k yields

$$M_{\parallel}(z) = \left(\frac{\eta_z^0 C_{\parallel}(t)}{(\psi_{\parallel}(t) - \varphi_{\parallel}^2(t))^{1/2}} + \frac{\varphi_{\parallel}(t)(1 - C_{\parallel}(t))(z - \eta_z^0 \varphi_{\parallel}(t))}{(\psi_{\parallel}(t) - \varphi_{\parallel}^2(t))^{3/2}} \right) \times \exp \left(\frac{\eta_z^0{}^2}{2} - \frac{z^2 + \psi_{\parallel}(t)\eta_z^0{}^2 - 2z\eta_z^2\varphi_{\parallel}(t)}{2(\psi_{\parallel}(t) - \varphi_{\parallel}^2(t))} \right). \quad (4.47)$$

Some algebraic manipulations lead to

$$M_{\parallel}(z) = \left(\frac{\eta_z^0 C_{\parallel}(t)}{(\psi_{\parallel}(t) - \varphi_{\parallel}^2(t))^{1/2}} + \frac{\varphi_{\parallel}(t)(1 - C_{\parallel}(t))(z - \eta_z^0 \varphi_{\parallel}(t))}{(\psi_{\parallel}(t) - \varphi_{\parallel}^2(t))^{3/2}} \right) \times \exp \left(- \frac{(z - \eta_z^0 \varphi_{\parallel}(t))^2}{2(\psi_{\parallel}(t) - \varphi_{\parallel}^2(t))} \right). \quad (4.48)$$

The last result can be expressed in terms of a probability distribution $P_{\parallel}(z)$,

$$M_{\parallel}(z) = \left\{ \eta_z^0 C_{\parallel}(t) - \frac{\eta_z^0 \varphi_{\parallel}^2(t)}{(\psi_{\parallel}(t) - \varphi_{\parallel}^2(t))} [1 - C_{\parallel}(t)] \right\} P_{\parallel}(z), \quad (4.49)$$

using the subensemble average of the position $\langle z(t) \rangle = \eta_z^0 \varphi_{\parallel}(t)$ and

$$P_{\parallel}(z) = \frac{1}{\sqrt{2\pi(\psi_{\parallel}(t) - \varphi_{\parallel}^2(t))}} \exp \left(- \frac{(z - \langle z(t) \rangle_S)^2}{2(\psi_{\parallel}(t) - \varphi_{\parallel}^2(t))} \right). \quad (4.50)$$

Equation (4.50) can also be found in [20]. There it was derived for a DCT approximation within the context of the V-Langevin equations.

Combined average for perpendicular motion

The conditional average of the perpendicular motion is found analogously,

$$M_{\perp}(\xi_x) \equiv \frac{\langle \eta_x(t) \delta(\xi_x - \xi_x(t)) \delta(\eta_x^0 - \eta_x(0)) \rangle_{\perp}}{\langle \delta(\eta_x^0 - \eta_x(0)) \rangle_{\parallel}}. \quad (4.51)$$

Due to the symmetry the same arguments hold for $M_{\perp}(\xi_y)$. Designating

$$\begin{aligned} \langle \eta_x(t) \eta_x(t) \rangle_{\perp} &= \langle \eta_x(0) \eta_x(0) \rangle_{\perp} = 1, \\ \langle \eta_x(t_1) \eta_x(t_2) \rangle_{\perp} &= \chi_{\perp} \nu e^{-\nu|t_1 - t_2|} \equiv C_{\perp}(t), \end{aligned} \quad (4.52)$$

and using the results for the classical transport,

$$\langle \xi_x(t) \eta_x(t) \rangle_{\perp} = \langle \xi_x(t) \eta_x(0) \rangle_{\perp} = \varphi_{\perp}(t), \quad (4.53)$$

we find a similar result for $M_{\perp}(x)$ as (4.49),

$$M_{\perp}(\xi_x) = \left\{ \eta_x^0 C_{\perp}(t) - \varphi_{\perp}(t)[1 - C_{\perp}(t)] \frac{d}{d\xi_x} \right\} P_{\perp}(\xi_x). \quad (4.54)$$

Here $P_{\perp}(\xi_x)$ is as given in Eq. (4.50).

4.2.4 The DCT approximation for $\mathcal{L}^{(0)}$ and the structure function $\mathcal{S}_0(t)$

The Lagrangian correlations are retrieved from Eq. (4.15) and (4.16). In $\mathcal{L}^{(0)}$ we need the subensemble contribution

$$\begin{aligned} & \left\langle \left\langle \langle \eta_{\parallel}(t) b_y[\mathbf{x}(t), z(t), t] \rangle_S \right\rangle_{\parallel} \right\rangle_{\perp} = \\ & \int_{-\infty}^{\infty} \int_{-\infty}^{\infty} \int_{-\infty}^{\infty} M_{\parallel}(z) \langle b_y(\mathbf{x} + \boldsymbol{\xi}, z, t) \rangle_S P(\xi_x) P(\xi_y) d\xi_x d\xi_y dz. \end{aligned} \quad (4.55)$$

The perpendicular integrals are performed and we use the prescriptions from the previous Sec. leading to

$$\left\langle \left\langle \langle \eta_{\parallel}(t) b_y[\mathbf{x}(t), z(t), t] \rangle_S \right\rangle_{\parallel} \right\rangle_{\perp} = \mathcal{N} F_{\perp}(\mathbf{x}; \lambda_{\perp} + \langle \xi^2(t) \rangle) \int_{-\infty}^{\infty} F_{\parallel}(z) M_{\parallel}(z) dz. \quad (4.56)$$

Note the appearance of the Corrsin term \mathcal{N} , which does not depend on the DCT. Within this picture the decorrelation trajectory itself appears only in the perpendicular coordinates x and y . The further integration can also be performed directly. With the results from the previous section the z -integration can be carried out, inserting the expression for $M_{\parallel}(z)$,

$$\begin{aligned} & \left\langle \left\langle \langle \eta_{\parallel}(t) b_y[\mathbf{x}(t), z(t), t] \rangle_S \right\rangle_{\parallel} \right\rangle_{\perp} = \\ & F_{\perp}(\mathbf{x}, \lambda_{\perp} + \langle \xi^2(t) \rangle) \mathcal{N} \left(\eta^0 \mathcal{M} \chi_{\parallel} \nu e^{-\nu t} - \frac{\eta^0 \varphi_{\parallel}^2 [1 - \chi_{\parallel} \nu e^{-\nu t}]}{\lambda_{\parallel}^2} \mathcal{M}^3 \right) e^{-\frac{\langle z(t) \rangle^2}{2\lambda_{\parallel}^2} \mathcal{M}^2}. \end{aligned} \quad (4.57)$$

In the latter equation we introduced the Corrsin term,

$$\mathcal{M} = \left(1 + \frac{(\psi_{\parallel} - \varphi_{\parallel}^2)}{\lambda_{\parallel}^2} \right)^{-1/2}. \quad (4.58)$$

At this stage the previous Corrsin result can be recognized as a special case. Only the integrations for the DCT are left. We split this integration into two parts and apply the main approximation of the DCT ($\mathbf{x} \approx \mathbf{X}$),

$$\begin{aligned} \mathcal{L}_{\text{DCT}}^{(0)} &= \frac{1}{b_0^2} \int_{-\infty}^{\infty} \int_{-\infty}^{\infty} \int_{-\infty}^{\infty} b_y^0 F_{\perp}(\mathbf{X}, \lambda_{\perp} + \langle \xi^2(t) \rangle) P(\mathbf{b}, \phi) db_x^0 db_y^0 d\phi^0 \\ &\times \int_{-\infty}^{\infty} \eta_z^0 P(\eta_z^0) \left(\eta_z^0 \mathcal{M} \chi_{\parallel} \nu e^{-\nu t} - \frac{\eta_z^0 \varphi_{\parallel}^2 [1 - \chi_{\parallel} \nu e^{-\nu t}]}{\lambda_{\parallel}^2} \mathcal{M}^3 \right) e^{-\frac{\langle z(t) \rangle^2}{2\lambda_{\parallel}^2} \mathcal{M}^2} d\eta_z^0, \end{aligned} \quad (4.59)$$

to find the following result,

$$\mathcal{L}_{\text{DCT}}^{(0)} = \mathcal{S}(t) \mathcal{N}_{\text{DCT}} \mathcal{M} \left(\chi_{\parallel} \nu e^{-\nu t} + \mathcal{M}^2 (\chi_{\parallel} \nu e^{-\nu t} - 1) \frac{\varphi_{\parallel}^2}{\lambda_{\parallel}^2} \right). \quad (4.60)$$

At last we apply the perpendicular average as shown in the previous section and after some algebraic manipulations and performing the perpendicular average the Lagrangian can be written as

$$\mathcal{L}_{\text{DCT}}^{(0)}(t) = \mathcal{S}_0(t) \mathcal{L}_{\text{Corrsin}}^{(0)}(t). \quad (4.61)$$

Here we used the Lagrangian correlation function derived with the Corrsin approximation,

$$\mathcal{L}_{\text{Corrsin}}^{(0)} = \frac{\beta^2}{b_0^2} \mathcal{M} \left\{ \chi_{\parallel} \nu e^{-\nu t} - \frac{\varphi_{\parallel}^2}{\lambda_{\parallel}^2} \mathcal{M}^2 \right\} \mathcal{N}_{\text{DCT}}, \quad (4.62)$$

but using \mathcal{N}_{DCT} instead of \mathcal{N} . This is allowed, because the difference between \mathcal{N}_{DCT} and \mathcal{N} does not change the correlation function significantly. A factor appears which we will call the structure function $\mathcal{S}_0(t)$,

$$\mathcal{S}_0(t) = \frac{1}{\left(1 + \frac{\mathcal{M}^2 \varphi^2}{\lambda_{\parallel}^2}\right)^{3/2}} \int_{-\infty}^{\infty} \int_{-\infty}^{\infty} \int_{-\infty}^{\infty} b_y^0 F_{\perp}(\mathbf{X}; \lambda_{\perp} + \langle \xi^2(t) \rangle) P(\mathbf{b}, \phi) db_x^0 db_y^0 d\phi^0. \quad (4.63)$$

In most cases this function has to be evaluated numerically. We comment on the details of the structure function later. A suitable algorithm to calculate \mathcal{S}_0 is described in Appendix D.4. The decorrelation trajectory is needed as an input for $\mathcal{S}_0(t)$.

4.2.5 The DCT approximation for $\mathcal{L}^{(1)}$

Averaging procedure for the correction term

Next we evaluate the correction term $\mathcal{L}^{(1)}$, which is more complicated than the zeroth order,

$$\begin{aligned} \mathcal{L}_{\text{DCT}}^{(1)} = & \left\langle \frac{\rho L^2}{v_t^2 b_0^2} \int_{-\infty}^{\infty} \int_{-\infty}^{\infty} \int_{-\infty}^{\infty} \int_{-\infty}^{\infty} \int_{-\infty}^{\infty} P(\eta_x^0) P(\eta_y^0) P(\eta_z^0) P(\mathbf{b}^0) P(\phi^0) \times \right. \\ & \left. \times \eta_z^0 b_x^0 \langle \eta_{\parallel}(t) \langle b_x'[\mathbf{x}(t), z(t), t] \rangle_S \rangle_{\parallel} d\eta_x^0 d\eta_y^0 d\eta_z^0 d\mathbf{b}^0 d\phi^0 \right\rangle_{\perp}. \end{aligned} \quad (4.64)$$

We proceed in a similar way as for $\mathcal{L}^{(0)}$ and introduce the derivative average for $\langle b_x'[\mathbf{x}(t), z(t), t] \rangle_S$ and the averaging integration for the parallel motion into the definition,

$$\begin{aligned} \mathcal{L}_{\text{DCT}}^{(1)} = & \frac{\rho L^2}{v_t^2 b_0^2} \left\langle \int_{-\infty}^{\infty} \int_{-\infty}^{\infty} \int_{-\infty}^{\infty} \int_{-\infty}^{\infty} \int_{-\infty}^{\infty} P(\eta_x^0) P(\eta_y^0) P(\eta_z^0) P(\mathbf{b}^0) P(\phi^0) \right. \\ & \times \eta_z^0 b_x^0 \int_{-\infty}^{\infty} \left\{ \left\{ T_1(\mathbf{x}, \lambda_{\perp}) \eta_x^0 \eta_x(t) + T_2(\mathbf{x}, \lambda_{\perp}) \eta_y^0 \eta_y(t) \right\} e^{-\frac{z^2}{2\lambda_{\parallel}^2}} M_{\parallel}(z) dz \right. \\ & \left. \left. + \left\langle b_x^0 T_3(\mathbf{x}, \lambda_{\perp}) \eta_z^{02} \eta_z^2(t) e^{-\frac{z^2}{2\lambda_{\parallel}^2}} \right\rangle_{\parallel} \right\} \right\rangle_{\perp}. \end{aligned} \quad (4.65)$$

We apply the perpendicular averages and get

$$\begin{aligned} \mathcal{L}_{\text{DCT}}^{(1)} = & \frac{\rho L^2}{v_t^2 b_0^2} \int_{-\infty}^{\infty} \int_{-\infty}^{\infty} \int_{-\infty}^{\infty} \int_{-\infty}^{\infty} \int_{-\infty}^{\infty} P(\eta_x^0) P(\eta_y^0) P(\eta_z^0) P(\mathbf{b}^0) P(\phi^0) \\ & \times \left[\eta_z^0 b_x^0 \left\{ \eta_x^0 \int_{-\infty}^{\infty} \int_{-\infty}^{\infty} \int_{-\infty}^{\infty} T_1(\mathbf{x} + \boldsymbol{\xi}) M_{\perp}(\xi_x) P_{\perp}(\xi_y) M_{\parallel}(z) e^{-\frac{z^2}{2\lambda_{\parallel}^2}} d\xi_x d\xi_y dz \right. \right. \\ & \left. \left. + \eta_y^0 \int_{-\infty}^{\infty} \int_{-\infty}^{\infty} \int_{-\infty}^{\infty} T_2(\mathbf{x} + \boldsymbol{\xi}) P_{\perp}(\xi_x) M_{\perp}(\xi_y) M_{\parallel}(z) e^{-\frac{z^2}{2\lambda_{\parallel}^2}} d\xi_x d\xi_y dz \right\} \right. \\ & \left. + \left\langle \eta_z^{02} \eta_z^2 \right\rangle_{\parallel} \int_{-\infty}^{\infty} \int_{-\infty}^{\infty} \int_{-\infty}^{\infty} T_3(\mathbf{x} + \boldsymbol{\xi}) P_{\perp}(\xi_x) P_{\perp}(\xi_y) P_{\parallel}(z) e^{-\frac{z^2}{2\lambda_{\parallel}^2}} d\xi_x d\xi_y dz \right] \\ & d\eta_x^0 d\eta_y^0 d\eta_z^0 d\mathbf{b}^0 d\phi^0, \end{aligned} \quad (4.66)$$

where we can identify equivalent terms to the Corrsin approximation applied for Eq. (3.30). Especially the last expression requires the same approximation on the quadratic velocity terms, namely the statistic independence between the average $\langle \eta_z^{02} \eta_z^2 \rangle_{\parallel} \approx v_t^4$ and the rest of the T_3 terms, which allows us to calculate the average by the integration of the distribution $P(z)$. In the following, rather lengthy calculation, we present details on the averaging method and derive expressions for the terms involving the T_i functions.

The \mathcal{T}_i -terms

We split the integration in different contributing terms beginning with the T_1 term, and evaluate the integrals using means of analytical software (due to the vast amount of terms within the T_i), yielding the result

$$\begin{aligned}
& \int_{-\infty}^{\infty} P(\eta_x^0) \eta_x^0 \int_{-\infty}^{\infty} \int_{-\infty}^{\infty} \int_{-\infty}^{\infty} T_1(\mathbf{x} + \boldsymbol{\xi}) M_{\perp}(\xi_x) P_{\perp}(\xi_y) M_{\parallel}(z) e^{-\frac{z^2}{2\lambda_{\parallel}^2}} d\xi_x d\xi_y dz d\eta_x^0 \\
&= \left\{ -\frac{\beta^2 C_{\perp}(t) \mathcal{T}_{1a}(\mathbf{x})}{\left(1 + \frac{\langle \xi^2 \rangle}{\lambda_{\perp}^2}\right)^3 \lambda_{\perp}^2} + \frac{3\beta^2 \varphi_{\perp}^2 (1 - C_{\perp}(t)) \mathcal{T}_{1b}(\mathbf{x})}{(\langle \xi^2 \rangle + \lambda_{\perp}^2)^{5/2} (\langle \xi^2 \rangle + \lambda_{\perp}^2 + \varphi_{\perp}^2)^{3/2} \lambda_{\perp}^4} \right\} \\
&\quad \times \left\{ \eta_z^0 \mathcal{M} \chi_{\parallel} \nu e^{-\nu t} - \frac{\eta_z^0 \varphi_{\parallel}^2 [1 - \chi_{\parallel} \nu e^{-\nu t}]}{\lambda_{\parallel}^2} \mathcal{M}^3 \right\}.
\end{aligned} \tag{4.67}$$

We have introduced the notation

$$\begin{aligned}
\mathcal{T}_{1a}(\mathbf{x}) &= \frac{1}{\left(1 + \frac{\langle \xi^2 \rangle}{\lambda_{\perp}^2}\right)^3 \lambda_{\perp}^4} [(\lambda_{\perp}^2 + \langle \xi^2 \rangle - x^2)(\lambda_{\perp}^2 + \langle \xi^2 \rangle - y^2) b_x^{\prime 0}] \\
&\quad + xy(3\lambda_{\perp}^2 + 3\langle \xi^2 \rangle - x^2) b_y^{\prime 0} \exp\left(-\frac{x^2 + y^2}{2(\langle \xi^2 \rangle + \lambda_{\perp}^2)}\right),
\end{aligned} \tag{4.68}$$

$$\begin{aligned}
\mathcal{T}_{1b}(\mathbf{x}) &= \\
& \frac{1}{3\left(1 + \frac{\langle \xi^2 \rangle + \varphi_{\perp}^2}{\lambda_{\perp}^2}\right)^4 \lambda_{\perp}^8} [(\langle \xi^2 \rangle - y^2 + \lambda_{\perp}^2) b_x^{\prime 0} (\langle \xi^2 \rangle + \lambda_{\perp}^2 + \varphi_{\perp}^2) (3\langle \xi^2 \rangle^2 - 6\langle \xi^2 \rangle x^2 \\
&\quad + x^4 + 6(\langle \xi^2 \rangle - x^2)\lambda_{\perp}^2 + 3\lambda_{\perp}^4 + 6(\langle \xi^2 \rangle - x^2 + \lambda_{\perp}^2)\varphi_{\perp}^2 + 3\varphi_{\perp}^4) \\
&\quad + xy(\langle \xi^2 \rangle + \lambda_{\perp}^2) b_y^{\prime 0} (15\langle \xi^2 \rangle^2 + x^4 - 10x^2\lambda_{\perp}^2 + 15\lambda_{\perp}^4 \\
&\quad - 10\langle \xi^2 \rangle(x^2 - 3\lambda_{\perp}^2) + 5\varphi_{\perp}^2(6\langle \xi^2 \rangle - 2x^2 + 6\lambda_{\perp}^2 + 3\varphi_{\perp}^2))] \\
&\quad \times \exp\left(-\frac{x^2}{2(\langle \xi^2 \rangle + \lambda_{\perp}^2 + \varphi_{\perp}^2)} - \frac{y^2}{2(\langle \xi^2 \rangle + \lambda_{\perp}^2)}\right).
\end{aligned} \tag{4.69}$$

These terms are already written in a special way, for easier comparison with the Corrsin results. The functions \mathcal{T}_i are dimensionless as they are normalized with the corresponding length λ_{\perp} . Furthermore, the numerical factors have been resorted so that $\mathcal{T}_i \rightarrow 1$ for $\lambda_{\perp} \rightarrow \infty$. Of course, the calculation of the integrations for the T_2 term are similar and yield

$$\begin{aligned}
& \int_{-\infty}^{\infty} P(\eta_y^0) \eta_y^0 \int_{-\infty}^{\infty} \int_{-\infty}^{\infty} \int_{-\infty}^{\infty} T_2(\mathbf{x} + \boldsymbol{\xi}) M_{\perp}(\xi_y) P_{\perp}(\xi_x) M_{\parallel}(z) e^{-\frac{z^2}{2\lambda_{\parallel}^2}} d\xi_x d\xi_y dz d\eta_y^0 \\
&= \left\{ -\frac{3\beta^2 C_{\perp}(t) \mathcal{T}_{2a}(\mathbf{x})}{\left(1 + \frac{\langle \xi^2 \rangle}{\lambda_{\perp}^2}\right)^3 \lambda_{\perp}^2} + \frac{15\beta^2 \varphi_{\perp}^2 (1 - C_{\perp}(t)) \mathcal{T}_{2b}(\mathbf{x})}{\lambda_{\perp}^4 \left(1 + \frac{\langle \xi^2 \rangle}{\lambda_{\perp}^2}\right)^{3/2} \left(1 + \frac{\langle \xi^2 \rangle + \varphi_{\perp}^2}{\lambda_{\perp}^2}\right)^{5/2}} \right\} \\
&\quad \times \left\{ \eta_z^0 \mathcal{M} \chi_{\parallel} v e^{-vt} - \frac{\eta_z^0 \varphi_{\parallel}^2 [1 - \chi_{\parallel} v e^{-vt}]}{\lambda_{\parallel}^2} \mathcal{M}^3 \right\}.
\end{aligned} \tag{4.70}$$

with

$$\begin{aligned}
\mathcal{T}_{2a}(\mathbf{x}) &= \frac{1}{3\left(1 + \frac{\langle \xi^2 \rangle}{\lambda_{\perp}^2}\right)^2 \lambda_{\perp}^4} \left[(3\langle \xi^2 \rangle^2 + y^4 - 6y^2 \lambda_{\perp}^2 + 3\lambda_{\perp}^4 - 6\langle \xi^2 \rangle (y^2 - \lambda_{\perp}^2)) b_x^0 \right. \\
&\quad \left. + x y (3\langle \xi^2 \rangle - y^2 + 3\lambda_{\perp}^2) b_y^0 \right] \exp\left(-\frac{x^2 + y^2}{2(\langle \xi^2 \rangle + \lambda_{\perp}^2)}\right),
\end{aligned} \tag{4.71}$$

$$\begin{aligned}
\mathcal{T}_{2b}(\mathbf{x}) &= -\frac{1}{15\left(1 + \frac{\langle \xi^2 \rangle + \varphi_{\perp}^2}{\lambda_{\perp}^2}\right)^4 \lambda_{\perp}^8} \\
&\times \left[-x y b_y^0 (\langle \xi^2 \rangle + \lambda_{\perp}^2 + \varphi_{\perp}^2) (15\langle \xi^2 \rangle^2 + y^4 - 10y^2 \lambda_{\perp}^2 + 15\lambda_{\perp}^4 \right. \\
&\quad \left. - 10\langle \xi^2 \rangle (y^2 - 3\lambda_{\perp}^2) + 5\varphi_{\perp}^2 (6\langle \xi^2 \rangle - 2y^2 + 6\lambda_{\perp}^2 + 3\varphi_{\perp}^2)) \right. \\
&\quad \left. - (\langle \xi^2 \rangle + \lambda_{\perp}^2) b_x^0 \right. \\
&\quad \left. (15\langle \xi^2 \rangle^3 - 45\langle \xi^2 \rangle^2 y^2 + 15\langle \xi^2 \rangle y^4 - y^6 + 15(3\langle \xi^2 \rangle^2 - 6\langle \xi^2 \rangle y^2 + y^4) \lambda_{\perp}^2 \right. \\
&\quad \left. + 45(\langle \xi^2 \rangle - y^2) \lambda_{\perp}^4 + 15\lambda_{\perp}^6 + 15\varphi_{\perp}^2 (3\langle \xi^2 \rangle^2 - 6\langle \xi^2 \rangle y^2 + y^4 \right. \\
&\quad \left. + 6(\langle \xi^2 \rangle - y^2) \lambda_{\perp}^2 + 3\lambda_{\perp}^4 + 3(\langle \xi^2 \rangle - y^2 + \lambda_{\perp}^2) \varphi_{\perp}^2 + \varphi_{\perp}^4) \right] \\
&\quad \times \exp\left(-\frac{x^2}{2(\langle \xi^2 \rangle + \lambda_{\perp}^2)} - \frac{y^2}{2(\langle \xi^2 \rangle + \lambda_{\perp}^2 + \varphi_{\perp}^2)}\right).
\end{aligned} \tag{4.72}$$

The last term has a slightly simpler form, because the integration involves only the gaussian distributions $P(\xi_x)$, $P(\xi_y)$ and $P(z)$,

$$\begin{aligned}
& \int_{-\infty}^{\infty} P(\eta_z^0) \eta_z^0 \int_{-\infty}^{\infty} \int_{-\infty}^{\infty} \int_{-\infty}^{\infty} T_3(\mathbf{x} + \boldsymbol{\xi}) P_{\perp}(\xi_x) P_{\perp}(\xi_y) P_{\parallel}(z) e^{-\frac{z^2}{2\lambda_{\parallel}^2}} d\xi_x d\xi_y dz d\eta_z^0 \\
&= -\frac{v_t^4 \beta^2 \mathcal{T}_3(\mathbf{x})}{\lambda_{\parallel}^4 \left(1 + \frac{\langle \delta z^2 \rangle + \varphi_{\parallel}^2}{\lambda_{\parallel}^2}\right)^{3/2} \left(1 + \frac{\langle \xi^2 \rangle}{\lambda_{\perp}^2}\right)^3}.
\end{aligned} \tag{4.73}$$

Here

$$\mathcal{T}_3(\mathbf{x}) = \frac{1}{\lambda_{\perp}^2} [(\langle z^2 \rangle - y^2 + \lambda_{\perp}^2) b_x{}^0 + x y b_y{}^0] \exp\left(-\frac{x^2 + y^2}{2(\langle \xi^2 \rangle + \lambda_{\perp}^2)}\right). \quad (4.74)$$

The structure functions \mathcal{S}_i for $\mathcal{L}^{(1)}$

We return to our calculation of $\mathcal{L}^{(1)}$ and use the results for the T_i integrations and perform the remaining integrals over $\eta_z{}^0$ and ϕ^0 leading to

$$\begin{aligned} \mathcal{L}_{\text{DCT}}^{(1)} = & -\frac{\rho_L^2 \beta^2 \mathcal{L}_{\lambda_{\perp} \rightarrow \infty}^{(0)}}{v_t^2 b_0^2} \left[\frac{C_{\perp}(t) (\mathcal{S}_{1a}(t) + 3 \mathcal{S}_{2a}(t))}{\left(1 + \frac{\langle \xi^2 \rangle}{\lambda_{\perp}^2}\right)^5 \lambda_{\perp}^2} \right. \\ & - \frac{3 \varphi_{\perp}^2 (1 - C_{\perp}(t)) \mathcal{S}_{1b}(t)}{\lambda_{\perp}^4 \left(1 + \frac{\langle \xi^2 \rangle}{\lambda_{\perp}^2}\right)^{5/2} \left(1 + \frac{\langle \xi^2 \rangle + \varphi_{\perp}^2}{\lambda_{\perp}^2}\right)^{3/2}} - \frac{15 \varphi_{\perp}^2 (1 - C_{\perp}(t)) \mathcal{S}_{2b}(\mathbf{x})}{\lambda_{\perp}^4 \left(1 + \frac{\langle \xi^2 \rangle}{\lambda_{\perp}^2}\right)^{3/2} \left(1 + \frac{\langle \xi^2 \rangle + \varphi_{\perp}^2}{\lambda_{\perp}^2}\right)^{5/2}} \left. \right] \\ & - \frac{\rho_L^2 \beta^2 v_t^2}{b_0^2} \frac{\mathcal{S}_3(\mathbf{x})}{\lambda_{\parallel}^4 \sqrt{1 + \frac{\psi_{\parallel}}{\lambda_{\parallel}^2}} \sqrt{1 + \frac{\lambda_{\parallel}^2}{1 + \frac{\psi_{\parallel}}{\lambda_{\parallel}^2}}} \left(1 + \frac{\langle \xi^2 \rangle}{\lambda_{\perp}^2}\right)^3}, \end{aligned} \quad (4.75)$$

given in terms of $\mathcal{L}_{\lambda_{\perp} \rightarrow \infty}^{(0)}$ which corresponds to the quasilinear limit including collisions. The structure functions are defined as,

$$\begin{aligned} \mathcal{S}_{1a}(t) &= \int_{-\infty}^{\infty} P(\mathbf{b}^0) \mathcal{T}_{1a}(\mathbf{x}) d\mathbf{b}^0, \quad \mathcal{S}_{2a}(t) = \int_{-\infty}^{\infty} P(\mathbf{b}^0) \mathcal{T}_{2a}(\mathbf{x}) d\mathbf{b}^0, \\ \mathcal{S}_{1b}(t) &= \int_{-\infty}^{\infty} P(\mathbf{b}^0) \mathcal{T}_{1b}(\mathbf{x}) d\mathbf{b}^0, \quad \mathcal{S}_{2b}(t) = \int_{-\infty}^{\infty} P(\mathbf{b}^0) \mathcal{T}_{2b}(\mathbf{x}) d\mathbf{b}^0, \\ \mathcal{S}_3(t) &= \int_{-\infty}^{\infty} P(\mathbf{b}^0) \mathcal{T}_3(\mathbf{x}) d\mathbf{b}^0. \end{aligned} \quad (4.76)$$

The correction function $\mathcal{L}^{(1)}$ found with the DCT has the same form like the function found within the Corrsin method. The functions \mathcal{T}_i and \mathcal{S}_i are dimensionless, the correction function appears therfor in the same dimension as the Corrsin result. The influence of the percolation structure is here also capsuled in the functions \mathcal{S}_i which still contain the complicated integrals of the \mathcal{T}_i over the b -field derivatives. This functions have to be evaluated numerically.

4.2.6 Properties of the $\mathcal{S}_i(t)$ structure functions in certain limits

Though a general treatment of $\mathcal{S}_0(t)$ and the other structure integrals appears impossible, we can still find asymptotic values in selected limits. We know already that the perpendicular correlation length is responsible for the percolation structure of the magnetic field. Therefore it is appropriate to discuss the $\mathcal{S}_i(t)$ for different limits of λ_\perp . For $\lambda_\perp \rightarrow \infty$ the structure terms become equal to one,

$$\lim_{\lambda_\perp \rightarrow \infty} \mathcal{S}_i(t) = 1, \quad (4.77)$$

which holds for all i . This reflects the fact that for small Kubo numbers no effect of the magnetic structure should be observed and our results from the Corrsin method are valid. Contrary to this limit we have

$$\lim_{\lambda_\perp \rightarrow 0} \mathcal{S}_i(t) = 0, \quad (4.78)$$

due to the dependence on the Eulerian correlator, e.g. in \mathcal{S}_0

$$\begin{aligned} \mathcal{S}_0(t) &= \frac{1}{\left(1 + \frac{\mathcal{M}^2 \varphi^2}{\lambda_\perp^2}\right)^{3/2}} \int_{-\infty}^{\infty} \int_{-\infty}^{\infty} \int_{-\infty}^{\infty} b_y^0 \\ &\times \frac{\beta^2}{\lambda_\perp^2} \{x \lambda_\perp^2 \phi^0 + x y b_x^0 + (\lambda_\perp^2 - x^2) b_y^0\} \\ &\times \exp\left(-\frac{X^2 + Y^2}{2\lambda_\perp^2}\right) P(b, \phi) db_x^0 db_y^0 d\phi^0. \end{aligned} \quad (4.79)$$

It decreases exponentially with decreasing λ_\perp and makes the structure term vanish. This explains the well-known problem that for high Kubo numbers the diffusion is expected to decay to zero as more and more field lines are trapped in the structures. Of course, this effect can be compensated by the collisions for large collisional frequencies ν , because $X \sim e^{-\nu t}$ and $Y \sim e^{-\nu t}$.

We can compare the numerical values of the structure functions in this limit with the numerical values presented in Sec. 3 within the Corrsin approximation. They are exactly equal. This result shows that the Corrsin results can be interpreted as the $\kappa \rightarrow 0$ limit of the DCT. Especially the relations

$$\lim_{\lambda_\perp \rightarrow \infty} \mathcal{L}_{\text{DCT}}^{(0)} = \mathcal{L}_{\text{Corrsin}}^{(0)}, \quad \lim_{\lambda_\perp \rightarrow \infty} \mathcal{L}_{\text{DCT}}^{(1)} = \mathcal{L}_{\text{Corrsin}}^{(1)} \quad (4.80)$$

hold, neglecting small differences in the exponents of the correlation terms. This important fact was not covered by any other work on the DCT so far.

4.3 Diffusion within the DCT approximation

In the end of Sec. 3 we gave an overview of various transport regimes found with the Corrsin approximation and presented details on some selected cases. The DCT tells us now, that the correlation functions from the Corrsin method are principally correct, but they have to be equipped with certain numerical factors which take care of the magnetic fields percolation structure. For increasing Kubo numbers $\kappa = \beta\lambda_{\parallel} / (b_0 \lambda_{\perp}) > 1$ these factors become relevant. Indeed the parameter λ_{\perp} has been identified to be the most crucial input value of the structure terms.

Two important questions remain, that are closely related to each other:

Does the percolative structure of high Kubo numbers always lead to a trapping and a reduction of the diffusion?

Have finite Larmor radii also significant effect on the diffusion in this regime?

We answer these questions by numerical solutions of the Green-Kubo formula for the anomalous transport contributions,

$$\frac{d^2}{dt^2} \langle \delta x^2(t) \rangle = 2 \frac{d}{dt} D(t) = \mathcal{L}_{\text{DCT}}^{(0)} + \mathcal{L}_{\text{DCT}}^{(1)}, \quad (4.81)$$

incorporated in an algorithm that solves also the DCT and the structure functions \mathcal{S}_i .

First, we are interested whether the DCT really reproduces the same gyro-radius effects as the Corrsin approximation. Therefore, we integrate Eq. (4.82) in time and show the asymptotic diffusion coefficient as a function of the Kubo number κ in Fig. 4.5. A first result is that the diffusion in the guiding center theory as well as in the case with Larmor radius corrections starts with the analytical values of $D_{\text{ql}}^{(0)}$ and $D_{\text{ql}}^{(0+1)}$ derived in Sec. 3.3. Here, we used $D_{\text{ql}}^{(0)}$ as a normalization factor. It can be seen from Fig. 4.5 that for small Kubo numbers within the DCT approximation the same influence of the Larmor radii occurs: a severe reduction of the diffusion rate. The magnitude of this reduction is of the same magnitude as the examples shown for the Corrsin approximation and shows very good agreement with our previous results.

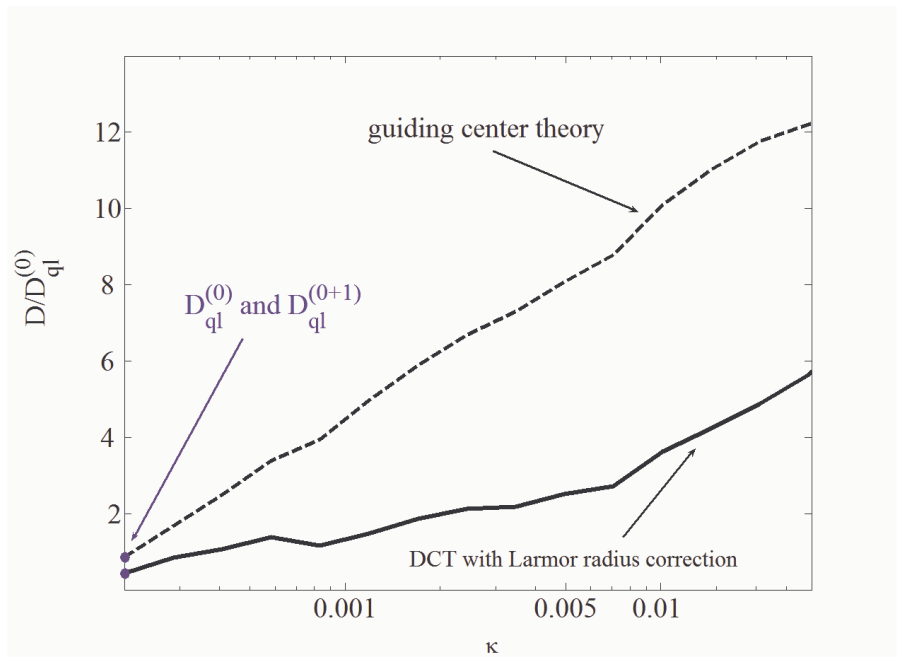


Figure 4.5: Solution of Eq. (4.82) for $\nu = 0$, $\lambda_{\parallel} \approx \rho_L$ and $b_0 = 1$. The curves originate in values given for the quasilinear limit presented in Sec. 3.3.

Next we investigate high Kubo numbers. In Fig. 4.6 we present the running diffusion coefficient normalized to the quasilinear coefficient (without Larmor radius corrections) in the collisionless case as a function of the time t (in units $1/\Omega$) for two values of the Kubo number. The guiding center result, that is a simulation of the zeroth order term in (4.82) alone, is compared with the complete integration of (4.82) yielding the Larmor radius influences. It can be seen, that for a larger Kubo number a smaller diffusion rate occurs. Additionally, and probably even more important: in this situation the finite Larmor radius terms lead to higher transport than predicted guiding center theory. Obviously guiding center theories will in such cases underestimate the diffusion dramatically.

Contrary we investigate a collisional situation to analyze in what way collisions may compensate this amplification effect. Figure 4.7 shows the again the normalized diffusion coefficient, but now we have collisions defined by the reduced collisional frequency $\nu/\Omega = 0.2$. Note that the Kubo numbers are larger compared to Fig. 4.5. Obviously the effect that the guiding center prediction is exceeded by the corrected results appears now for higher Kubo numbers. The qualitative result of an amplification of transport at high Kubo numbers is not changed by the collisions. Indeed, extreme high collisionalities may remove any influence of the structure as the the occurrence of the amplification is shifted to infinite Kubo numbers. So far we note, that for a fixed value of ν/Ω a certain Kubo number can be found at which diffusion is amplified by the Larmor radius effects.

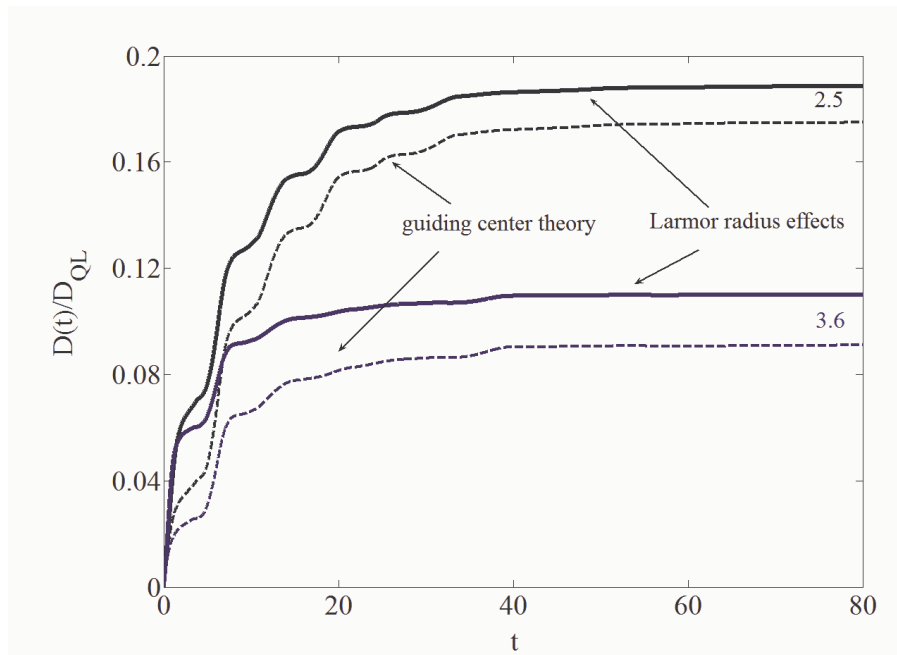


Figure 4.6: Solution of (4.82). The ratio of $D(t)$ and D_{QL} is presented in the collisionless case for two different Kubo numbers, $\kappa = 2.5$ and $\kappa = 3.6$, and compared with the guiding center theory. The time appears here in units $1/\Omega$. As stochastic values $\lambda_{\parallel} = 25 \rho_L$ and $\beta/b_0 = 0.1$ were used.

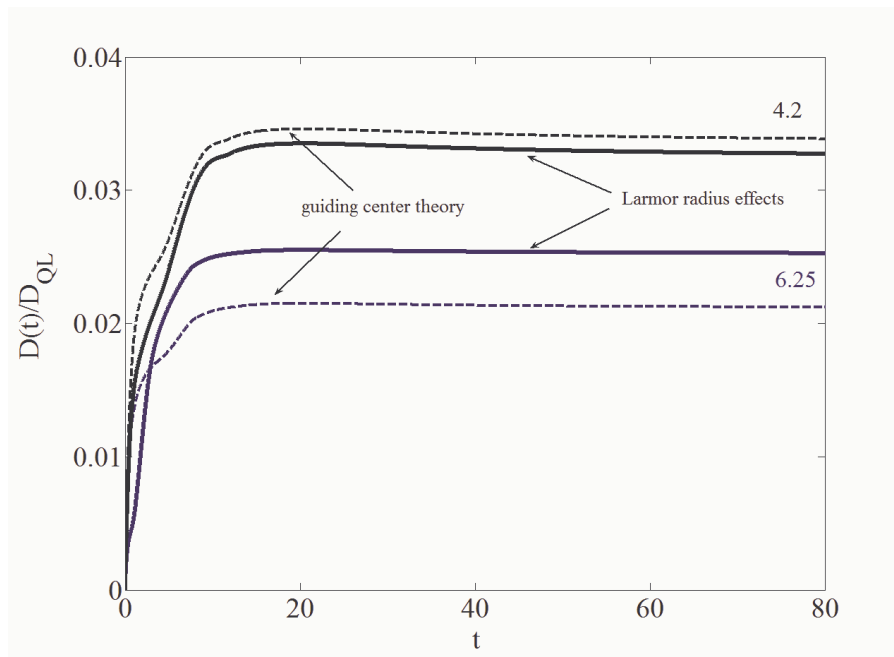


Figure 4.7: Solution of (4.82). The ratio of $D(t)$ and D_{QL} is presented in a collisional case with $\nu/\Omega = 0.2$ for two different Kubo numbers, $\kappa = 4.2$ and $\kappa = 6.25$, and compared with the guiding center theory. The time appears here in units $1/\Omega$. The stochastic values were defined by $\lambda_{\parallel} = 25 \rho_L$ and $\beta/b_0 = 0.1$.

An overview of the functional dependency between diffusion coefficient and Kubo number is presented in Fig. 4.8, where we show the effect of the finite Larmor radii. For large Kubo numbers, the increase of the diffusion occurs due to the Larmor radius. The Larmor radius corrections lead to a strong amplification of the diffusion for very high Kubo numbers. A maximum between $\kappa = 100$ and $\kappa = 1000$ occurs. Of course, in the limit $\kappa \rightarrow \infty$ both rates, the guiding center diffusion and the corrected diffusion, decay to zero. If collisions were included, the effect would still prevail.

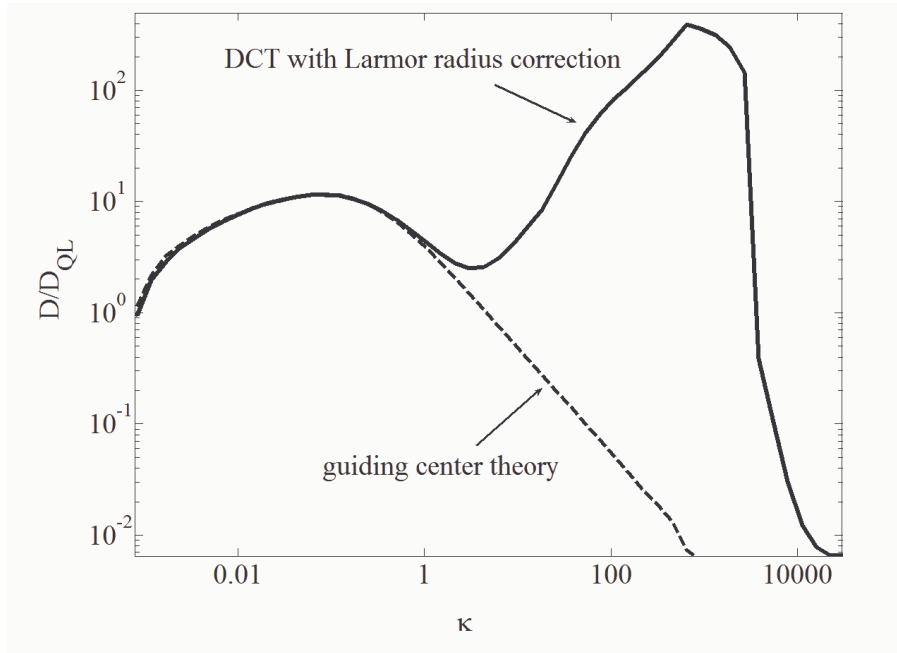


Figure 4.8: Amplification of the diffusion caused by finite Larmor radii for a collisionless situation $\nu = 0$. The normalized diffusion coefficient is plotted as a function of the Kubo number, using $\beta/b_0 = 0.1$, $\rho = 2$ measured in units of $v_t/(\Omega b_0)$. The guiding center diffusion was also calculated within the DCT.

Our results can be interpreted as follows:

First of all, the qualitative result from Isichenko et al. [22] could be reproduced. Namely the guiding center diffusion gradually decreases with Kubo number. It becomes zero for infinite Kubo numbers. In such a regime all field lines are trapped in the structures which are very small, because of $\lambda_{\perp} \rightarrow 0$.

The situation is changed when we take Larmor radius effects into account. Though the qualitative result of Isichenko et al. remains, the diffusion tends to zero for $\kappa \rightarrow \infty$, a distinct maximum of the diffusion is found in a certain area of the Kubo number. In this area, the diffusion rate is dramatically higher than predicted by the guiding center theory. While the field lines are entangled in the percolation structure, the particles are able to detach from this trapped state and contribute to the diffusion.

Another important conclusion from this analysis is the fact, that the transport is always diffusive, despite the very special case $\kappa \rightarrow \infty$. So even in higher Kubo number regimes a linearly time-dependence of the MSD prevails.

- For very small Larmor radii and high Kubo numbers the diffusion is reduced. Infinite Kubo numbers lead to an extinction of diffusion.
- The influence of large Larmor radii is essential. The qualitative reduction of the transport at high Kubo numbers is now turned into a significant increase of the diffusion.

Our investigations so far concerned the physics that underlies the anomalous transport. From a more mathematical point of view [28,29,30], it is interesting to compare both methods involved and to find estimates for the range of validity for the Corrsin approximation [17]. In Fig. 4.9 the results of both theories are compared. Indeed for $\kappa \rightarrow 0$ the difference between both approximations vanishes. But for increasing Kubo numbers, a strong deviation is found around $\kappa \gtrsim 0.3$. Of course, qualitative results, such as principal scalings derived with the Corrsin approximation, remain valid. Even the amplification effect discussed above (though several times higher) can also be observed within the Corrsin treatment.

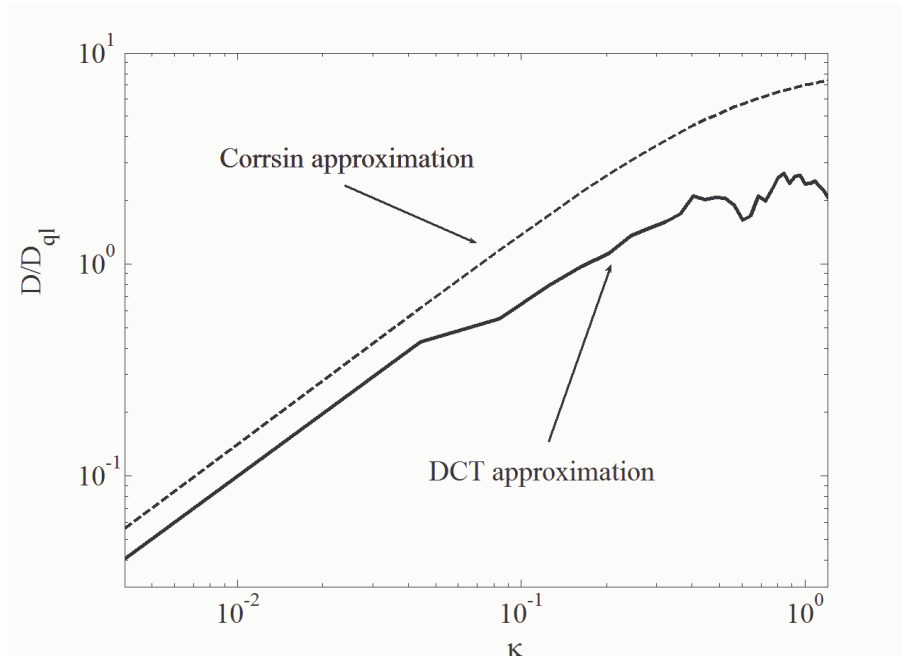


Figure 4.9: Comparison of the diffusion coefficients derived with the Corrsin approximation and the DCT. We used a parameter regime with $\nu = 0$, $\lambda_{\perp} = 50 \rho_L$, $\beta = 0.4$ and $b_0 = 1$.

5 Numerical simulations of the A-Langevin equation

Various analytical predictions are presented in Secs. 3 and 4 for the diffusion. We will now compare these analytical results with numerical simulations of the A-Langevin equation. A special interest lies in the effect of the correction terms. Though these corrections appear in small order, our numerical solution and the analytical predictions are in great agreement.

5.1 Verification of the diffusion predictions for small Kubo numbers

5.1.1 Motivation for numerical analysis

In order to independently check the analytical predictions for the anomalous transport and the finite Larmor radius corrections, we performed numerical simulations of the complete A-Langevin equation. The results of this simulations are compared with the formulas and models presented in Secs. 3 and 4.

Though various works covered separate aspects of the anomalous transport problem, e.g. starting from the V-Langevin equations [11], numerical simulation have (so far) not been performed with the original A-Langevin equation. The following verification of our results is also a proof of quality for the used stochastic methods and approximations. Especially the Corrsin method turns out to be highly accurate, within the permitted range of turbulence and Kubo numbers.

5.1.2 Comparisms in the Rechester-Rosenbluth parameter regime

In Sec. 3 we derived a model equation for the MSD and the running diffusion coefficient, the A-MSD-equation. It was shown that this equation leads to all well-known diffusion regimes in certain limits. Now we use the simulation of the complete A-Langevin equation to verify the prediction of the A-MSD-equation. The parameters are mainly chosen to fit into the most famous diffusion regime, the Rechester-Rosenbluth scaling. It can be regarded as a paradigm of transport regimes.

Figure 5.1 shows the MSD as a result of a direct A-Langevin integration and from the prediction of the A-MSD-equation, respectively. First parameters are chosen such that the guiding center approximation applies. The noisy character of the simulation curve is due to the random values introduced by the Monte-Carlo method.

In Fig. 5.2 we reduced the guiding field b_0 to values that allow the observation of transport in a domain where Larmor radius effects occur. We see a clear deviation from the guiding center result. The latter overestimates the diffusion. Instead, the solution of the A-MSD-equation, including the higher order correction terms, shows a very good coincidence with the simulation. The MSD of the simulation has nearly the same dependence as our prediction. We observed this effect for all simulations with small guiding fields, though the Larmor radius correction may sometimes be small. Indeed the parameters in Fig. 5.2 are adjusted to values at which the effect of the correction terms can be clearly recognized.

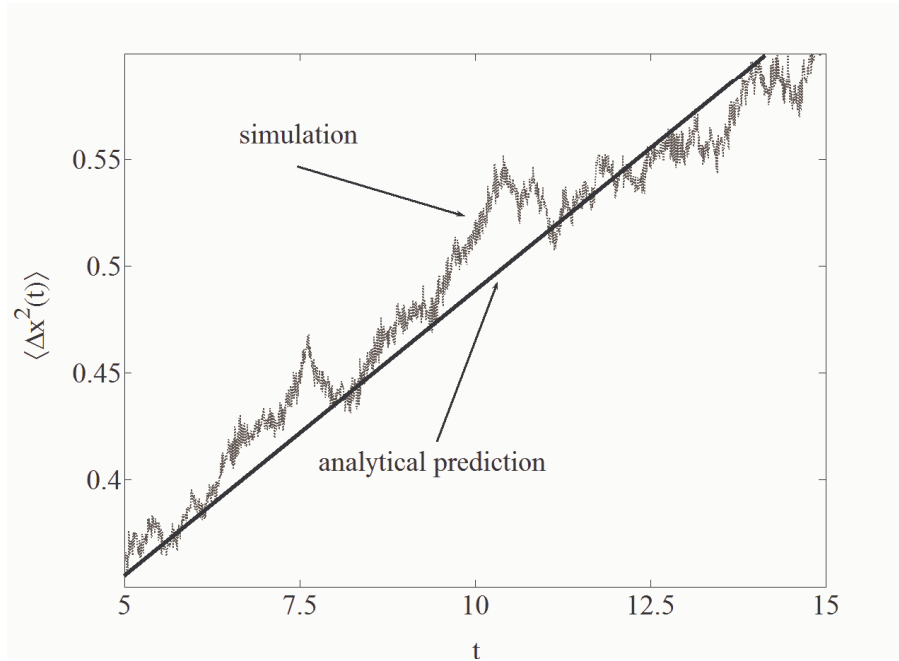


Figure 5.1: Numerical simulation of the Rechester-Rosenbluth regime within the guiding center limit compared with the analytical prediction. $\lambda_{\perp} = \lambda_{\parallel} = 15 \rho_L$, $\beta = 0.7$, $b_0 = 5$, and $\nu/\Omega = 0.4$.

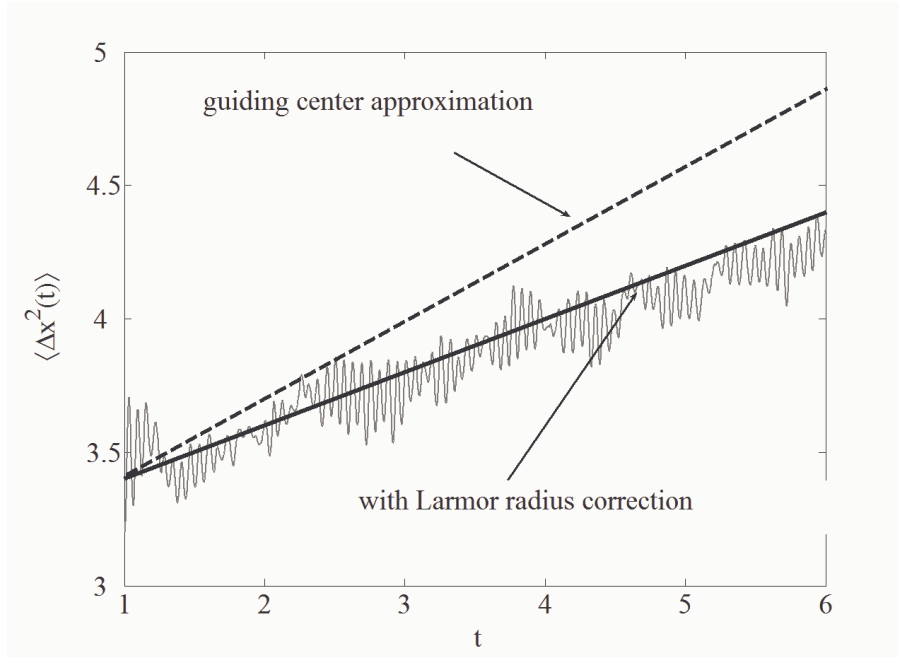


Figure 5.2: Numerical simulation of the A-Langevin equation and comparison with the analytical predictions, for the case of a strong guiding field. Shown is the MSD (in unit v_t^2/Ω^2) versus time (in units Ω^{-1}). The parameters are $\lambda_{\parallel} = \lambda_{\perp} = 2 [v_t/\Omega]$, $\varepsilon = \beta/b_0 = 0.4$, $b_0 = 1.5$ and $\nu/\Omega = 0.05$.

Of course, we also investigated further regimes with our numerics such as the quasilinear and the subdiffusive regime. We found the same agreement.

5.1.3 Verification of the regime with dominant stochastic fields

A second major result was the analytical prediction of the diffusion for zero guiding fields. There are not many predictions in the literature covering this regime. We compared our formula for the diffusion coefficient with the simulation and present in Fig. 5.3 presents a comparison between the standard classical diffusion and the diffusion with a stochastic perturbation field.

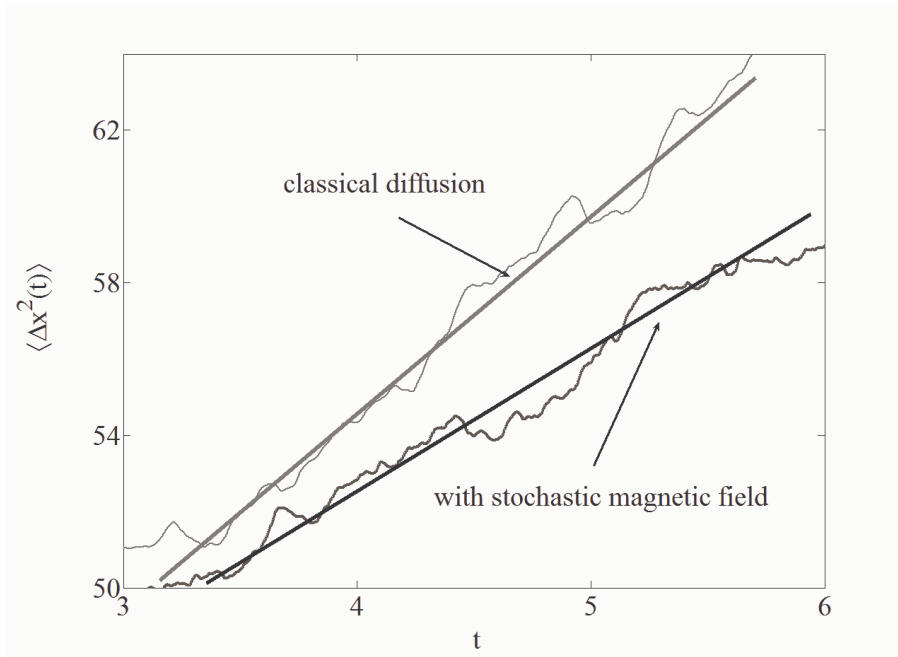


Figure 5.3: Numerical simulation, with and without stochastic magnetic field, respectively, in the case of no guiding field. Straight lines indicate the analytical predictions. Shown is the MSD (in unit v_t^2 / Ω^2) versus time (in unit Ω^{-1}). The parameters are $\lambda = 0.1[v_t / \Omega]$, $\beta = 0$ and $\beta = 0.9$, respectively, $b_0 = 0$ and $v / \Omega = 0.2$.

Though the effect of the perturbation field is small, it can be clearly seen from the simulation. The classical diffusion coefficient is now given by $\chi = v_t^2 / (2\nu)$ for all directions. Random fields appear as additional interactions for the particles and can be accounted for a new virtual friction. This additional friction reduces the diffusion coefficient to values below the classical diffusion.

5.2 Numerical simulations in the percolation regime

5.2.1 Test of the predicted reduction of the diffusion rate for high Kubo numbers

We first investigate the reduction of the diffusion caused by high Kubo numbers. In Fig. 5.4 we have got $\kappa = 438$ which would reduce the anomalous diffusion to zero in the collisionless case. We therefore use a collisional frequency of $\nu/\Omega = 0.1$ to achieve a visible reduction effect, which still leaves the anomalous transport greater than the classical diffusion.

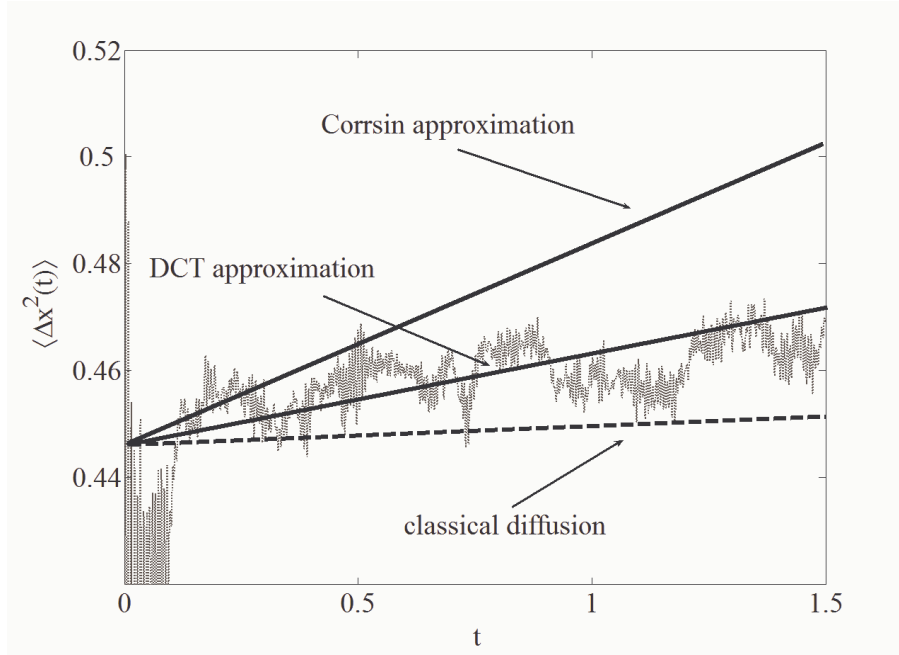


Figure 5.4: Numerical simulation for high Kubo number (grey dots) and comparison of the DCT results and the Corrsin estimates. $b_0 = 5$, $\beta = 0.9$, $\lambda_{\parallel} = 365 \rho_L$, $\lambda_{\perp} = 0.85 \rho_L$, $\kappa = 438$ and $\nu/\Omega = 0.1$. The dashed line shows the classical diffusion coefficient.

Note the result by the Corrsin approximation. It overestimates the diffusion and gives the wrong result: the gradient of the Corrsin MSD curve is twice as large as the gradient of the DCT line. There is also quantitative agreement with the results of Isichenko et al. [22] in regimes where the predictions for the percolation threshold hold.

5.2.2 Validation of the diffusion rates for high Kubo numbers and large Larmor radii

Large Larmor radii were found to be responsible for an increase of the diffusion in systems with a high Kubo number. Figure 5.5 presents a simulation of the A-Langevin equation and the predictions of the DCT. We compare the DCT results with Larmor radius corrections to the DCT results for guiding center diffusion. The Larmor radius is in this example even larger than the perpendicular correlation length. The diffusion is found to be much larger than proposed by the guiding center theory. In contrast to other works about the DCT, our simulation in Fig. 5.5 was performed in a collisional regime, proving the existence of the predicted amplification of the diffusion also for system with $\nu \neq 0$.

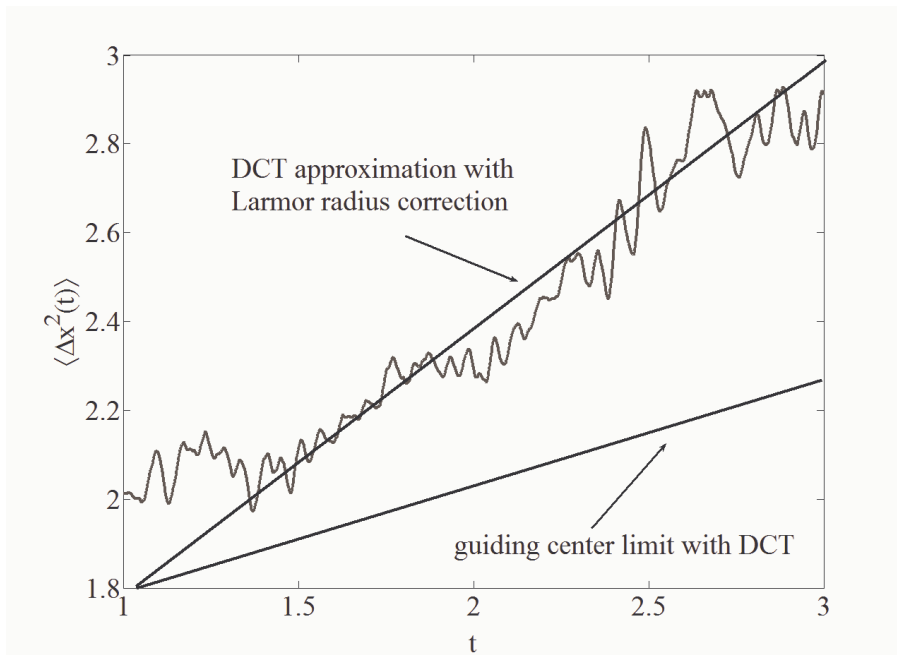


Figure 5.5: A simulation for a high Kubo number and large values of ρ_L . Comparison of the DCT results and the guiding center estimates. $b_0 = 1$, $\beta = 0.5$, $\lambda_{\parallel} = 50 \rho_L$, $\lambda_{\perp} = 0.2 \rho_L$, $\kappa = 125$ and $\nu/\Omega = 0.2$. Straight lines indicate the analytical predictions for the DCT with Larmor radius corrections and the guiding center limit (also calculated with the DCT).

Of course in this case, the Corrsin method with Larmor effects would have predicted even larger values for the diffusion. Nevertheless the typical guiding field theory dramatically underestimates the transport in this regime.

We verified our predictions and found in all cases extremely good coincidences between the analytical formulas and the numerical simulations. It shows not only the reliability of our theory, but also the quality of the applied approximations, the Corrsin method and the DCT technique. Both yield very good results, where the Corrsin results have to be taken only for small Kubo numbers. The results in the high Kubo number regime are also an evidence that the criterion for the Corrsin approximation used in many other works is correct, as far as only the DCT is capable of producing consistent behaviour.

6 Conclusion

The aim of this work was a theory of anomalous test particle transport in the presence stochastic magnetic fields. Therefore, we were mainly interested in analytical equations for the mean-square-displacement and the running diffusion coefficient.

In contrast to other works based on the guiding center assumption, we used the more general A-Langevin equation, a stochastic differential equation for the velocity of a particle, to incorporate also the Larmor motion of the particles and to extend the range of regimes to the vanishing guiding field limit.

To achieve our aim, we solved the A-Langevin equation in Sec. 2 and found an expression for the perpendicular velocity correlation function. The general velocity correlation functions showed analytically the coincidence of perpendicular and parallel diffusion in the case of vanishing guiding fields. We approximated this function for strong mean fields. The finite Larmor radius effects appeared as higher order corrections to the results of the guiding center approximation. The Green-Kubo formalism was presented as the method of choice for the relation between Lagrangian correlation functions and the transport properties.

Depending on the Kubo number, the fundamental parameter that defines the state of turbulence in the stochastic system, we divided our investigation into two parts, distinguishing between small and high Kubo numbers. Two different approximations were applied to transform the correlation functions to the Lagrangian frame of reference: the Corrsin approximation for small Kubo numbers, presented in Sec. 3 and the Decorrelation Trajectory Method for high Kubo numbers, as shown in Sec. 4.

In Sec. 3 we transformed the correlation function to the Lagrangian frame of reference by applying the more intuitive Corrsin approximation. Introduced into the Green-Kubo formula the Lagrangian correlators lead to ordinary differential equations for the transport properties, the A-MSD-equations.

How do the fluctuations contribute to the diffusion of the particles?

In the range of small Kubo numbers we recovered well-known diffusion regimes of anomalous transport, including the Rechester-Rosenbluth regime, as results of a zeroth-order treatment of the A-MSD equations. The fluctuations lead to diffusion rates much higher than predicted by the classical transport theory.

What is the influence of the Larmor radius on the diffusion?

Finite Larmor radii were discovered to reduce the diffusion. We presented analytical as well as numerical estimates for the quantitative description of this reduction. Additionally for higher Kubo numbers the transport was serverely enhanced by taking the gyration into

account. It also insistently proves our claim that a rigorous treatment of anomalous transport has to start with a dynamical equation that includes the complete movement of the particle.

What happens with the transport if the mean field is not present?

In the limit of zero guiding fields we presented analytical expressions for the diffusion. The magnetic perturbation field acts then as an additional virtual friction and reduces the diffusion in a similar manner as the collisional frequency.

Is the diffusion affected by the percolative structure of the perturbation field?

Large Kubo numbers correspond to the percolation regime, a regime in which complicated trapping processes and additional decorrelations can appear. In Sec. 4 we investigated this regime and found the Corrsin results to be the limiting cases of the more general DCT method. An explicit analytic relation between the Corrsin correlators and the DCT correlators was derived, leading to the conclusion that the Corrsin results have to be multiplied with a certain structure function given by the DCT to remain valid in the high Kubo number regimes.

Generally, the influence of the percolation structure alone leads to a dramatic reduction of the diffusion, caused by a trapping of field lines within the maxima of the flux function. We observed this reduction and found the diffusion decreasing to zero as the Kubo number tends to infinity. These results confirmed the predictions of Isichenko et al., where the percolation theory was used to find the scaling of the diffusion coefficient.

Finite Larmor radii lead to important corrections. The coincidence of a percolation structure with high Kubo numbers and relevant Larmor radius effects can also increase the diffusion to decisively elevated levels.

In Sec. 5 we verified our results with a numerical simulation of the A-Langevin equation. First we showed in the guiding center limit the general agreement of the transport data derived from the direct simulation and the predictions of the A-MSD equations. Then we also resolved the deviations due to finite Larmor radii at smaller guiding fields and found excellent agreement with our correction formulas.

The predictions for the percolation regime were also compared with the complete simulation. The increase due to finite Larmor radii and the decrease of the diffusion in the guiding center limit due to the field line trapping were also verified.

A possibility for future works would be the inclusion of fluctuating electric fields, which are still not covered by the common theory.

Summarizing we can state the major results as follows: Based on the A-Langevin equation a framework for the description of transport in stochastic plasmas was derived. The approach allows the treatment of finite Larmor radius effects. We investigated diffusion regimes for different Kubo numbers and found a significant decrease of the transport for large Larmor radii when the Kubo numbers are small and an increase of the diffusion for large Kubo numbers.

Appendix A

A.1 Necessary properties of the matrix V

Here, we evaluate the matrix V ,

$$V = -\Omega R^+ \mathbf{b} L R^-. \quad (\text{A.1})$$

It has an anti-symmetric structure induced by the L_i -generators and can be calculated directly by inserting the magnetic perturbation vector \mathbf{b} ,

$$V(t', t'') = -\Omega_0 \begin{pmatrix} 0 & -V_z(t'') & V_y(t') \\ V_z(t'') & 0 & -V_x(t') \\ -V_y(t') & V_x(t') & 0 \end{pmatrix}. \quad (\text{A.2})$$

yielding the entries

$$\begin{aligned} V_x(t') &= \cos(\alpha(t')) b_x(t') - \sin(\alpha(t')) b_y(t'), \\ V_y(t') &= \sin(\alpha(t')) b_x(t') + \cos(\alpha(t')) b_y(t') \\ V_z(t'') &= b_z(t''), \end{aligned} \quad (\text{A.3})$$

with $\alpha(t) = \Omega b_0 t$. Note the different variables t' and t'' . We will sometimes write $V(t', t'' = t') \equiv V(t')$. For $b_0 \rightarrow 0$ the matrix reduces to the simple expression,

$$V = -\Omega \mathbf{b} L, \quad V_x(t') = b_x(t'), \quad V_y(t') = b_y(t'), \quad V_z(t'') = b_z(t''). \quad (\text{A.4})$$

The Eigenvalues of V are

$$\lambda_0 = 0, \quad \lambda_{\pm} = \pm i \Omega |\mathbf{b}|. \quad (\text{A.5})$$

Next we investigate how $V(t)$ transforms by multiplication with the rotational matrices. First we let R_i^{\pm} act at the same time as V ,

$$R^-(t) V(t) R^+(t) = -\Omega \mathbf{b} L = -\Omega_0 \begin{pmatrix} 0 & -b_z & b_y \\ b_z & 0 & -b_x \\ -b_y & b_x & 0 \end{pmatrix}. \quad (\text{A.6})$$

Obviously this operation cancels all guiding field entries in V . The effect is different when we apply rotations at arbitrary times,

$$R^-(t) V(\tau, \tau) R^+(t) = V(\tau - t, \tau). \quad (\text{A.7})$$

Now the rotation matrices cause a timeshift in the perpendicular entries of V .

A.2 The rotational group $SO(3)$

The rotational group $SO(3)$ turns out to be a useful tool in constructing a solution of the ALE. Let us define the following matrices,

$$R_1 \equiv \begin{pmatrix} 1 & 0 & 0 \\ 0 & \cos \alpha & -\sin \alpha \\ 0 & \sin \alpha & \cos \alpha \end{pmatrix}, R_2 \equiv \begin{pmatrix} \cos \alpha & 0 & \sin \alpha \\ 0 & 1 & 0 \\ -\sin \alpha & 0 & \cos \alpha \end{pmatrix}, R_3 \equiv \begin{pmatrix} \cos \alpha & -\sin \alpha & 0 \\ \sin \alpha & \cos \alpha & 0 \\ 0 & 0 & 1 \end{pmatrix}. \quad (\text{A.8})$$

Then the $R_i(\alpha)$ are a base of the $SO(3)$ and can be expressed in terms of the generators L_i of an infinitesimal rotation,

$$R_i(\alpha) = e^{L_i \alpha} \quad (\text{A.9})$$

using

$$L_1 = \begin{pmatrix} 0 & 0 & 0 \\ 0 & 0 & -1 \\ 0 & 1 & 0 \end{pmatrix}, \quad L_2 = \begin{pmatrix} 0 & 0 & 1 \\ 0 & 0 & 0 \\ -1 & 0 & 0 \end{pmatrix}, \quad L_3 = \begin{pmatrix} 0 & -1 & 0 \\ 1 & 0 & 0 \\ 0 & 0 & 0 \end{pmatrix}, \quad \mathbf{L} \equiv \begin{pmatrix} L_1 \\ L_2 \\ L_3 \end{pmatrix}. \quad (\text{A.10})$$

The vector-product of two vectors \mathbf{a} and \mathbf{b} is given by the operator representation involving the vector of the generators \mathbf{L} ,

$$\mathbf{a} \times \mathbf{b} = -(\mathbf{b} \cdot \mathbf{L}) \mathbf{a}. \quad (\text{A.11})$$

In the most cases we will drop the argument in R_i . Finally we define a set of damped-rotational-operators,

$$R^\pm(t) \equiv R_3(\pm \Omega_0 b_0 t) e^{\pm \nu t}. \quad (\text{A.12})$$

That can be used to solve the ALE. As often as possible we will use the short notation $\alpha \equiv \alpha(t) = \Omega_0 b_0 t$ for the argument. In the special case $b_0 \rightarrow 0$ the rotational matrices reduce to the unity matrix, and

$$R^\pm(\alpha(t))|_{b_0 \rightarrow 0} = I e^{\pm \nu t}, \quad (\text{A.13})$$

is left. A further helpful representation of R^\pm is found by transformation into the complex space by using the vector $\mathbf{q} = (x + i y, z)$

$$R^\pm \mathbf{q} = \begin{pmatrix} e^{\pm i \Omega b_0 t - \nu t} & 0 \\ 0 & e^{-\nu t} \end{pmatrix} \begin{pmatrix} x + i y \\ z \end{pmatrix}. \quad (\text{A.14})$$

The original variables can, of course, be recovered by $x = \mathcal{R}(q_x)$, $y = \mathcal{I}(q_x)$ and $(R^\pm \mathbf{r})_x = \mathcal{R}[(R^\pm \mathbf{q})_x]$, $(R^\pm \mathbf{r})_y = \mathcal{I}[(R^\pm \mathbf{q})_x]$.

A.3 Short review of the velocity correlation function for classical transport

The solution of the A-Langevin equation without magnetic fluctuations reads

$$\boldsymbol{\eta}(t) = R^- \mathbf{u}_0 + R^- \int_0^t R^+ \mathbf{a}(\tau) d\tau, \quad (6.15)$$

and we can calculate the velocity correlation functions by successively apply our information about the stochastic data of \mathbf{a} and \mathbf{u}_0 . The product of two perpendicular velocities is given by,

$$\begin{aligned} \langle \eta_x(t_1) \eta_x(t_2) \rangle_a &= [\cos(\Omega b_0 t_1) \cos(\Omega b_0 t_2) u_{0,x}^2 + \sin(\Omega b_0 t_1) \sin(\Omega b_0 t_2) u_{0,y}^2] \\ &\times \exp[-\nu(t_1 + t_2)] + \frac{A}{2\nu} [1 - \exp(-\nu t_2)] \cos(\Omega b_0(t_1 - t_2)). \end{aligned} \quad (A.16)$$

Here we used already the correlation of the random velocities $\langle \mathbf{a}(t_1) \mathbf{a}(t_2) \rangle = \mathbf{1} A \delta(t_1 - t_2)$. The choice of the constant A is still at our disposal [5]. Next we assume a Maxwellian distribution of the initial velocities,

$$P(\mathbf{u}_0) = \pi^{-3/2} v_t^{-3} \exp\left(-\frac{u_0^2}{v_t^2}\right), \quad (A.17)$$

and average the initial velocities, yielding

$$\langle \langle \eta_x(t_1) \eta_x(t_2) \rangle_a \rangle_{\mathbf{u}_0} = \left(\frac{A}{2\nu} e^{-\nu|t_1-t_2|} + \frac{1}{2} \left(v_t^2 - \frac{A}{\nu} \right) e^{-\nu|t_1+t_2|} \right) \cos(\Omega b_0(t_1 - t_2)). \quad (A.18)$$

Obviously this correlation function is not stationary in time, it still depends on t_1 and t_2 separately. To fulfill the constraint [10], that $\langle \langle \eta_x(t_1) \eta_x(t_2) \rangle_a \rangle_{\mathbf{u}_0}$ should depend only on the difference of two times, $\tau = t_1 - t_2$, we choose the constant A to be

$$A = v_t^2 \nu. \quad (A.19)$$

Substituting this value for A , we directly find the relations presented in the main text.

A.4 Multiscale perturbation series for strong guiding fields

The evaluation of the correlation functions needs an approximation [31] for strong guiding fields. We present here a suitable method to estimate the integrals up to the desired order. Following types of integrals have to be solved,

$$I_1 = \int_0^t \cos\left(\frac{\tau-t}{\varepsilon}\right) b_y(\tau) d\tau, \quad I_2 = \int_0^t \sin\left(\frac{\tau-t}{\varepsilon}\right) b_x(\tau) d\tau. \quad (A.20)$$

For $b_0 \gg 1$ we use the smallness parameter $\varepsilon = (\Omega b_0)^{-1}$. Substituting $x = \varepsilon^{-1}(\tau - t)$ and expanding in ε leads to

$$I_1 = \int_{-\varepsilon^{-1}t}^0 \cos(x) b_y(t + \varepsilon x) dx \approx \varepsilon b_y(t) [\sin(x)]_{-\varepsilon^{-1}t}^0 - \varepsilon^2 \int_{-\varepsilon^{-1}t}^0 \sin(x) b_y'(t_1 + \varepsilon x) dx. \quad (\text{A.21})$$

A second partial integration by path enables us to derive an approximation to the second order of ε ,

$$I_1 = \varepsilon b_y(t) \sin(\varepsilon^{-1}t) - \varepsilon^2 b_x'(t) - \varepsilon^2 b_x' \cos(\varepsilon^{-1}t) + \mathcal{O}(\varepsilon^3). \quad (\text{A.22})$$

The second integral can be estimated in the same way,

$$I_2 = -\varepsilon b_y(t) - \varepsilon b_y(t) \cos(\varepsilon^{-1}t) + \varepsilon^2 b_y'(t) \sin(\varepsilon^{-1}t) + \mathcal{O}(\varepsilon^3). \quad (\text{A.23})$$

Due to the fast oscillations the trigonometric terms vanish and the contribution of the perturbation field \mathbf{b} are found to be

$$I_1 \approx -\varepsilon^2 b_x'(t), \quad I_2 \approx -\varepsilon b_y(t). \quad (\text{A.24})$$

Appendix B

B.1 Combined average

The average of mixed terms combined of the stochastic function and the characteristic function is more involved [31,32] than the standard cumulant expansion. Let $\sigma(t_1, t_2) = \langle a(t_1) a(t_2) \rangle$, we can calculate the combined average as,

$$\begin{aligned}
\left\langle a(t_1) a(t_2) \exp \left\{ -ik \int_{t_2}^{t_1} a(\theta) d\theta \right\} \right\rangle &= \frac{1}{k^2} \frac{\partial^2}{\partial t_1 \partial t_2} \left\langle \exp \left(-ik \int_{t_2}^{t_1} a(\theta) d\theta \right) \right\rangle \\
&= \frac{1}{k^2} \frac{\partial^2}{\partial t_1 \partial t_2} \exp \left(-\frac{1}{2} k^2 \int_{t_2}^{t_1} \int_{t_2}^{t_1} \langle a(\theta_1) a(\theta_2) \rangle d\theta_1 d\theta_2 \right) \\
&= \left\{ \sigma_a(t_1, t_2) - k^2 \int_{t_2}^{t_1} \sigma_a(t_1, \theta_2) d\theta_2 \int_{t_2}^{t_1} \sigma_a(\theta_1, t_2) d\theta_1 \right\} \times \\
&\quad \exp \left\{ -\frac{1}{2} k^2 \int_{t_2}^{t_1} \int_{t_2}^{t_1} \sigma_a(\theta_1, \theta_2) d\theta_2 d\theta_1 \right\}.
\end{aligned} \tag{B.1}$$

which can be written with the using φ_a and ψ_a from the main text, defined in (3.22),

$$\left\langle a(t_1) a(t_2) \exp \left\{ -ik \int_{t_2}^{t_1} a(\theta) d\theta \right\} \right\rangle = \left\{ \sigma_a(t_1, t_2) - k^2 \varphi_a^2 \right\} \exp \left\{ -\frac{1}{2} k^2 \psi_a \right\}. \tag{B.2}$$

This prescription can also be found in [10,12] and is used throughout the derivation of the Lagrangian correlation functions. A more generalized procedure for mixed or combined averages is presented in Sec. 4.2.

B.2 Analytical derivation of the Rechester-Rosenbluth diffusion coefficient

The derivation follows Vanden-Eijnden et al. [12] where a detailed treatment of the method and the calculation can be found. In order to derive the asymptotic diffusion coefficient for the MSD $\mu^{(0)}$ given by

$$\frac{d^2}{d\tau^2} \mu^{(0)}(\tau) = k^2 \bar{\chi}_{\parallel}^2 \left(1 + \bar{\chi}_{\parallel} \tau - \frac{1}{2} \bar{\chi}_{\parallel} \right)^{-\frac{3}{2}} \left(1 - \left(1 + \bar{\chi}_{\perp} \left(\tau - \frac{1}{2} \right) + \frac{1}{2} \mu^{(0)}(t) \right)^{-2} \right), \tag{B.3}$$

we approximate (B.3) with

$$\frac{d^2}{d\tau^2} \mu^{(0)}(\tau) = \theta \left(\tau - \frac{1}{2} \right)^{-\frac{3}{2}} \left(1 - \left(1 + \bar{\chi}_\perp \left(\tau - \frac{1}{2} \right) + \frac{1}{2} \mu^{(0)}(\tau) \right)^{-2} \right), \quad (\text{B.4})$$

for $\bar{\chi}_\parallel \gtrsim 1$. $\theta = \kappa^2 \bar{\chi}_\parallel^{1/2}$. This Eq. should be solved with the initial conditions $\mu^{(0)}(1) \approx 0$ and $\frac{d}{d\tau} \mu^{(0)}(\tau) |_{\tau=1} \approx 0$. A solution can now be found by dividing the evaluation of the differential Eq. (B.4) into two parts. First we solve (B.4) for $\bar{\chi}_\perp \left(\tau - \frac{1}{2} \right) + \frac{1}{2} \mu_1^{(0)}(\tau) \ll 1$. In this case, the last term in (B.4) can be approximated using the expansion

$$\left(1 + \bar{\chi}_\perp \left(\tau - \frac{1}{2} \right) + \frac{1}{2} \mu_1^{(0)}(\tau) \right)^{-2} \approx 1 - 2 \bar{\chi}_\perp \left(\tau - \frac{1}{2} \right) - \mu_1^{(0)}(\tau), \quad (\text{B.5})$$

which leads to the differential equation (in the regime 1),

$$\frac{d^2}{d\tau^2} \mu_1^{(0)} = \theta \left(\tau - \frac{1}{2} \right) (2 \bar{\chi}_\perp \bar{\tau} + \mu_1^{(0)}(\tau)). \quad (\text{B.6})$$

using $\bar{\tau} = \tau - \frac{1}{2}$. The solution of this Eq.,

$$\mu_1^{(0)} = -2 \bar{\chi}_\perp \bar{\tau} + \bar{\chi}_\perp \sqrt{\bar{\tau}} \{c_1 I_2[4 \sqrt{\theta} \bar{\tau}^{1/4}] + c_2 K_2[4 \sqrt{\theta} \bar{\tau}^{1/4}]\}, \quad (\text{B.7})$$

is given in terms of the modified Bessel functions I_2 and K_2 . The coefficients c_1 and c_2 are found by using the initial conditions,

$$c_1 = \sqrt{2} [a K_1(a) + 4 K_2(a)], \quad c_2 = \sqrt{2} [a I_1(a) - 4 I_2(a)], \quad a = 2^{7/4} \sqrt{\theta}. \quad (\text{B.8})$$

We use the asymptotic expansions of the Bessel functions,

$$K_2 \sim \sqrt{\frac{\pi}{2x}} e^{-x}, \quad I_2 \sim \frac{1}{\sqrt{2\pi x}} e^x, \quad \text{for } x \gg 1. \quad (\text{B.9})$$

With this substitution, the solution (B.7) simplifies to

$$\mu_1^{(0)} + 2 \bar{\chi}_\perp \bar{\tau} \sim \frac{1}{2 \sqrt{2\pi}} \bar{\chi}_\perp \bar{\tau}^{3/8} \theta^{-1/4} c_1 \exp(4 \sqrt{\theta} \bar{\tau}^{1/4}), \quad (\text{B.10})$$

if we assume $\sqrt{\theta} \bar{\tau}^{1/4} \gg 1$. The second regime is defined by the condition

$$\bar{\chi}_\perp \left(\tau - \frac{1}{2} \right) + \frac{1}{2} \mu_2^{(0)}(\tau) \gg 1, \quad (\text{B.11})$$

and leads to a very simple differential equation of the form,

$$\frac{d^2}{d\bar{\tau}^2} \mu_2^{(0)} = \theta \bar{\tau}^{-3/2}, \quad (\text{B.12})$$

which can be integrated once in time,

$$\frac{d}{d\bar{\tau}} \mu_2^{(0)} = D - \theta \bar{\tau}^{-1/2}. \quad (\text{B.13})$$

In the latter formula the diffusion coefficient appears as a principally unknown integration constant. Obviously both regime have to be matched at a certain time $\bar{\tau}^*$, where we assume that both approximations are valid. Using (B.6) and (B.12) we get

$$1 = \frac{1}{2\sqrt{2\pi}} \bar{\chi}_\perp \bar{\tau}^{*3/8} \theta^{-1/4} c_1 \exp(4\sqrt{\theta} \bar{\tau}^{*1/4}), \quad (\text{B.14})$$

as a defining equation for the fitting time $\bar{\tau}^*$. (B.10) leads together with (B.13) to the matching relation,

$$D - \theta \bar{\tau}^{*-1/2} = \frac{1}{4\sqrt{2\pi}} \bar{\chi}_\perp \bar{\tau}^{*-3/8} \theta^{1/4} c_1 \exp(4\sqrt{\theta} \bar{\tau}^{*1/4}) \approx 0. \quad (\text{B.15})$$

One obtains the matching time

$$\bar{\tau}^{*-1/2} = \frac{D}{\theta}. \quad (\text{B.16})$$

Introducing this matching time into (B.14) gives us an implicit equation for D ,

$$1 = \frac{1}{2\sqrt{2\pi}} \bar{\chi}_\perp D^{-3/4} \theta^{-1/2} c_1 \exp(4\theta D^{-1/2}), \quad (\text{B.17})$$

which can be iterated around $D \approx 16\theta^2$, reproducing the famous Rechester-Rosenbluth diffusion coefficient as it can be found in the main text,

$$D = \frac{16\theta^2}{\log^2[16\sqrt{2\pi}\theta^2\bar{\chi}_\perp^{-1}]}. \quad (\text{B.18})$$

Appendix C

C.1 Conditional probabilities in the DCT

We present here a simple example to explain the calculation of the involved conditional probabilities in the DCT [33,34,35]. Therefore we concentrate in finding the subensemble average of the form,

$$\langle b \rangle_S = \int_{-\infty}^{\infty} b P(b | \phi^0) db. \quad (\text{C.1})$$

b may be one dimensional and $\phi(0) = 0$ the only condition. For $P(b | \phi^0)$ we use

$$P(b | \phi^0) = \frac{\langle \delta(b - b(x)) \delta(\phi^0 - \phi(0)) \rangle}{\langle \delta(\phi^0 - \phi(0)) \rangle}. \quad (\text{C.2})$$

Next we define the correlation between $b(x)$ and $\phi(0)$ as $C_{b\phi} = \langle b(x) \phi(0) \rangle$. All other correlations are either one or zero, e.g. $\langle b(x) b(x) \rangle = 1$. Inserting the Fourierrepresentation of the Deltafunction and applying the cumulant expansion in the exponent, we arrive at

$$P(b | \phi^0) = \frac{\frac{1}{4\pi^2} \int dk \int dl \exp[ikb + il\phi^0 - \frac{1}{2} k^2 - \frac{1}{2} l^2 - klC_{b\phi}]}{\frac{1}{2\pi} \int dm \exp[im\phi^0 - \frac{1}{2} m^2]}. \quad (\text{C.3})$$

The integration is straightforward and yields,

$$P(b | \phi^0) = \frac{1}{\sqrt{2\pi(1 - C_{b\phi}^2)}} \exp\left(-\frac{(b - C_{b\phi}\phi^0)^2}{2(1 - C_{b\phi}^2)}\right). \quad (\text{C.4})$$

Performing also the last integration we find the ensemble average to be

$$\langle b \rangle_S = \phi^0 C_{b\phi}. \quad (\text{C.5})$$

Of course, the extension of Eq. (C.2) with more conditional terms is straightforward and leads to similar expressions like Eq. (C.5). The probabilities used in the main text are derived by the same method as presented here. Some details and further examples can be found in the works of Vlad et.al. [18,19,20].

Appendix D

D.1 The *Matlab7* environment

All algorithms are programmed and implemented in the mathematical interpreter language Matlab7. The major advantage of the interpreter environment is the possibility to use internal random generators and differential equation solvers which are very fast and reliable. Subroutines are placed in separate program modules to provide individual maintenance for single parts of the calculation and the possibility to exchange or reuse single modules for other purposes.

The guided user interface **patric**@Matlab7 was developed. It automatically controls all steps of the ALE integration process and the corresponding Green-Kubo model equations.

D.2 Numerical solution of the A-Langevin equation

Principle

The ALE is a second order stochastic differential equation for the trajectory \mathbf{r} of a particle. It is solved by a direct Monte-Carlo integration [36]. Calculating the differential equation system is straightforward and is performed with a standard fourth order Runge-Kutta procedure with fifth-order error correction. The stochastic values are basically provided by a random generator that produces distributed or correlated random numbers.

Integration of the trajectory

An ensemble of particles is propagated through the system, solving the ALE once for each particle. With fixed values of the magnetic field and the acceleration, the ALE is, of course, equal to a damped and accelerated 3D-Lorentz equation system. To establish useable results, the number of trajectories should be large enough. Every single particle is equipped with an individual random starting point and a random starting velocity in each direction. The random data have a Gaussian distribution. These data are used as initial condition for the integration. We found that the precision of the calculation is no longer significantly increased using more than 50 particles. So, typically, we propagate around 50 to 100 particles for our statistics.

Stochastic collisions

Within the steps of the numerical integration, an acceleration \mathbf{a} is provided by a random generator. It models the collisional events a particle will experience along its trajectory. The strength of the collisions is scaled by the factor $\sqrt{A} = v_t \sqrt{\nu}$, as derived in Sec. 2. As the collisions appear now at each integration step, the friction parameter ν requires rescaling with the step size of the integrator.

Stochastic magnetic field

The magnetic fluctuation field \mathbf{b} is also changed randomly, but it is still correlated by the rules of the Eulerian correlation function. We generate the perturbation field at a position $X(i)$, by using the state of the perturbation field at $X(i-1)$ and adding a random number scaled with the inverse of the correlation value at the position $X(i)$ [36,37]. The latter is possible, because the position of the particle is always known at the temporary point of integration.

Polynomial fitting and transport properties

A set of trajectories is obtained and the numerical analysis is completed by averaging these trajectories to provide the MSD. From the MSD other transport properties can be derived. To derive numerical data on the diffusion coefficient, a polynomial fitting routine is applied to take care of noise and oscillation of the MSD data, causing large derivatives in the calculation of the diffusion.

D.3 Integration of the Green-Kubo differential equations

In most cases the Green-Kubo equations are solved by an internal Matlab7 routine. It is based on an explicit Runge-Kutta method using the Dormand-Prince pair and is an 4th order integrator with a 5th order error correction [38]. In some rare cases the differential equation is stiff. Then the algorithm is switched to an integrator for stiff equations, applying a second order Rosenbrock formula.

D.4 Monte-Carlo integration of the DCT structure function

Principle

The numerical calculation of the DCT structure function requires an efficient and fast way to solve the triple integral for ϕ^0 and \mathbf{b}^0 . This is a non-trivial task, because for each integration step $(\phi_i^0, \mathbf{b}_i^0)$, the decorrelation trajectory $\mathbf{X}_i(t; \phi_i^0, \mathbf{b}_i^0)$ has to be retrieved by an additional integration of the non-stochastic 3D-Lorentz differential equation system determining \mathbf{X}_i .

Monte-Carlo method

The basic idea of the Monte-Carlo integration (more precisely, it should be called quadrature here) is to replace the integration with a summation [36,38]. But instead of using a regular grid to cover the integration points in fixed steps, we choose a random set of ϕ_i^0 and \mathbf{b}_i^0 . Again the number of random points has to be large enough to find precise results. Due to the special characteristics of the integral, we generate the values for ϕ_i^0 and \mathbf{b}_i^0 from a Gaussian distribution and select in that way only numbers with maximal contribution to the integral. The algorithm has proven to be extremely efficient.

Bibliography

- [1] R.D. Hazeltine and J.D. Meiss, *Plasma confinement* (Addison-Wesley, Redwood City, Calif., 1992).
- [2] R. Balescu, *Aspects of anomalous transport in plasmas* (Institute of Physics Publishing, Bristol, 2005).
- [3] R. Balescu, *Transport processes in plasmas: 2. Neoclassical transport theory* (North-Holland, Amsterdam, 1988).
- [4] T.E. Evans, Phys. Rev. Lett. **92**, 235003 (2004).
- [5] R. Balescu, Statistical Dynamics, *Matter out of Equilibrium* (Imperial College Press, London, 2000).
- [6] W.H. Matthaeus, G. Qin, J.W. Bieber and G.P. Zank, *Nonlinear collisionless perpendicular diffusion of charged particles*, Astr. Phys. J. **590**, L000 (2003).
- [7] F. Casse, M. Lemoine, and G. Pelletier, *Transport of cosmic rays in chaotic magnetic fields*, Phys.Rev.D **65**, 023002 (2001).
- [8] N. Van Kampen, *Stochastic processes in physics and chemistry* (North-Holland, 1981).
- [9] J.M. Rax and R.B. White, Phys. Rev. Lett. **68**, 1523 (1992).
- [10] R.Balescu, H.D.Wang, and J.H.Misguich, *Langevin equation versus kinetic equation: Subdiffusive behavior of charged particles in a stochastic magnetic field*, Phys.Plasmas1, 3827 (1994).
- [11] H.D. Wang, E. Vanden-Eijnden, F. Spineanu, J.H. Misguich, and R. Balescu, *Diffusive processes in a stochastic magnetic field*, Phys. Rev. E **51**, 4844 (1995).
- [12] E. Vanden-Eijnden and R. Balescu, *Statistical description and transport in stochastic magnetic fields*, Phys. Plasmas **3**, 874 (1996).
- [13] S. Corrsin, in: *Atmospheric Diffusion and Air Pollution*, edited by F.N.Frenkiel and P.A.Sheppard, p.161 (Academic Press , New York, 1990).
- [14] J. Weinstock, *Lagrangian-Eulerian relation and the independance approximation*, Phys. Fluids **19**, 1702 (1996).
- [15] W.D. McComb, *The Physic of Fluid Turbulence* (Clarendon Press , Oxford, 1990).
- [16] J.L. Lumley, *The mathematical nature of the problem of relating Lagrangian and Eulerian statistical functions in turbulence*, Pages 17-16 in: *Mécanique de la turbulence Colloq. Intern. CNRS, Marseille (CNRS, Paris, 1962)*.

- [17] P.G. Saffman, *An approximate calculation of the Lagrangian auto correlation coefficient for stationary homogeneous turbulence*, Appl. Sci. Res. A **11**, 245 (1963).
- [18] M. Vlad, F. Spineanu, J.H. Misguich, and R. Balescu, *Diffusion with intrinsic trapping in two-dimensional incompressible stochastic velocity fields*, Phys. Rev. E **58**, 7359 (1998).
- [19] M. Vlad, F. Spineanu, J.H. Misguich, and R. Balescu, *Diffusion in biased turbulence*, Phys. Rev. E **63**, 066304 (2001).
- [20] M. Vlad, F. Spineanu, J.H. Misguich, and R. Balescu, *Magnetic line trapping and effective transport in stochastic magnetic fields*, Phys. Rev. E **67**, 026406 (2003).
- [21] M.B. Isichenko, *Effective plasma heat conductivity in 'braided' magnetic field-I*, Plasma Phys. Contr. Fusion **33**, 795 (1991).
- [22] M.B. Isichenko, *Effective plasma heat conductivity in 'braided' magnetic field-I*, Plasma Phys. Contr. Fusion **33**, 809 (1991).
- [23] M.B. Isichenko, *Percolation, statistical topography, and transport in random media*, Rev. Mod. Phys. **64**, 961 (1992).
- [24] B.B. Kadomtsev and O.P. Pogutse, *Electron heat conductivity of plasma across a 'braided' magnetic field*, Pages 649-663 in: Plasma Physics and Controlled Nuclear fusion Research, Proceedings of the 7th International Conference Innsbruck, 1978. IAEA-CN-37/O-1.
- [25] R. Kubo, *Stochastic Liouville Equations*, J. Math. Phys. **4**, 174 (1963).
- [26] A.B. Rechester and M.N. Rosenbluth, *Electron heat transport in a Tokamak with Destroyed Magnetic Surfaces*, Phys. Rev. Lett. **40**, 38 (1978).
- [27] J.-D. Reuss and J.H. Misguich, *Low-frequency percolation scaling for particle diffusion in electrostatic turbulence*, Phys. Rev. E **54**, 1857 (1996).
- [28] R.H. Kraichnan, *Kolmogorov's Hypothesis and Eulerian Turbulence Theory*, Phys. Fluids **6**, 1603 (1964).
- [29] R.H. Kraichnan, *Lagrangian-History Closure Approximation for Turbulence*, Phys. Fluids **8**, 575 (1965).
- [30] J.L. Lumley, *Stochastic tools in turbulence*, Applied mathematics and mechanics No. 12 (Academic Press, New York, 1970).
- [31] A.H. Nayfeh, *Perturbation methods* (John Wiley, New York, 1973).

-
- [32] C.W. Gardiner, *Handbook of Stochastic Methods*, Second edn. Springer Series in Synergetics No. 13. (Springer Verlag, Berlin, 1985).
- [33] R. Balescu, M. Vlad, F. Spineanu, and J.H. Misguich, *Anomalous Transport in Plasmas*, *J. Quantum Chemistry* **98**, 125-130 (2004).
- [34] M. Vlad, F. Spineanu, J.H. Misguich, J.-D. Reuss, R. Balescu, K. Itoh, and S.-I. Itoh, *Lagrangian versus Eulerian correlations and transport scaling*, *Plasma Phys. Control. Fusion* **46**, 1051 (2004).
- [35] R. Balescu, *Drift-wave turbulence and zonal flow generation*, *Phys. Rev. E* **68**, 046409 (2003).
- [36] G. Grimmet, *Probability and random processes 3.ed.* (Oxford Univ. Press, Oxford, 2001).
- [37] J.E. Gentle, *Random number generation and Monte Carlo methods* (Springer Verlag, New York, 2005).
- [38] W.H. Press, S.A. Teukolsky, W.T. Vetterling and B.P. Flannery, *Numerical recipes in C* (Cambridge Univ. Press, Cambridge, 1997).

Danksagung

Am Ende dieser Arbeit möchte ich all denjenigen danken, die mich im Verlaufe der letzten Jahre maßgeblich unterstützt haben.

Herrn Prof. Dr. K.H. Spatschek danke ich, meine Faszination an der Theoretischen Physik geweckt zu haben, einen Gebiet das mich für immer geprägt hat. Seine stets offene, hilfreiche und manches mal geduldige Betreuung der vorliegenden Arbeit war nicht nur eine fachliche Bereicherung. Frau Prof. Dr. D. Bruß danke ich für die Übernahme des Koreferats dieser Arbeit und ihre überaus freundliche Unterstützung. Einer Vielzahl von weiteren Personen gebührt Dank für ihre Unterstützung und an erster Stelle sei hierbei Herr Dr. E.W. Laedke erwähnt. Die vielen regen Diskussionen und Gespräche waren dabei immer mehr als nur eine Hilfe, sein schier unerschöpflicher Humor war vielmehr eine große Quelle an Kraft die alle Mitglieder unserer Institutsgruppen bereichert. Herrn Dr. H. Wenk sei für seine Unterstützung bei Computerfragen und für das reibungslose Funktionieren der Computernetze gedankt. Herzlicher Dank an Fr. E. Gröters, dem organisatorischen Engel des Instituts. Sie stand mit Rat und Tat zur Seite und nahm einem stets die Angst von den schlimmsten bürokratischen Fragen. Herrn E. Zügge danke ich für die Computerunterstützung und vor allem dafür, dass es ausreicht an seinem Büro vorbeizugehen und dort genug gute Laune für den gesamten Tag tanken zu können. Es bleibt den weiteren Mitarbeitern des Instituts zu danken, insbesondere Matthias Dellweg, Wolfgang Lellinger, Teodora Baeva, und einigen Ehemaligen, deren Unterstützung nie ausblieb, wie z.B. Dr. Silvie Defrasne, Dr. Dimitry Lesnik und Dr. Alexander Posth. Christoph Karle, Götz Lehmann und Zelimir Marojevic motivierten, stärkten den Rücken und halfen bei der Durchsicht wichtiger Textpassagen, ihnen sei an dieser Stelle nochmals herzlich gedankt. Ein besonderer Dank gilt auch Andreas Wingen für seine Freundschaft und Hilfsbereitschaft während des Studiums, der Diplomarbeit und der Promotion. Marlene Tomkowski stand stets bereit um mir auch in schweren Zeiten neue Kraft zu schenken und dem Herzen neuen Mut verleihen, ihr und den Menschen an meiner Seite, Ulf Bressel, Nikola Sasse, Anja Winter, Anke Strauch und selbstverständlich Nils Bittner, Holger Freymann und Michael Wessolowski, sei an dieser Stelle nochmals dafür gedankt. Letztlich möchte ich meinen Eltern für ihre uneingeschränkte Unterstützung, ihr Vertrauen und ihre Hilfe danken, ihnen sei diese Arbeit gewidmet.

Erklärung

Die hier vorgelegte Dissertation habe ich eigenständig und ohne unerlaubte Hilfe angefertigt. Die Dissertation wurde in der vorgelegten oder in ähnlicher Form noch bei keiner anderen Institution eingereicht. Ich habe bisher keine erfolglosen Promotionsversuche unternommen.

Düsseldorf, den 7.12.2005

(Marcus Neuer)